OPTIMAL OPERATION AND SIZING OF A COMBINED HEAT AND POWER SYSTEM INTEGRATED WITH DEMAND SIDE RESPONSE IN A SMART ENERGY HUB

Haijie Qi

A thesis presented in fulfilment of the requirements for the degree of
Doctor of Philosophy

Department of Electronic and Electrical Engineering
University of Strathclyde, Glasgow, UK
August 2020

This thesis is the result of the author's original research. It has been composed by the author and has not been previously submitted for examination which has led to the award of a degree.

Signed:

Date:

Dedicated to my family

ACKNOWLEDGEMENTS

I would like to express my deepest gratitude to my supervisor Dr Hong Yue, who is always there to provide me with helpful feedback and suggestions with her tremendous knowledge and experience. Her supervision and valuable guidance during my PhD education have been very much appreciated. She is a prestigious researcher who always pursues both professional excellence and moral integrity. Her attitude to life and passion for academic research is a real motivation to me, especially when I experience setbacks and lose my resilience and creativity. I cherish the days of fighting for this thesis under her guidance and wish for the opportunity to work with her again in my future research.

My special gratitude to my former supervisor Dr Jiangfeng Zhang for his continued help throughout my PhD study, for his patient and effective guidance on this thesis revision. I would also like to thank my co-supervisor Prof. Steve Lo for his precious comments which guide my PhD research and academic writings.

A gracious acknowledgement is made to my friends--- Dr Hui Yu, Dr Wei Zheng, Connie Qiu, Dr Yanyi Sun, Huaye Wen, Banghao Zhou, Zhao Wang, Shangen Tian, Kai Huang for being there for me, sharing all the happiness and challenges during my PhD study. I would also like to thank my roommates Dr Ding Zhou, Jian Song, Ximingle Liu, Chen Gao and Xuanwei Hai for their accompany during these years, making me feel at home in Glasgow.

Finally, I would like to take this special chance to thank my love Shiyu Zhong for her accompany, care and encouragement for all these years. She is the one who can always motivate me especially when I was in negative mood. I would also like to thank my parents, Kun Qi and Hongning Wang, for their mental and financial support. Without their love and support, I would not be able to complete this journey.

LIST OF ABBREVIATION

CCGT	Combined Cycle Gas and steam Turbines
CHP	Combined Heat and Power
DOD	Depth of Discharge
DSR	Demand Side Response
EMS	Energy Management System
ESS	Electrical Storage System
GA	Genetic Algorithm
HRSG	Heat Recovery Steam Generator
HVAC	Heating, Ventilation, and Air-Conditioning
IDR	Integrated Demand Response
LP	Linear Programming
NPV	Net Present Value
S.E. Hub	Smart Energy Hub
SMES	Superconducting Magnetic Energy Storage
SOC	State of Charge
TSS	Thermal Storage System
TOU	Time of Use

LIST OF NOMENCLATURE

Chapter 3 Methodology

a	Positive charging/discharging power for TSS, kW
a_{ik}	Average annual energy saving of component i size k, kWh
b_i	Decision variables indicating appliances on/off status
B	Average annual year energy cost saving, £
c_{boiler}	Unit cost of heat generated by the boiler, £/kWh
c_{grid}	Electricity tariff of the power grid, £/kWh
c_t	Operational cost in year t, £
d_{ik}	Decision variables indicating the size k of component i
d_t	Average discount rate of each year, %
e	Positive charging/discharging power for TSS, kW
$EC_{existing}$	Energy consumption of the existing components, kWh
$EC_{proposed}$	Energy consumption of the proposed components, kWh
I	Number of appliances
I_0	Total investment of new components, £
I_{budget}	Investment budget, £
J	Index set of characteristic points of the CHP
k	Alternative size choices
L_{power}	Lower power bound in optimal design model, kW
P_{ik}	Rated power of component i size k, kW
p_j	Power value of characteristic point j CHP, kW

P_{excess}	Excess power generated by CHP, kW
P_{grid}	Electricity power purchased from the power grid, kW
P	Power production of CHP, kW
P_{s+}	ESS charging power, kW
P_{s-}	ESS discharging power, kW
q_j	Heat value of characteristic point j CHP, kW
Q	Heat demand of the S.E. Hub, kW
Q_{boiler}	Heat output of the boiler, kW
Q	Heat production of CHP, kW
Q_{s+}	TSS charging power, kW
Q_{s-}	TSS discharging power, kW
S_P	Energy stored in ESS, kWh
S_Q	Energy stored in TSS, kWh
$S_P^{\min}$	Minimum storage levels of ESS, kWh
$S_P^{\max}$	Maximum storage levels of ESS, kWh
$S_Q^{\min}$	Minimum storage levels of TSS, kWh
$S_Q^{\max}$	Maximum storage levels of TSS, kWh
Δt	Interval of sampling time, h
T	Total sampling time, h
x_j	Decision variable of CHP
u_j	Cost at characteristic point j of CHP, £
U_{power}	Upper power bound in optimal design model, kW

U	Operating unit cost of CHP, £/h
η_P	Storage efficiency of ESS considering self-discharging rate, %
η_Q	Storage efficiency of TSS considering self-discharging rate, %
∂	Electricity price annual increasing rate, %
λ	Upper bound integer that makes NPV nonnegative, years
Z	Maximal expected payback period, years
$EC_{\exp}$	Minimal energy saving, kWh

Chapter 4 Optimal Operation of CHP Combined with DSR

a	Positive charging/discharging power for TSS, kW
$b_{l_{HVAC}}$	Binary variable indicating working levels of HVAC
c_1	TOU tariff, £/kWh
c_2	Natural gas price, £/kWh
c_3	Sale price from CHP to the grid, £/kWh
$c_{electricity}$	Electricity cost, £
c_{gas}	Natural gas cost, £
c_{income}	Income from selling excess electricity, £
c_{total}	Total cost of an S.E. Hub, £
$C_{building}$	Heat capacity of the building, kW/℃
e	Positive charging/discharging power for ESS, kW
GMF_{CHP}	Gas mass flow of CHP input, kW
GMF_{boiler}	Gas mass flow of boiler input, kW
H^{ig}	Heat conductance between indoor air and ground, kW/℃

H^{io}	Heat conductance between indoor air and outdoor air, kW/℃
H^{iv}	Heat conductance between indoor air and ventilation air, kW/℃
HF_{boiler}	Heat flow generated by gas boiler, kW
j	Index of CHP characteristic points
l_{HVAC}	HVAC operating levels
p_j	Power value of CHP characteristic point *j*, kW
P_1	Power generated by CHP, kW
$P_{CHP}^{\max}$	Maximum rated power of CHP, kW
P_{CHP}^{rate}	Power ramping rate of CHP, kW/h
P_{excess}	Excess power generated by CHP, kW
P_{grid}	Purchased power from the power grid, kW
P_{HVAC}	Power of HVAC system, kW
$P_{l_{HVAC}}$	Operating power levels of HVAC, kW
P_L	Power of the sum of inflexible appliances, kW
q_j	Heat value of CHP at characteristic point j, kW
Q	Heat demand of end users, kW
Q_1	Thermal power generated by CHP, kW
T^g	Ground temperature, ℃
T^i	Indoor air temperature, ℃
$T_{\min}^i$	Minimal indoor air temperature, ℃
$T_{\max}^i$	Maximal indoor air temperature, ℃
T^o	Outdoor air temperature, ℃

T^{v}	Ventilation temperature, ℃
Δt	Length of sampling time slot, h
u_j	Hourly cost of CHP unit, £
x_j	Decision variables for CHP modeling
ϕ	Set of all decision variables
η^{boiler}	Energy efficiency of centralized boiler, %
η_1^{heat}	Heat utilization efficiency for thermal demand, %
η^{HVAC}	Energy efficiency of HVAC, %

Chapter 5 Optimal Operation of CHP and Energy Storages Integrated with DSR

a	Positive charging/discharging power for TSS, kW
c_{con}	Construction cost of ESS, £
$c_{storage}$	Cost of storage system, £
c_{SOC}^{ESS}	SOC−related degradation cost of ESS, £
c_{DOD}^{ESS}	DOD-related degradation cost of ESS, £
C_{ESS}	Storage capacity of ESS, kWh
C_{TSS}	Storage capacity of TSS, kWh
C_{water}	Water heat capacity in tank, kJ/(kg · ℃)
$CF_{\max}$	The ESS maximum capacity fade constant, %
e	Positive charging/discharging power for TSS, kW
P_s	Charging/discharging electrical power of ESS, kW

Q_s	Charging/discharging thermal power of TSS, kW
S_P	Electrical energy stored in ESS, kWh
S_Q	Thermal energy stored in TSS, kWh
$S_P^{\min}$	Minimum storage levels of ESS, kWh
$S_P^{\max}$	Maximum storage levels of ESS, kWh
$S_Q^{\min}$	Minimum storage levels of TSS, kWh
$S_Q^{\max}$	Maximum storage levels of TSS, kWh
SOC_{ESS}	State of charge of ESS, %
SOC_{TSS}	State of charge of TSS, %
V	Water volume in TSS, m^3
Z	Number of lifecyle for DOD degradation
α	Linear regression parameter for SOC degradation
β	Linear regression parameter for SOC degradation
η_P	Storage efficiency of ESS considering self-discharging rate, %
η_Q	Storage efficiency of TSS considering self-discharging rate, %
ρ	Water density, kg/m^3
φ	ESS charging/discharging efficiency, %
ψ	TSS charging/discharging efficiency, %
η_{CHP}	Average energy conversion efficiency of CHP, %

Chapter 6 Optimal Sizing of CHP Considering DSR

B	Annual energy cost saving, £

c_{daily}^{S2}	Average daily energy cost of Scenario 2, £
I_{CHP}	CHP investment, £
I_{budget}	Investment budget, £
K	Decision variable indicating CHP capacity
λ_1	Weighting factor related to operational cost compensation
λ_2	Weighting factor related to payback period compensation
ξ	Maximum payback period, years

LIST OF FIGURES

LIST OF TABLES

CONTENT

1. INTRODUCTION

As a distributed high-efficient generation technology, combined heat and power (CHP) has been widely applied to generate thermal and electrical energy in residential and commercial buildings. This thesis aims to investigate the efficient operation and optimal sizing problems of CHP to guide optimal operations of a smart energy hub (S.E. Hub). For this purpose, the detailed background, objectives, motivation, novelty, and outlines of the thesis are introduced below.

1.1. Background

With the modernization of power grid, technologies of power generation and transmission have been developed quickly. In light of the rising significance of distributed energy resources, research on electric power distribution is attracting increasing attention. Electric power systems have been undergoing a radical transformation and new challenges have been raised due to renewable energy sources, distributed generations, demand-driven planning ambitions, microgrids and smart grid technologies, climate change related pressures and increasing consumer preferences [1].

The technologies such as demand side response (DSR) and CHP have been proposed and developed to meet the requirement of energy efficiency improvement. Meanwhile, the idea of S.E. Hub becomes an advanced technology and a suitable choice to integrate DSR [2], CHP [3] and storage systems [4] as a potential solution to tackle challenges such as efficient energy usage, optimal design, etc.

1.1.1. S.E. Hub

In view of environmental concerns and diverse power consumption by demand side, future energy supply systems will take the form of sustainable multi-energy systems [5], which is described as an S.E. Hubs or a microgrid comprised of multiple

S.E. Hubs, as shown in Fig. 1.1. Energy hub is defined as the place where the energy generation, conversion, storage and consumption take place [6]. An S.E. Hub is considered as an upgraded energy hub deploying intelligent devices such as smart meters and smart appliances [7], it is a new topic of past few years in multi-energy management [8].

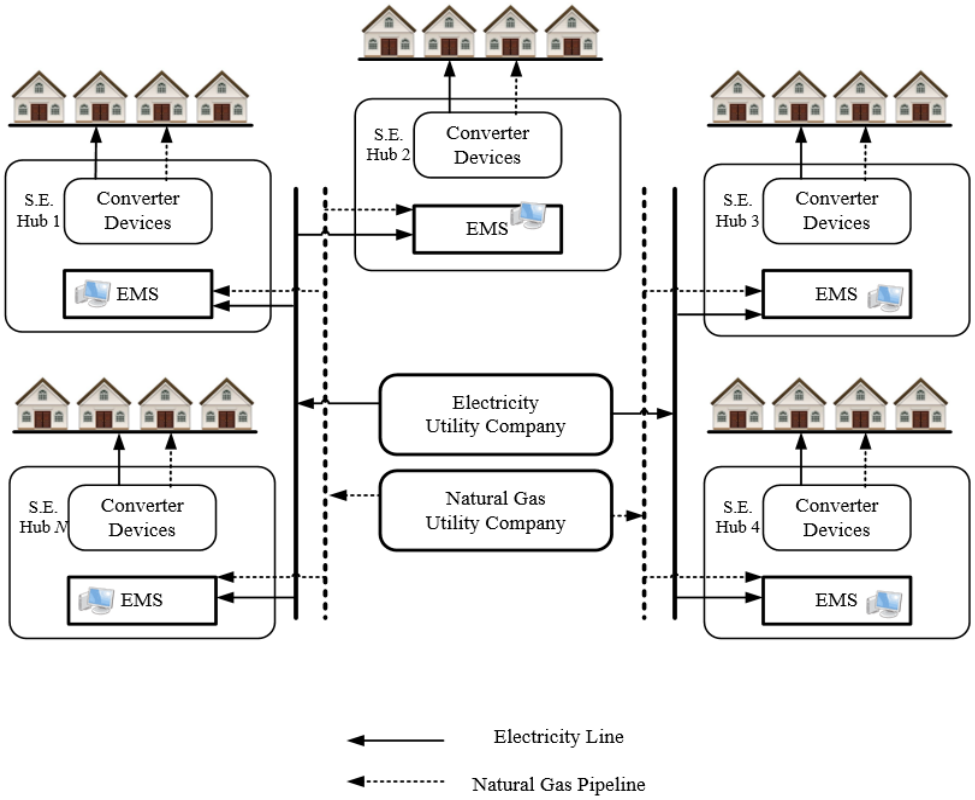

Fig. 1.1 Illustrative diagram of S.E. Hubs equipped with EMS and communication lines (taken from [9])

The establishment of S.E. Hubs becomes a popular trend to improve energy efficiency and decrease environmental pollution, with benefits on integration of highly-efficient devices, adoption of advanced control approaches, and establishment of bi-directional communications between utilities and consumers. On the other hand, the control of S.E. Hub provides system operators and prosumers opportunities to enhance the grid flexibility [10]. This flexibility is defined as the grid system capability of modifying generation and/or consumption patterns in response to an external signal (such as a change in energy price) [11]. Additionally, an S.E. Hub can enhance the

reliability of the energy system [12] as different energy sources back up each other to satisfy the load demands of end-users [13]. The development of S.E. Hubs has significantly strengthened the integration of various energy resources [14, 15]. Thus, optimal operation of S.E. Hubs has become increasingly important to ensure coordinated operation of multi-energy sources, and has attracted great research interests.

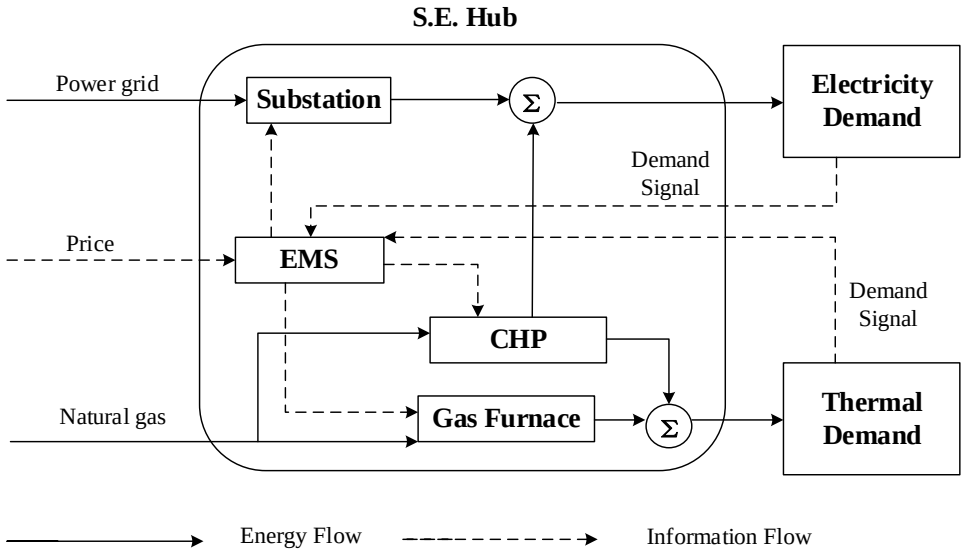

Fig. 1.2 The schematic of a typical S.E. Hub

As shown in Fig. 1.2, a typical S.E. Hub is comprised of an energy management system (EMS), an energy conversion system, such as CHP, and energy and information flows between demand side and supplier side [16, 17]. The EMS is functioned to analyze the demand signals and electricity tariff information, so as to send commands to local power and heat generations while making decisions for energy purchase from the external. In developed countries, the building energy consumption (both residential and commercial) increases steadily occupying 30-40% of total energy consumption, and it exceeds the industrial and transportation energy consumption in most countries [18]. Thus, it is crucial to manage the building's demands of an S.E. Hub, where DSR is proposed.

1.1.2. Demand side response

DSR is an economic operational strategy widely used in building demand management [19]. It is a program encouraging end-users to reduce or shift their electricity load during peak electricity price period in response to varying electricity price (price-based DSR) or other forms of financial incentives (incentive-based DSR). With respect to the current technologies of power distribution, DSR is an efficient solution to improve the energy usage efficiency of end-users [20]. Instead of treating end-users as passive electricity consumers, DSR enables end-users to save energy costs against the varying electricity price [21].

In power systems, DSR has been in use for over ten years in various forms like load shifting to satisfy the needs of industrial users [22]. Nevertheless, over the past few years, there has been an increasing interest in DSR programs because of the prevalence of intermittent renewable energy sources [23]. DSR programs is particularly useful for enhancing renewable generation and improving power systems' flexibility, reliability, and energy efficiency [24]. Additionally, DSR programs can engage in the energy market by offering peak-shaving and load-changing services so as to reduce the demand for expensive plants during the peak time [25], decrease the financial investment in extra generators, and reduce the pressure on current transmission and logistics infrastructure [24].

In conventional DSR programs, the optimization is achieved by pre-acting or delaying some flexible loads from the peak electricity price region to the valley electricity price region [26]. However, this single energy carrier DSR is not suitable for end-users without energy storage facilities. Thus, the end-users' DSR capability cannot be fully exploited [17]. In an S.E. Hub, DSR is integrated with multi-energy system, known as integrated demand response (IDR).

In this thesis, IDR scheme is implemented along with CHP dynamic control, where the EMS can not only shift the load demand in the peak tariff period but also increase the power output of CHP generation instead of purchasing electricity from the power grid. The IDR scheme of this thesis depends on a TOU tariff, which is a price-based DSR program [27].

1.1.3. CHP system

Employment of on-site CHP can greatly strengthen a building's energy security. Meanwhile, it can also serve as a protector from rising electricity prices. In this regard, CHP systems are suitable for a large range of applications, both in industries and commerce [28]. Commercial buildings are suitable for CHP installations particularly due to their relatively large heating, cooling, and electrical loads that can be well predicted. This enables CHP systems to realize sufficient operating hours so as to achieve the purposes of environmental protection or energy conservation [29]. Additionally, a DSR program enables an extra source of revenues, making it more feasible to apply CHP technology in commercial buildings. With the increasing prevalence of decentralized energy generation, CHP can be considered as more useful both for system operators and for owners of buildings, as it can offer reliable, secure, and cost-effective energy.

CHP units and heat pumps are two efficient systems that constitute an S.E. Hub, producing the required energy demand such as electricity, heating, and cooling [30]. Notably, some types of CHP systems can use sustainable fuels as energy resource such as biomass and wood chips [31], recognized as possessing good potential to mitigate climate change [32]. CHP systems are considered as distributed sustainable energy generations in power systems with nearly 90% energy conversion efficiency [33]. Because of these advantages, traditional centralized boilers tend to be replaced by

community-sized CHP units in buildings [34], such as hotels, hospitals, university campuses, and office buildings [35].

In this thesis, the optimal operation control of CHP and the optimal design for new CHP installation are explored through case studies. Under the proposed optimal operation strategies of an S.E. Hub, the power and heat split ratio of CHP is determined dynamically for CHP cost minimization. The optimal design for CHP operation reduces the investment and also helps the building owner save energy cost based on the proposed S.E. Hub operational strategy.

1.2. Motivation of Research

Most DSR schemes are developed for cost saving (price-based) or revenue generating (incentive-based) for residential consumers [36, 37], or for improving network stability [38-41]. A recent move is to combine DSR technology with microgrid optimization.

A hybrid renewable energy system operational optimization model with DSR has been presented in [42] considering solar, wind, diesel, and storage systems, where the energy management is formulated as a two-layer optimization problem. The DSR is taken as the first layer and then total energy cost is minimized through optimal control of components under regulated load. However, this approach decreases the function of controllable components such as CHP system and storage systems, which are flexible to manage under time-varying electricity prices.

Jin et al. [43] assume a building as a virtual energy storage system, its internal space can be pre-warmed under a DSR method and the virtual energy storage system is integrated with dispatchable hybrid distributed generators including a CHP unit to reduce daily operational cost. A multi-objective optimization of microgrid with DSR including different types of heat and electricity generators is developed in [44]. Firouzmakan et al. propose a day-ahead energy management system including CHP

units to minimize the microgrid operational cost and improve the reliability under DSR [45]. However, these CHP units in [44, 45] are considered as generators with fixed power-heat ratio to follow the optimal strategies.

A research gap is identified as that CHP units are generally considered as fixed heat-power output generators in most microgrid optimization systems including CHP and DSR. The capability of CHP dynamic generation in response to varying electricity price and demands has been largely ignored, and the fixed CHP units may not operate optimally since the electricity and thermal demands may change significantly from one time to another. To fill this gap in research, this thesis proposes several S.E. Hub operational strategies, in which the ration of the electrical power over thermal heat output of CHP is dynamically controlled along with DSR and energy storage technologies to achieve the overall energy cost minimization.

For residential buildings, energy are mainly used for space cooling and heating, consuming more than 50% of the total energy demand in developed countries [46]. In Europe, space heating is generally supplied by heating, ventilation, and air-conditioning (HVAC) systems in smart commercial buildings [47]. HVAC is therefore taken as the main load in DSR. Through the integrated optimization scheme in this thesis, the load management of HVAC can be attained by combining optimal controls of CHP, electricity storage system (ESS) and thermal storage system (TSS).

After S.E. Hub optimal operation strategies are proposed, controllable components, such as CHP, can be optimally re-designed following the strategies for better operation performance or investment reduction. This can be supported by an optimization with the aim to find the optimal size of CHP considering the building owner/designer's preference with respect to saving operational cost and reducing CHP investment payback period.

1.3. Aims and Objectives

The power grid will be able to save a huge amount of energy with improved energy efficiency of each S.E. Hub. Therefore, it is crucial to optimize operation of S.E. Hubs. This thesis aims to integrate optimal operation control of CHP and energy storage with DSR to achieve the overall cost savings of an S.E. Hub.

The following are the three main objectives of this thesis:

i. The first objective is to reduce the S.E. Hub operational cost through dynamically changing the thermal and power output ratio of the CHP so that the overall cost can be minimized. Most of the CHPs are operated with a fixed ratio of thermal to power output, although the thermal and electrical load demand always change with time, therefore, this fixed thermal/power ratio is often not the most economical way to operate CHP. This first objective will be achieved through optimally control the CHP along with other S.E. Hub energy facilities under price-based DSR.

ii. The second objective is to integrate controllable buffer components, i.e., ESS and TSS, to further optimize the economic performance of CHP and extend the scale of the S.E. Hub for system flexibility improvement. This is because that an S. E. Hub without energy storage facilities has to meet the load demand in real time, which may cause higher operating cost under peak tariff period and also cause unnecessary burden to the power grid. Furthermore, the storage of surplus thermal energy from CHP when supply is greater than demand can also make CHP run at a high energy efficiency operating point. Therefore, inclusion of ESS and TSS will further reduce the overall operating cost of an S.E. Hub.

iii. The third objective is to optimally design the size of CHP regarding investing a CHP unit in building retrofit. After obtaining the optimal operation strategies for an S.E. Hub, the optimal sizing of CHP will be studied so as to invest and install a properly sized CHP within a given budget for cost-saving purpose. The operational cost after CHP installation will be calculated by considering the building operated under the proposed strategy, which combines dynamic control of CHP operation with DSR. The optimization design will prioritize building owner/designer's preference on saving operational cost and reducing CHP investment payback period.

1.4. Novelty of Research

The main contributions of this thesis with novelties are summarized as follows.

i. A modeling framework of an S.E. Hub for a smart building system has been established in Chapter 4, based on which the operational cost of the overall system is minimized through the demand side management and the optimal selection of CHP's power-heat generation ratio. In this optimization scheme, efficient CHP operation and HVAC scheduling are determined under a TOU tariff. It is the first time in literature to minimize an SEH operational cost through CHP power and heat split ratio control cooperating with DSR simultaneously.

ii. The controllable energy storage systems (ESS and TSS) are implemented to further improve the effectiveness of the proposed optimization scheme in Chapter 5. The most suitable storage capacities and charging/discharging power flows of ESS and TSS are discussed to enhance the optimization effect. Furthermore, two methods of ESS and TSS modeling are explored to ensure the optimization scheme practical.

iii. A multi-factors optimization model has been established to find the optimal size of CHP for investment decision in Chapter 6. The obtained two objectives are to minimize the building operational cost and the CHP investment payback period, respectively. Depending on the preference of the building owner/designer with respect to the two objectives, the optimal solution of CHP capacity can be obtained through the proposed model.

1.5. Outline of Thesis

This thesis is arranged as follows.

Chapter 2 provides literature reviews on the technologies of key components, such as CHP, ESS and TSS, the applications of DSR, optimal operational strategies in S.E. Hubs and microgrids, and the optimal design for component investment.

Chapter 3 presents general methodologies of S.E. Hub energy cost minimization including CHP hourly dynamic control, appliances load management and optimal design for high-efficiency energy components investment.

Chapter 4 proposes an energy cost minimization model, which combines the dynamic control of CHP with DSR, for an S.E. Hub. Since the HVAC system consumes the majority of the electricity required at the building, the corresponding HVAC load management strategy is developed to verify the feasibility of the DSR. The optimization of S.E. Hub operation under a TOU tariff considers factors such as the capacity and constraints within CHP operation, the operating condition of HVAC, and the range of indoor air temperature. Efficient CHP operation and optimal HVAC scheduling are determined through optimization. The effects of the proposed optimization strategies are verified in case studies by comparing with two existing S.E. Hub operational strategies, which consider CHP optimal control and DSR separately.

Chapter 5 develops an expanded energy cost minimization model for an S.E. Hub with the deployment of controllable storage systems. ESS and TSS are designed as on/off components with fixed power level options. The power and heat split ratio of CHP, scheduling of HVAC, and charging/discharging of energy storage systems are determined through the optimization solution. Technically available SOC ranges of ESS and TSS, and state of charge (SOC) and depth of discharge (DOD) related degradations of ESS are taken into consideration in the optimization problem. Besides, different capacity sizes and charging/discharging power levels of TSS and ESS are tested for a better optimization effect. Moreover, two methods of ESS and TSS modeling are explored in Chapter 5. The first method, without consideration of charging/discharging efficiency, simplifies the calculation whereas performances of ESS and TSS are relatively amplified. Charging/discharging efficiencies are considered in the second method thus improved the modeling accuracy.

Chapter 6 proposes an optimization method to determine the optimal size of CHP for building retrofit. The investment budget, maximal payback period and the preference of the building owner/designer with respect to these two objectives are considered in the optimization model design. The optimization problem has been solved by combing the two objectives into a single-objective function using weighting factors. The new building system after CHP installation is considered to operate with the operational strategy proposed in Chapter 4 for operational cost minimization, which combines the CHP dynamic control with HVAC scheduling. The energy saving after CHP installation is compared to a benchmark system, which is also considered to operate with HVAC load management for a conservative estimation on CHP investment payback period. Different building owner/designer's intentions with different optimal CHP sizes are discussed in the case study.

Chapter 7 draws conclusions and gives perspectives of future research.

The appendix delivers a short history of CHP, detailed reviews of CHP and ESS technologies. The popular types of CHP generation, such as CCGT, Stirling engine, microturbine system and fuel cell system, are introduced. Suitable types of generation for a small-scale CHP system are recommended. The operating methods, advantages and disadvantages of ESS technologies are discussed.

1.6. Publications

[1] H. Qi, H. Yue, J. Zhang, and S. Lo, "Optimal Control of CHP Plant Integrated with Load Management on HVAC System in Microgrid," in *2019 IEEE 15th International Conference on Control and Automation (ICCA)*, 16-19 July 2019 2019, pp. 1073-1078, doi: https://doi.org/10.1109/ICCA.2019.8899972. (Chapter 4)

[2] H. Qi, H. Yue, J. Zhang, and S. Lo, " Optimization of a Smart Energy Hub through Integration of Combined Heat and Power, Energy Storage and Demand Side Response," submitted to *Applied Energy*. (under review, Ms. Ref. No. APEN-D-20-07243) (Chapters 4 and 5)

[3] W. Zheng, P. Crossley, B. Xu, and H. Qi, "Transient stability of a distribution subsystem during fault-initiated switching to islanded operation," *International Journal of Electrical Power & Energy Systems*, vol. 97, pp. 418-427, 2018/04/01/ 2018, doi: https://doi.org/10.1016/j.ijepes.2017.11.024.

2. LITTERATURE REVIEW

In this Chapter, the relevant literature on CHP system, energy storage system, DSR applications and optimal operation and design of S.E. Hubs are discussed.

In Section 2.1, the technologies of CHP, ESS and TSS are reviewed, where the focus is on advantages and disadvantages of those technologies for applications in S.E. Hubs. Section 2.2 delivers the applications of different DSR programs in power systems, along with microgrids optimization models including both CHP units and DSR. Section 2.3 reviews optimal operational control of S.E. Hubs with CHP systems or energy storage systems. In Section 2.4, optimal design of S.E. Hubs has been reviewed to facilitate the investigation of CHP optimal sizing for S.E. Hubs. A brief summary is given in Section 2.5.

2.1. CHP and Energy Storage Systems in S.E. Hubs

2.1.1. CHP technologies and economic analysis

CHP is a power generation system with capability of using waste heat. There are many approaches to generate heat in various CHP systems [48], which can be categorized as three types: gas liquefaction from high-pressure steam to low-pressure hot water, heat conduction from hot gas or heated air, absorption from a refrigeration process. Different operating mechanisms and steam turbines such as combined cycle gas and steam turbines (CCGT), gas turbines, reciprocation engines, microturbines, fuel cells, and the Stirling engine are used in CHP systems. Different CHP generation types also have different output power ranges, power efficiency ranges, and peak energy utilization rates, as shown in Table 2.1. The requirement of thermal demand is the key factor to choose a suitable type of CHP; for example, a mill requiring steam should be best served by a gas turbine CHP. Additionally, the power range and heat to

power ratio also need to be considered to match applications. The output of a CHP plant is expected to match the power and heat demands.

Table 2.1 Overall CHP generation types [49]

CHP Generation Types	Power Range (MW)	Power Efficiency Range (%)	Peak Energy Utilization Rate (%)
CCGT	20-600	30-55	85
Gas Turbine	2-500	20-45	80
Steam Turbine	0.5-100	15-40	75
Reciprocating Engine	0.005-10	25-30	85
Micro-turbine	0.03-0.25	25-35	75
Fuel Cell	0.005-1	30-40	75
Stirling Engine	0.001-0.05	10-25	80

The information in Table 2.1 comes from historical data, with the development of various CHP technologies, each CHP technology may have flexible power ranges and higher power efficiency. For example, a gas turbine CHP system already has 100-500 kW power levels application for residential and commercial buildings ADDIN EN.CITE <EndNote><Cite><RecNum>0</RecNum><IDText>Sokratherm</IDText><DisplayText>[50]</DisplayText><record><urls><related-urls><url>https://www.sokratherm.de/en/compact-chp-units/compact-chp-units-of-the-500-kw-class/</url></related-urls></urls><titles><title>Sokratherm</title></titles><pages>500kW class CHP production</pages><number>12 April</number><added-date format="utc">1586696866</added-date><ref-type name="Web Page">12</ref-type><rec-number>301</rec-number><last-updated-date format="utc">1586697066</last-updated-date><volume>2020</volume></record></Cite></EndNote>[50]. The S.E. Hub

under study is based on a community sized smart building whose peak power value is around 450-500kW. Considering both power efficiency and construction cost, a 500 kW gas turbine CHP is a suitable choice other than a steam turbine CHP or a reciprocation engine CHP. More details of different CHP types are discussed in Appendix.

The role of CHP unit in an S.E. Hub is not only a conversion component, but also a key player for energy cost reduction. The economic analysis of CHP is directly related to electricity price, fuel price and the respective efficiency of output power and heat. The relationship among these factors and their efficiencies are described by a metric named “spark spread”, which is used to indicate the gross income of one-unit electricity sold after purchasing the necessary fuel.

The spark gap is another metric used to measure the competitiveness of a CHP, which is the price gap between electricity and gas price [51]. A huge difference between electricity price and gas price at any time point indicates the strong competitiveness of CHP. In the electricity market, high electricity demand leads to high electricity prices where a larger spark gap will be generated. To date, electricity price in the UK has been shifting between £0.13 and £0.16 per kWh [52], with gas price fluctuating around £0.028 per kWh [52]. This large spark gap indicates the economic advantage of employing a CHP system in UK energy market. However, a spread gap does not include all necessary data of a CHP system, such as data about levies or levy exemptions, operational expenses, energy distribution, ability to utilize waste heat, emissions trading permits, etc.

CHP generation tends to be located in buildings or at the community level [53], such as in hotels, hospitals, university campuses, and office buildings [35]. From an economic perspective, distributed CHP generation provides many advantages in

comparison to traditional centralized electricity generation. These advantages have been summarized in Table 2.2.

Table 2.2 Advantages of distributed CHP generation

Advantages	Description
Enable to utilize waste heat	CHP enables waste thermal energy to be utilized onsite or nearby for residents heating or other productive purposes.
Easy installation	Contrary to large scale centralized electrical generation, distributed CHP is modular and can be installed quickly.
Carbon saving	As electricity is generated onsite, a huge amount of carbon is saved due to reduced losses. Moreover, the micro CHP system is expected to meet up to 50% of a home's electricity needs.
Reduced transmission and distribution losses	Near the point of demand leads to less transmission and distribution losses.
Diversity of energy sources	Many types of primary fuels can be used for distributed generation, such as wood chips, biomass, etc.

However, there are still some disadvantages and challenges of distributed CHP generation. The main disadvantage is that most CHP systems are currently fueled by natural gas. Unless biogas is widely adopted as the main energy source, CHP cannot be seen as a true sustainable generation. The other disadvantage is that CHP systems are only suitable for sites which have both electricity and thermal heat demands. And the high installation cost of CHP makes a hard decision for CHP investment.

2.1.2. ESS technologies and applications in S.E. Hubs

According to the Low Carbon Transition Plan, the UK government has guaranteed that over 30% of total electricity and 15% of total energy will be generated with renewable sources by 2020 [54]. This objective has already been achieved;

however, the increase in renewable energy generation is accompanied by many problems. For example, most renewable generations are affected by weather conditions, which may cause intermittent dispatch. Unstable electricity generation increases the difficulty of grid network management [54]. Under these challenges, ESS is considered as an effective way to support the balance of electricity supply and demand in a highly renewable generation penetrated power grid.

Selection of suitable ESS technologies poses a challenge for grid applications depending on a series of factors such as network capacity and geographical environment [55]. For instance, as per the 2018 UK *Hydropower Status Report* [56], the UK power network already has a total hydropower installed capacity of over 4600 MW, including 2744 MW of pumped storage. However, the potential of pumped hydroelectric storage scheme is considered to be restricted in UK [57]. Some of the pumped hydroelectric storage projects were initially developed to support coal and nuclear generation. After those coal generation is replaced by renewable generation, many pumped hydroelectric storages in UK have not been operating on daily cycles [56]. Thus, the selection of ESS needs comprehensive consideration and long-term planning.

The most widely used method to categorize ESS technologies is based on the form of energy stored in ESS [58, 59], as shown in Table 2.3.

Table 2.3 Classification of ESS technologies

ESS Types	Specific Technologies
Mechanical ESS	Pumped Hydroelectric Storage Compressed Air Energy Storage Flywheel Energy Storage
Electrochemical ESS	Secondary Battery (Lead-acid/NaS/Lithium-ion) Flow Battery (Redox flow/Hybrid flow)
Electrical ESS	Capacitor/Supercapacitor Superconducting Magnetic Energy Storage
Thermochemical ESS	Solar Fuels

Chemical ESS	Hydrogen (Fuel cell)

Details of ESS technologies and relevant research studies have been provided in Appendix (Section 8.2). The ESS in this work employ electrochemical batteries for a commercial building-based S.E. Hub. Commercially-available sodium-sulfur (NaS) batteries, relatively low-cost redox-flow batteries, and lithium-ion batteries are usually selected for S.E. Hub applications [60], in which lithium-ion batteries are most popular and have the highest storage efficiency [61]. A Li-ion battery is comprised of a cathode (positive electrode), an anode (negative electrode), and an electrolyte. Many materials can be used for electrodes in a lithium-ion battery. The most commonly selected material for the cathode and anode is lithium cobalt oxide and graphite respectively. Lithium-ion batteries have been used as ESS in this work. When a lithium-ion battery is charging, the lithium ions move from the cathode to the anode and absorb electrons from the outside electricity. Contrarily, in the discharging status, electrons are transmitted to outside loads, and lithium ions move back towards the cathode.

- Advantages of lithium-ion batteries

Compared to other rechargeable batteries, lithium-ion batteries have one of the highest energy densities, which can reach $100\text{-}265 Wh/kg$ or $250\text{-}670 Wh/L$ [62]. A Lithium-ion battery cell can drive up to 3.6 volts, thrice more than a Ni-Cd (Nickel-cadmium) battery cell or a Ni-MH (Nickel-metal hydride) battery cell. Moreover, lithium-ion batteries have a relatively low maintenance cost and do not need to schedule cycling to maintain their life. Their self-discharging rate is approximately 1.5%-2% [62], which is lower than other battery technologies. Most importantly, lithium-ion batteries do not contain toxic cadmium; it is easier to be disposed of than Ni-Cd batteries. Accompanied with the development of renewable generations, lithium-ion batteries possess the potential to be applied in small-scale renewable generations in a microgrid.

- Disadvantages of lithium-ion battery:

Lithium-ion batteries still have a number of shortcomings, especially in terms of safety. They tend to become overheat and suffer damage at a high voltage, which may result in thermal runaway and combustion. Thus, a safety mechanism is required to limit lithium-ion batteries' voltage and internal pressures. Furthermore, lithium-ion batteries are characterized by the problem of ageing, which may lead to loss of capacity or operation failure over several years. Another factor limiting the wide adoption of lithium-ion batteries is their expensive cost, it is around £15000/100 kWh [63] which is 40% higher than Ni-Cd's [62].

2.1.3. Necessity of TSS in S.E. Hubs

In the future, energy systems should be designed to utilize various renewable energy resources, waste energy, and effective techniques, as mentioned in many studies [64, 65]. To improve the energy efficiency for future power grid requirements, it is crucial to install and enhance district heating and cooling, where both systems have played a critical role in European energy systems due to the possibility of combining the following options [66, 67]:

- Renewable resources such as solar energy or biomass [68-70]
- Pumps for air and groundwater heat [71, 72]
- Waste heating collected from industrial or energy plants [73-75]
- Cogeneration plants to produce both electricity and heat (e.g. CHP) [76]
- Traditional plants such as boiler systems [77]
- Heat created by prosumers linked to the system [78]

It should be noted that there are two major gaps in district heating and cooling systems [79]. The first gap is the dynamic unbalance between demand and supply sides caused by time difference between them. For instance, this can be caused by the

intermittent characteristics and dynamic feature of energy produced by solar resources or economic reasons due to variations in the daily price of thermal energy. The second gap is the great loss of heat during the thermal power transmission from production plants to consumers.

The existence of a gap between production and consumption may result in the waste of thermal energy. TSS is integrated into district heating and cooling systems to better bridge the gap between demand and supply. This integration can optimize both the flexibility and performance of district heating and cooling systems, and improve the smart combination of renewable energy sources and thermal systems.

TSS has a storage medium (adopted to reserve thermal energy for heating and cooling), and the energy stored can be used later. The use of TSS systems in commercial buildings can save energy by 7.8% on an annual basis in the EU [79]. Meanwhile, it can also reduce CO2 emissions by 5.5% [79]. In general, the adoption of TSS can reduce 1.4 million GWh of energy on an annual basis in Europe [79]. When integrated with a thermal system, TSS can increase the flexibility of an energy hub [80, 81].

In an ideal situation, demand should be kept stable to make full use of the capacity of thermal plants. However, in winter time, the daily demand for heating is higher. Similarly, in summer, the requirement for cooling is high. Additionally, the demand of heating and cooling are changing during the day based on the behaviors of end-uses, types of heating devices, or regulatory facilities of an energy hub. Therefore, the long-run or short-run TSS can be used to actively balance the supply and demand in an S.E. Hub. Another critical feature of TSS is associated with thermal production, particularly when heat is wasted in an industrial process. Many thermal production sources generate a great surplus, which can be stored conveniently. Advantages and disadvantages of TSS application in S.E. Hubs are summarized in the following.

- Benefits of TSS can be found in technical, economic and environmental aspects [82].
  - Flexibility can be increased with a reservation system which also influences the design of CHP. It can especially reduce the heat production of CHP at the peak heat demand, which implies that the capacity of the CHP can be optimized for construction cost saving [83].
  - When connected to the major line of a district heating and cooling system, smaller pipelines can be used for energy distribution [84].
  - The stored heat can relieve over demand.
  - Time-varying management can boost overall performance of an S.E. Hub.
  - The management and operation of TSS can reduce the impact of thermal heat demand on CHP operation, and enhance CHP power generation when the electricity price is high [85, 86].
  - Reducing the intermittent characteristics of renewable energy sources can provide microgrids with better flexibility in choosing different energy sources.
  - Operational costs can be reduced through storage, such as costs for pumping systems, as flow rates can be reduced in a certain network during the peak time. Pumping cost cannot be ignored, which takes around 1% of primary energy use, particularly in large district heating networks, as seen in [87, 88].
  - Installing TSS can prevent the integration of a pressurization vessel under circumstances [89].
  - Users can save money with a flexible heat request, as TSS will allow them to change their peak-time load.

- Disadvantages of TSS
  - TSS entails non-negligible installation costs and investment.

- A space is needed for TSS - a typical issue for all storage-related aspects at different levels.
- Significant thermal losses throughout the storage process are an important issue to consider in energy conservation, thus, further research is required.
- New challenges will arise in terms of system design and connection planning.

The TSS can be divided into short-run and long-run storages [19, 90]. The first refers to storage used to satisfy daily demand at the peak time with a duration varying from a few hours to a day. A long-run TSS ensures long-term energy storage from several weeks to months. In an S.E. Hub, short-run TSS can extend technological limits and strengthen the advantages of some components such as a CHP system. As CHP-district heating systems are the most widely used technology in an S.E. Hub, it is very important to analyze the potential installation of a TSS [91]. Designed with both CHP and boiler plants, TSS can enhance system flexibility and bring profits from sale of electricity and reduction in CHP installation capacity [92]. In plants supported by CHP, heat production is based on the generation of electricity while heat storage reduces the impact of thermal demand and enables full-power operation during the peak electricity price. In this regard, TSS can save operational energy cost and ensure a CHP system to achieve optimal operation [93]. Furthermore in [94], integrating fuel cells with TSS in district heating systems can increase energy efficiency by up to 350% while reducing CO2 emission by half.

In this thesis, a short-run TSS is employed to enhance the S.E. Hub's flexibility under a TOU tariff. The TSS is integrated with a CHP unit to enable the best power-heat generation ratio for CHP so as to minimize the overall operational energy cost.

2.2. DSR Applications in S.E. Hubs

Most DSR schemes include cost saving (price-based DSR) or revenue generating (incentive-based DSR) options for residential consumers. The DSR programs can be

divided into two types: incentive-based DSR and price-based DSR. These two DSR types complement each other and can be employed in the same system, therefore enabling a wide range of customers to engage in the DSR program. Additionally, these systems can be adopted in energy, capacity, and ancillary markets on the basis of a regulatory system. Table 2.4 summarizes different DSR types. For this work, the price-based DSR under a TOU tariff is selected.

Table 2.4 DSR program classification and description [95]

Incentive Types	Incentive -based	Price-based	Explanation
Direct Load Control	√		Participants are controlled by the system operator to a certain extent, but they receive payment in return.
Load Curtail	√		Incentives are used to adjust the load or need for energy.
Demand Building	√		Load reduction bids are submitted to the market.
Capacity Market	√		Participants can bid in the capacity market to change their load on request.
Ancillary Market	√		Participants in an ancillary market reduce their load on request, but usually for a short period of time.
TOU Tariffs		√	Electricity rates are solid in response to daily changes.
Critical Peak Pricing		√	It is used to avoid the electricity usage during a peak electricity price period. However, this is not popular in the market and operationally depends on time.
Real Time Pricing		√	This entails daily changes in electricity prices, in accordance with the wholesale market price, marginal price or other pricing schemes.

To allow wide applications of DSR programs, challenges need to be addressed, such as controlling and optimizing market demand with effective price indicators, constructing a favorable market situation and setting up profitable business models

[96]. Moreover, there are barriers such as regulation, policy issues, and requirements for infrastructure need to be overcome [25]. Additionally, issues such as limited user experience and uncertainty of DSR programs are still in place due to the fact that much of the current work is still confined by certain aspects.

2.2.1. Price-based DSR

The price-based DSR allows participants to change their load on a voluntary basis in a manual or automatic manner, as a response to the price signals in electricity market. This technology activates a large amount of industrial, commercial and residential end-users, which can participate individually or through aggregators. With the development of information communication technologies, the range of appliances has been expanded to be used in DSR. However, at the time of saving cost through price-based DSR, the convenience and experience of end-users need to be carefully protected.

A typical example for price-based DSR was presented in [97]. This paper considers residential appliances such as lights, dishwasher, bread maker, swimming pool pump, electric water heater, TV, DVD player, decoder, clothes drier and washing machine, and also considers the operation relationship, for example, clothes drier must follow the washing machine, TV and decoder must operate at the same time. The electricity storage system is implemented to store electricity at the off-peak time and to discharge at the peak time. All the energy cost reduction in [97] is based on the electrical appliances' load management. Safdarian et al. [98] design real time operating models for electric water heater and HVAC considering DSR. Their models consider various factors such as the internal water circulation inside the electric water heater, ambient temperature of HVAC, resident comfortable level, and also switching actions of electric water heater and HVAC. The power levels of the electric water heater and HVAC are modeled as binary variables, which are similar to the modeling approach

in this thesis. Setlhaolo et al. [36] establish a residential operational cost minimization model through the scheduling of typical home appliances. In their model, the consumers can shift their consumption in response to the varying prices by choosing an inconvenience level in the DSR program.

Caprino et al. [99] present a peak shaving approach through applying price-based DSR to aggregators of electricity users. The authors mainly focus on modeling and management of household appliances. The predicable reduction of the peak load was achieved while guaranteeing the users' comfort. Mohsenian-Rad et al. [100] apply game theory and formulate an energy cost scheduling game for a group of DSR participants. The authors assume that each user simply applies his/her best load management strategy under real-time energy price. All consumers are served by a single utility company; therefore, the utility company can change the pricing tariffs to influence the energy usage for energy generation optimization.

In [101], an automated DSR program for residential appliances is proposed to reduce the electricity bill under the dynamic electricity price while fulfilling comfort constraints. Juan et al. [102] propose a DSR scheme for smart buildings to balance the customers' requirements and energy cost by integrating a novel cost structure that encourages load shifting. Customer response is studied considering demand price elasticity and historical response curve in [103, 104] in order to achieve better performance under the TOU based DSR programs. For electricity retailers, risk management has been discussed in [105] considering the difference between time-varying wholesale purchase price and the fixed retail selling price. By comparing several DSR programs based on TOU, critical peak pricing and peal time pricing, the effectiveness of DSR programs on economic savings and load shifting is discussed in [106].

2.2.2. Incentive-based DSR

The incentive-based DSR requires participants to shift their load patterns on request and then obtain direct payment. The industrial and commercial users can participate individually or through aggregators, where residential users usually only can participate through aggregators. Increase-based DSR can create short term response for grid balancing, reduce the peak electricity usage and improve the grid reliability. This technology highly depends on the policy of electricity market, thus the main challenge for operators is to control and optimize market demand with effective price indicators.

Wang et al. [107] analyze the effectiveness of incentive-based DSR through the data from large-scale DSR trials and matching questionnaires. They combine trial data and survey data together, which provides important references with respect to policies implemented and participants' attributes. Three incentive-based DSR programs with four different incentives are discussed in [108], in which the consumers' willingness and interest among different incentive-based DSR programs are analyzed. A suitable incentive-based DSR program for a typical subsidized market is obtained considering the consumers' preference and a linear relationship between incentivization and load reduction. Aalami et al. [109] develop a non-linear model of incentive-based DSR for a real-world power system, based on the demand elasticity on price and benefit function of consumers. The authors provide network operators references about the effect of incentives and the economic performance of the power system. Similar references about the incentives policy determination for network operators are discussed in [110], in which the aim is to minimize generators' fuel cost while considering the emission cost.

An incentive-based DSR scheme for a microgrid containing different types of generations is proposed in [111] to generate optimal energy dispatch strategies for

cost minimization. In [112], a dynamic pricing-based buy-back scheme is used to encourage end users to generate more renewable energy, thereby enhance the energy efficiency of a smart grid. Similar direct load control-based DSR schemes are proposed in order to reduce the peak system load [113, 114], save operational cost [115, 116], and optimize customer satisfaction [117]. The elastic price of demand is achieved in [118] through a scheduling model of smart home energy management. For larger consumers, such as electricity retailers, a linear bidding function based DSR program is proposed in [119] to improve social welfare.

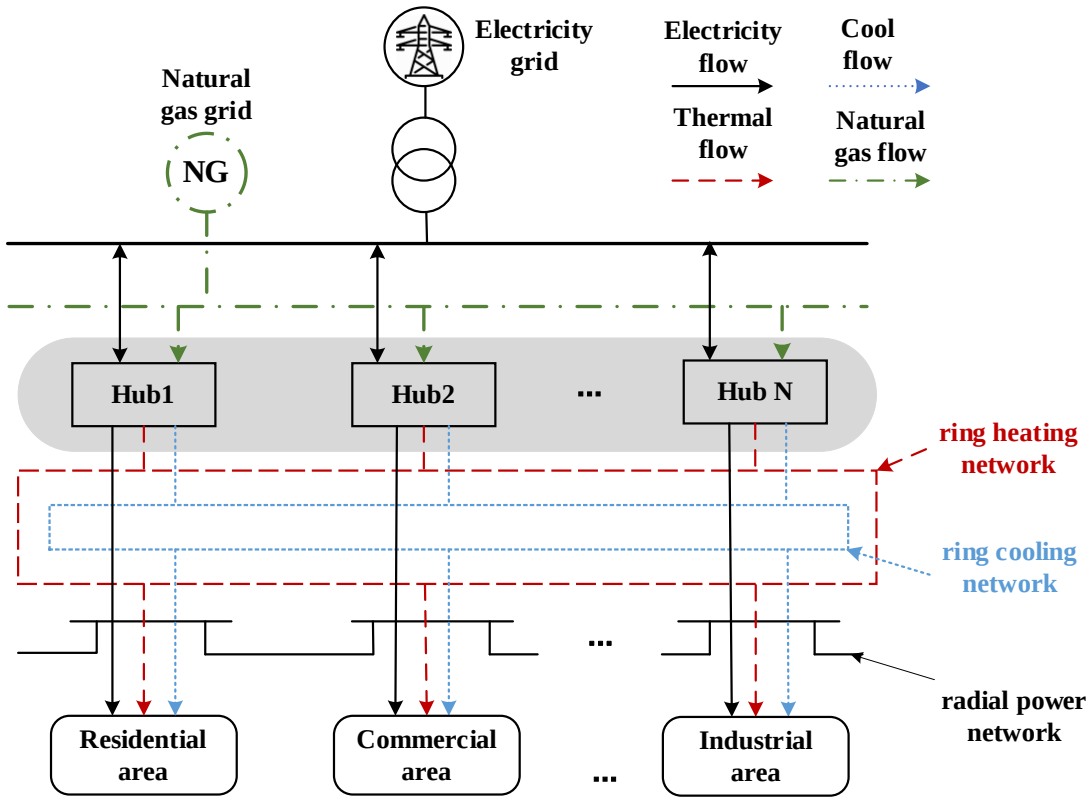

Fig. 2.1 A typical microgrid comprising multi-S.E. Hubs (taken from [120])

The methodologies in the above references can also be generalized to study multiple S.E. Hubs as described in Fig. 2.1, which has significant applications for distribution operators or load aggregators to implement price-based or incentive-based DR within a microgrid optimization.

2.3. Optimal Operation Control of S.E. Hubs

An S.E. Hub is established based on a commercial building system in this thesis. According to [121], around 40% of the energy consumption is consumed by buildings, with half of it on commercial buildings, resulting in one-third of total greenhouse gas emissions. Therefore, the energy efficiency of commercial buildings has great potential to be improved in order to save energy, reduce buildings' energy cost and reduce pollution emissions. Power and heat at commercial buildings are traditionally provided by the power grid and large boilers, respectively. However, with the development of distributed generation technologies and the increase of electricity prices, CHP systems become preferred solutions in commercial buildings. A CHP unit can be operated together with renewable energy sources and energy storage systems to improve overall energy performance. The operational optimization of such systems has great potential for cost reducing and energy saving for an S.E. Hub. In the following, the optimal operations of S.E. Hubs are reviewed on CHP system and energy storage system, respectively.

2.3.1. Optimal operation of CHP system

As a popular energy conversion system in S.E. Hubs, CHP generation can be controlled by dynamically optimizing its power and heat split ratio to improve the energy efficiency and economic performance of S.E. Hubs. A general evaluation of a CHP in a commercial building is proposed in [122] from the aspects of operation cost and carbon emission. Two non-convex operation regions with four or five operating points (based on the power to heat ratio) of a CHP are defined in [123]. The operation of different types of CHPs under such non-convex operation regions has been discussed in [124], and a short-term optimal scheduling strategy has been proposed to reduce the operational cost.

It has been pointed out in [125] that the CHP operating points highly affect its energy efficiency and economic performance. Meanwhile, the flexible operation strategies under different external conditions, such as varying electricity prices and buyback prices, of a CHP enhance the economic benefits [126, 127]. Several operation modes have been discussed in [128], including different lengths of daily operation time and intervals. However, the CHP was only modeled with fixed power and heat ratios. Three CHP operation modes known as heat-driven, electricity- driven and cost- driven modes have been defined in [129]. The economic performances of these operation modes have been evaluated where the results show that the cost-driven mode can improve the economic performance.

Different operation strategies of a CHP system integrating solar thermal system in a commercial building are proposed and compared in [130] regarding to the CHP's economic performance, where different demand types have also been considered. Xie et al. propose a CHP operational optimization model in [131], taking the real heat, electricity and gas prices into account to enhance the CHP economic performance. Their case studies reveal that the power to heat ratio should be regulated according to the time day and the energy prices, in order to pursue higher profits. However, the CHP operation in [131] is simply modeled by different loading levels with corresponding power-heat ratios. The real-time CHP control based on varying demands and energy prices is not achieved.

On another aspect, the greenhouse gas emission regarding to different CHP operation strategies has been considered by Peacock et al. in [132], where the results show that the great emission reduction can be achieved by proper operation strategies such as minimizing the thermal surplus generated on 'warm' days in a Stirling engine based CHP. The carbon emission has also been considered in [133] together with the operational cost, forming a multi-objective operational optimization strategy of a CHP. With the S.E. Hub and CHP operational optimization strategy, £110 million can be

saved in a time frame of 20 years, based on the energy consumption data of University of Bath [133].

However, the CHP operational optimization are rarely considered with DSR technology, and no previous work focuses on the CHP heat-power split ratio control together with load management of a HVAC system under a TOU tariff. Even in some microgrid models including both CHP and DSR technologies, CHP is considered as a generator with fixed heat-power ratio. In this thesis, the S.E. Hub's energy cost can be reduced by enhancing CHP economic performance along with regulating HVAC load optimally.

2.3.2. Optimal operation of energy storage systems

To cope with energy demand and environmental challenges, renewable energy, such as wind energy and solar energy, has been integrated into the power distribution network gradually [134, 135]. However, the inherent characteristic of such renewable generations makes their reliability highly affected by the natural conditions (e.g. weather and the time of the day). Therefore, the renewable generations should be implemented along with reliable distributed generators, such as CHPs, and energy storage systems [136, 137], in order to assure their power supply reliability. More importantly, the implementation of storage systems in an S.E. Hub can greatly improve the overall system energy efficiency with operational flexibility [138, 139], and delivers better economic performance to the owners [140].

Nowadays, the most mature and widely used energy storage system is battery energy storage system [141-143], such as lithium-ion battery, which is also the storage system used in this thesis. The proper control and operation of storage systems in an S.E. Hub provide significant potential for energy efficient enhancement and economic performance improvement.

A wide range of studies have been focused on optimal operation of battery ESS in building systems. Generally, the storage system enables building owners to store energy during lower electricity price periods and discharge during high electricity price periods. In this way, the overall energy cost can be reduced [144]. Oudalov et al. propose an optimal operational strategy based on dynamic programming for a battery ESS in the peak load shifting process in order to achieve the operational cost minimization [145]. The optimal sizing problem of the battery ESS also has been considered in literature to minimize the investment cost while fulfilling the demand.

In [146], the next day electricity price is forecasted to optimize the battery ESS operation, aiming to improve the overall economic performance. Proper scheduling of battery ESS has been determined and longer lifetime (reduced investment cost) of batteries is achieved [146]. In [147], an optimal scheduling of storage system has been proposed to reduce the energy cost and minimize the power loss considering the batteries' charging/discharging efficiency. Similar work has been done in [148], where the energy storage system is composed of both battery ESS and TSS.

In [149], energy storage constraints such as the charging/discharging rates of electrical and thermal energy storage, and the heat loss of thermal energy storage, are considered. The thermal energy storage system is usually implemented along with CHPs to reduce the heat loss. It has also been considered in an S.E. Hub to reduce the energy cost of the HVAC system, which consumes nearly 50% of the total energy in a commercial building [150]. Thermal energy storage also participates in day-ahead energy dispatch scheduling program in a building [151]. The energy consumption is predicted one day ahead, and the stored energy is scheduled to release for the heating demand during the high electricity/gas price period. The effectiveness of the proposed optimal operation strategy is significantly affected by the predicted next-day thermal load.

Simple battery degradation models are used in [152-155] for modeling of the energy storage systems and optimization of their operation. The battery degradation is often considered as a fixed cost per kWh while evaluating the economic performance of a storage system. However, as discussed in [156], the actual lifetime of a battery is largely affected by the DOD and SOC, which are the significant factors need to be considered when optimizing the storage system operation. Therefore, it is necessary to apply more accurate battery degradation models in S.E. Hub studies. In [157, 158], battery ESS cost function and optimal control are formulated considering battery degradation as a function of DOD, charge rate and SOC. It has been indicated in [159] that the lifetime of a battery highly depends on its operations, thus an optimal operation strategy has been proposed to find the balance between the building operational cost and the batteries' lifetime. The results in [155] show that 40% of the battery degradation cost and 8.5% to 16% of the building overall operational cost can be saved with a good balance point.

According to the research, an optimal operational scheme of ESS and TSS can greatly improve the overall S.E. Hub energy efficiency. However, rare research combines the optimal controls of CHP and storage system under a TOU tariff and varying demands. In this thesis, the optimal controls of ESS and TSS are integrated with CHP dynamic heat-power split ratio control and HVAC load management to achieve the overall S.E. Hub operational cost saving.

2.4. Optimal Design of S.E. Hubs

As mentioned above that the energy consumed by buildings around the world shares 40% of the total energy [160], it is worthwhile to invest in the building energy efficiency improvement. Multiple actions can be taken such as energy efficient lighting and heating, advanced controller for HVAC, on-site energy production components improvement, and energy storage systems improvement [161-163]. Since CHP is the

main object of study in this thesis, the relevant sizing and investment studies on CHP are reviewed in this section.

The purpose of installing CHPs in commercial buildings is to improve energy efficiency and reduce operational cost, however, unreasonable size of the CHP units will not achieve such a target, and sometimes it may cause unnecessary investment and operational costs. In [164], a maximum rectangle method, which is usually used in finding proper capacity of generators [165], is used to find the optimal size of CHP in a building. The load distribution curve (demands versus number of sampling points) is drawn firstly using the building's load data sampled every minute through a year. Then the width of the rectangle with the largest area under the load distribution curve is considered as the optimal capacity for the given load data. The same method has been used in [166] to determine the CHP size and several case studies have been carried out to evaluate its effectiveness. The maximum rectangle method aims to find the most efficient CHP capacity with the purpose to fulfill the demand without considering the investment cost.

Another method based on linear programming of CHP operation model has been used in [167, 168], and the purpose of optimal sizing of CHP is included in the model in order to determine the sufficient capacity to fulfill the demand and minimize the overall operational and investment cost. The balance between meeting demand and minimizing cost affects the results significantly, and the result depends on the owner's preferences among these two objectives. Similar work has been reported in [169] using non-linear programming, where the sizing of CHP is affected by investment cost and operational strategies. Another economic factor known as net present value has been used for CHP optimal sizing [170], in which the increase of electricity price and depreciation of equipment are taken into consideration when optimizing the CHP size for commercial and office buildings.

The payback period has been considered for the CHP capacity design in [171]. The proposed method is used to evaluate the optimal capacities of a micro turbine-based CHP unit for buildings with different power and thermal demand. Kim et al. considered the relationship between the efficiency and size of CHP in [172]. With improved efficiency by CHP size optimization, the economic performance can be enhanced.

Another significant factor, which is carbon emission, has been discussed in designing the CHP capacities [173]. A more comprehensive evaluation of CHP sizing considering multiple objectives such as operational cost, primary energy consumption and the pollution emission has been proposed in [174]. Liu et al. consider the total annual cost of the entire S.E. Hub while optimizing the CHP size [175].

The expensive installation cost leads to a hard decision for CHP investment. Previous researchers provide different models to find a suitable CHP size depending on various considerations. However, there is no method optimally determining the CHP capacity by both considering building's energy cost saving and payback period reduction. In this thesis, the newly installed CHP system operates along with HVAC load management to achieve building operational cost minimization.

2.5.Summary

A literature review is given in this chapter on optimal operation control of S.E. Hubs in building systems with CHP and DSR. Firstly, key components in S.E. Hubs are introduced including CHP, ESS and TSS in Section 2.1, followed by DSR applications in S.E. Hubs in Section 2.2. Next optimization of CHP and energy storage systems operation are reviewed in Section 2.3. Then the optimal design of CHP generator is discussed for building systems in Section 2.4. From the literature review, it is found that CHP plays an important role to improve the energy performance of an S.E. Hub, and existing studies have neglected the dynamic control of CHP power to

heat ratios to improve the overall S.E. Hub operational and economic performance. In the following chapters, this power to heat ratio in CHP will be modeled and controlled to achieve minimal operating cost in S.E. Hubs, together with the HVAC load management, optimal sizing of CHP under DSR. In addition to the operational cost, the CHP investment payback period will also be investigated.

3. METHODOLOGY

This thesis establishes an optimization scheme for an S.E. Hub to minimize the overall cost of the hub system. The main development includes the following four parts:

i. Establish a modeling framework for S.E. Hubs including hourly operations of a CHP unit, an electricity storage and a thermal storage combined with DSR under a time-of-use tariff.

ii. Develop optimal operation of CHP, ESS and TSS in the S.E. Hub, with the hourly dynamic control of the CHP heat and power split ratio.

iii. Implement DSR programs in S.E. Hub, mainly focusing on the load management of centralized/grouped appliances.

iv. Investigate the optimal sizing of CHP for the purpose of energy cost saving and investment payback.

This chapter delivers the general methodologies to support studies in the later chapters, especially on CHP modeling, load management and optimal sizing of CHP investment. The outline of this chapter is arranged as follows.

In Section 3.1, a general S.E. Hub operational cost minimization methodology including CHP dynamic control is presented. Section 3.2 introduces a load management method on appliances of an S.E. Hub, and the logic correlations between appliances are discussed. In Section 3.3, a component investment modeling algorithm is studied, and an optimization example is cited for optimal design problem in building energy system retrofit. A summary is given in Section 3.4.

3.1. S.E. Hub Optimization

3.1.1. CHP dynamic control

Linear Programing (LP) [176] and non-linear programing [176] are two techniques used in CHP dynamic operation. LP methods are suitable for most CHP generation types, e.g. gas turbine CHP, steam turbine CHP and micro CHP. Non-linear programming algorithm is usually used for complex CHP technologies, for example, CCGT CHP system which is generally used in large-scale power plant. In this thesis, the S.E. Hub is studied under a typical commercial building system, and the gas turbine CHP generation is selected. Thus, LP is applied to determine the CHP operational strategy.

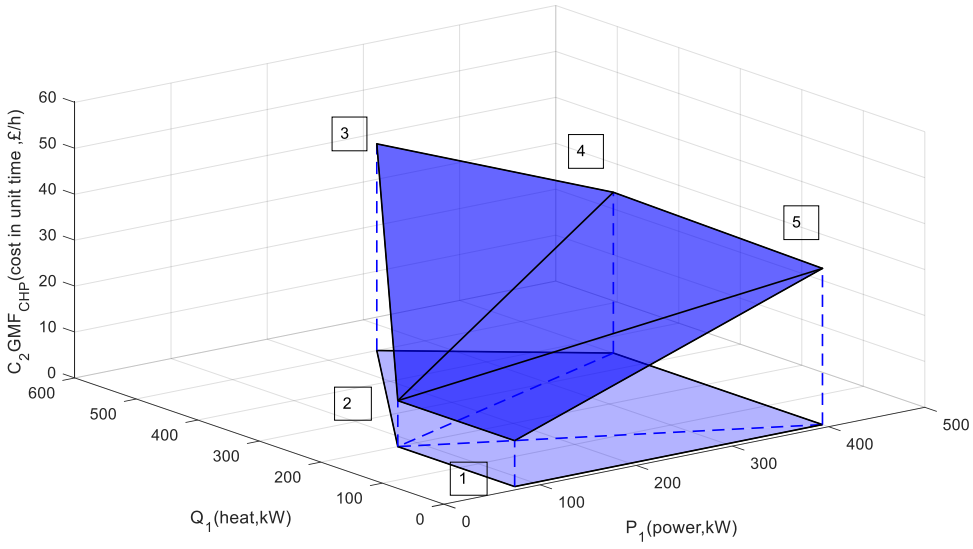

Fig. 3.1. The convex operating region of a CHP unit

Assume that the operating region of each CHP unit is convex in terms of the areas formed by the output of power and heat, meanwhile the cost of each CHP is also a convex function with respect to its power and heat production, see an illustration in Fig. 3.1. This convexity property implies that any operating point in the operating

region can be represented as a vector combination of characteristic points (u_j, p_j, q_j), where u_j, p_j and q_j are the cost, power and heat values of the characteristic point j of a CHP unit, respectively. The five characteristic points correspond to 5 extreme CHP operations (See Fig. 3.1): minimal power and minimal heat (point 1), maximal heat when power is minimal (point 2), maximal heat (point 3), maximal heat when power is maximal (point 4), and maximal power and minimal heat (point 5). In order to simplify the later calculation in Chapter 3-6, all hourly energy flows in kJ/h are transferred into kW ($3.6 \times 10^3\ kJ/h = 1kW$).

Then the operating cost U, power production P and heat production Q can be expressed as a vector combination of characteristic points [177]:

$$U\ (t) = \sum_{j \in J} u_j \cdot x_j\ (t) \tag{3.1}$$

$$P\ (t) = \sum_{j \in J} p_j \cdot x_j\ (t) \tag{3.2}$$

$$Q\ (t) = \sum_{j \in J} q_j \cdot x_j\ (t) \tag{3.3}$$

$$\sum_{j \in J} x_j\ (t) = 1,\ 0 \le x_j\ (t) \le 1 \tag{3.4}$$

where J is the index set of characteristic points of the CHP unit; x_j is the decision variable encoding the vector combination of the operating region.

These functions allow the shape of the operating region to change over time, but always keep convexity. When a CHP unit is turned off, the characteristic points will be changed to (0,0,0) for all (u_j, p_j, q_j). The optimal control of CHP unit should include the turn-on and turn-off cost.

3.1.2. S.E. Hub energy cost minimization

In an S.E. Hub with only one CHP unit, other common components such as heat-only boiler, ESS and TSS, also need to be considered in the energy cost minimization model. The excess electricity P_{excess} generated by the CHP unit can be sold to the power grid to generate additional revenue. In the following grid – connected system, a boiler and a CHP are included. Without considering the operation cost of ESS and TSS, the objective function to minimize energy cost can be formulated as

$$\min \sum_{t=1}^{T} \left(\sum_{j \in J} u_j \cdot x_j(t) + c_{boiler}(t) \cdot Q_{boiler}(t) + c_{grid}(t) \cdot P_{grid}(t) - c_{excess}(t) \cdot P_{excess}(t) \right) \cdot \Delta t \tag{3.5}$$

subject to the constraints of CHP decision variables x_j in Eq. (3.4). c_{boiler} is the unit cost of heat generated by the boiler; Q_{boiler} is the heat output of the boiler; c_{grid} is the electricity tariff of the power grid; P_{grid} is the electricity power purchased from the power grid; c_{excess} is the excess electricity selling price; Δt is the length of sampling time, which is generally set as one hour for building systems.

The power balance function is represented as

$$\sum_{j \in J} p_j \cdot x_j(t) + P_{s-}(t) - P_{s+}(t) + P_{grid}(t) - P_{excess}(t) = P(t) \tag{3.6}$$

where P_{s+} and P_{s-} are the ESS charging power and discharging power, respectively; P is the power demand of the S.E. Hub.

The heat balance function is written as an inequality constraint, which implies that the excess heat is produced to ensure sufficient supplies and it can be freely disposed. The minimized operational cost will also make the excess heat minimal. The heat constraint is written as

$$\sum_{j\in J} q_j \cdot x_j(t) + Q_{s-}(t) - Q_{s+}(t) + Q_{boiler}(t) \geq Q(t) \tag{3.7}$$

where Q_{s+} and Q_{s-} are the TSS charging power and discharging power, respectively; Q is the heat demand of the S.E. Hub.

For ESS and TSS, the storage efficiencies caused by their self-discharging rates are considered as follows [176].

$$S_P(t) = \eta_P \cdot S_P(t-1) - P_{s-}(t) + P_{s+}(t) \tag{3.8}$$

$$S_Q(t) = \eta_Q \cdot S_Q(t-1) - Q_{s-}(t) + Q_{s+}(t) \tag{3.9}$$

where S_P and S_Q are the energy stored in ESS and TSS, respectively; η_P and η_Q are the self-discharging related storage efficiencies of ESS and TSS, respectively.

The energy stored in ESS and TSS are subject to equipment capacity limitations.

$$S_P^{\min} \leq S_P(t) \leq S_P^{\max} \tag{3.10}$$

$$S_Q^{\min} \leq S_Q(t) \leq S_Q^{\max} \tag{3.11}$$

where $S_P^{\min}$ and $S_P^{\max}$ are the minimum and the maximum energy stored in ESS; similarly $S_Q^{\min}$ and $S_Q^{\max}$ for TSS.

With the above model, the operating points of CHP, or equivalently the heat/power split ratio of the CHP, can be determined dynamically so as to minimize the overall operating cost. In this general framework, the boiler system is a backup component for thermal demand, which is not necessary if the CHP heat output is sufficient. In this thesis, only CHP is considered for power and heat generation within a building. Different from this framework, the charging/discharging efficiencies of ESS and TSS, and the degradation cost of ESS are considered in Chapter 5.

3.2. Appliances Operation Modeling under DSR

DSR can be used to achieve energy cost minimization in an S.E. Hub. In this thesis, the DSR is employed on centralized/grouped appliances, i.e., the HVAC. In this section, an appliance operation method proposed by Xia and Zhang [178] is introduced considering five main types of appliances constraints.

Assume that an energy hub consists of I appliances, each of them can be independently controlled as on/off status. The appliances are divided into two groups:

i. The i-th appliance operates at its rated power, P_i kW, if it is switched on, where $i = 1, 2, \cdots, I_1$;

ii. The i-th appliance operates at any power value between 0 and its rated power, P_i, if it is switched on, where $i = I_1 + 1, I_1 + 2, \cdots, I$; and $I_1 \le I$.

In the first group, I_1 appliances operate with only simple on/off status, for example, electric kettles, electric water heater and night lights. In the second group, $I - I_1$ appliances can operate with variant powers, for example, air conditions or HVAC, washing machines.

Assume all electricity is purchased from the power grid, and the electricity price is c_{grid}, which generally takes real-time pricing or a TOU tariff in price-based DSR. The on/off status of the i-th appliance is represented by b_i and is defined as

$$b_i(t)\begin{cases} = 1, \text{ if the } i\text{-th appliance is on and } 1 \le i \le I_1 \\ = 0, \text{ if the } i\text{-th appliance is off and } 1 \le i \le I_1 \\ \in [0,1], \text{ if } I_1 \le i \le I \end{cases} \tag{3.12}$$

Then the energy cost function f_c over a fixed time interval $[t_o, t_f]$ is formulated as

$$f_c = \sum_{i=1}^{I} P_i \cdot \int_{t_0}^{t_f} b_i(t) \cdot c_{grid}(t)\,\mathrm{d}t \tag{3.13}$$

In [178], five types of constraints are presented on appliances, including logic correlations, mass balance, energy balance, process and service correlations, and boundary constraints. The logic correlations of appliances are shown as below.

i. When the i-th appliance is switched on at time t_1, the y-th appliance must be switched off at time t_2, where $y \in [0, I]; y \neq i;$ and $t_1, t_2 \in \left[t_o, t_f\right]$.

In this case, a new sign function is introduced to cover the appliances with variable powers, and the sign function is given as

$$\mathrm{sign}\left(b_i(t)\right) = \begin{cases} 1, \text{ if } b_i(t) > 0 \\ 0, \text{ if } b_i(t) = 0 \end{cases} \tag{3.14}$$

The mathematical equivalent expression can be formulated as

$$\left(\mathrm{sign}\left(b_i(t_1)\right)+1\right)\cdot\left(\mathrm{sign}\left(b_y(t_2)\right)+2\right) \neq 6 \tag{3.15}$$

Consider a simple example with an electric appliance which can be powered by the grid or by a distributed generation, such as CHP, but it cannot be supplied by both at same time. The connection status of the power grid to this appliance can be represented as $\mathrm{sign}(a_1)$, while the connection status of the distribution to this appliance corresponds to $\mathrm{sign}(a_2)$. $\mathrm{sign}(a_1)$ and $\mathrm{sign}(a_2)$ are both binary variables, where equaling one means on and equaling zero means off. Then the connection constraint can be derived as

$$\left(\mathrm{sign}\left(a_1(t_1)\right)+1\right)\cdot\left(\mathrm{sign}\left(a_2(t_1)\right)+2\right) \neq 6 \tag{3.16}$$

ii. When the i-th appliance is switched on at time t_1, the y-th appliance must be switched on at time t_2.

The constraint function is formulated as the following inequality.

$$\left(\text{sign}\left(b_i\left(t_1\right)\right)+1\right)\cdot\left(\text{sign}\left(b_y\left(t_2\right)\right)+2\right)\neq 4 \tag{3.17}$$

iii. When the i-th appliance is switched off at time t_1, the y-th appliance must be switched on at time t_2.

The constraint function under this case is formulated as the following inequality.

$$\left(\text{sign}\left(b_i\left(t_1\right)\right)+1\right)\cdot\left(\text{sign}\left(b_y\left(t_2\right)\right)+2\right)\neq 2 \tag{3.18}$$

iv. When the i-th appliance is switched off at time t_1, the y-th appliance must be switched off at time t_2.

The constraint function under this case is formulated as the following inequality.

$$\left(\text{sign}\left(b_i\left(t_1\right)\right)+1\right)\cdot\left(\text{sign}\left(b_y\left(t_2\right)\right)+2\right)\neq 3 \tag{3.19}$$

v. The on/off status of the i-th appliance does not affect the status of y-th appliance. In this case, no mathematical constraint is required.

3.3. Optimal Design for Building Energy System Retrofit

To optimally sizing components in building energy system retrofit, assume that there are I components to be retrofitted with more energy efficient ones, among them the i-th component has K_i different choices, and denote the k-th alternative choice of the i-th component by d_{ik}, where $i=1,2,\cdots I$, and $k=1,2,\cdots K_i$. Each component d_{ik} corresponds to an installation cost represented by c_{ik}. The choosing

activity of each d_{ik} is the decision variable in optimal design model, and this variable is defined as

$$x_{ik} = \begin{cases} 1, \text{ if } d_{ik} \text{ is chosen} \\ 0, \text{ if } d_{ik} \text{ is not chosen} \end{cases} \tag{3.20}$$

Then the total investment of the energy retrofit, denoted by I_0, can be formulated as

$$I_0 = \sum_{i=1}^{I} \sum_{k=1}^{K_i} x_{ik} \cdot c_{ik} \tag{3.21}$$

The total investment of energy system retrofit must be limited by the allowed maximum budget.

$$\sum_{i=1}^{I} \sum_{k=1}^{K_i} x_{ik} \cdot c_{ik} \le I_{budget} \tag{3.22}$$

Assume the rated power output of d_{ik} is P_{ik}. The overall total power of these I components must be within a lower bound L_{power} and an upper bound U_{power}, which is formulated as

$$L_{power} \le \sum_{i=1}^{I} \sum_{k=1}^{K_i} x_{ik} \cdot P_{ik} \le U_{power} \tag{3.23}$$

Malatji et al. [161] proposed a multi-objective model for new components investment in building retrofit, the two objectives are to minimize the investment payback period and to maximize the energy saving. They also considered the electricity price change by years and the net present value (NPV) constraint. Their method is briefed below, which will be applied in Chapter 6.

Assume a_{ik} is the average annual energy savings of component i, which can be represented as

$$a_{ik} = EC_i^{existing} - EC_{ik}^{proposed} \tag{3.24}$$

where $EC_i^{existing}$ is the energy consumption of the existing component i and $EC_{ik}^{proposed}$ is the energy consumption of the proposed component i with investment choice k. The average annual year energy cost saving B is formulated as

$$B = \frac{1}{T} \cdot \sum_{t=1}^{T} \sum_{i=1}^{I} \sum_{k=1}^{K_i} a_{ik} \cdot x_{ik} \cdot c_{grid} \left(1+\sigma\right)^t \tag{3.25}$$

where $t = 1, 2, \cdots, T$ stands for year index, T is the minimum number of years needed for a nonnegative NPV as defined later in (3.28), c_{grid} is the electricity price of the power grid; σ is an averaged electricity price annual increasing rate.

The two objectives functions for minimum payback period and maximum energy saving are formulated as

$$\min f_1 = \frac{I_0}{B} = \frac{T \cdot \sum_{i=1}^{I_1} \sum_{k=1}^{K_r} x_{ik} \cdot c_{ik}}{\sum_{t=1}^{T} \sum_{i=1}^{I_1} \sum_{k=1}^{K_r} a_{ik} \cdot x_{ik} \cdot c_{grid} \left(1+\sigma\right)^t} \tag{3.26}$$

$$\max f_2 = \sum_{i=1}^{I_1} \sum_{k=1}^{K_r} a_{ik} \cdot x_{ik} \tag{3.27}$$

subject to

$$\text{NPV}:= \sum_{t=1}^{T} \frac{B - c_t}{\left(1+d_t\right)^t} - I_0 \geq 0 \tag{3.28}$$

$$0 \leq T \leq \lambda \tag{3.29}$$

$$f_1 \leq Z \tag{3.30}$$

$$f_2 \geq EC_{\exp} \tag{3.31}$$

and also subject to investment budget constraint in Eq. (3.22). In the above optimization model, c_t is the operational cost in year *t*; d_t is the average discount rate of each year; λ is the upper bound integer that makes NPV non negative. Z and $EC_{\exp}$ are the maximal expected payback period and minimal energy savings, respectively.

3.4. Summary

The methodologies presented in this chapter provide strong support to the later studies of this thesis, especially on CHP modeling and optimization, HVAC modeling and operation in DSR, and optimal sizing of CHP investment. The detailed optimization scheme and constraints are proposed in Chapter 4-6.

4. OPTIMAL OPERATION OF CHP COMBINED WITH DSR

In this chapter, the ratio of the electricity and thermal output of the CHP unit is controlled, along with HVAC load management, so as to minimize the overall microgrid operational cost. A model is established for the energy cost minimization of an S.E. Hub, which includes factors such as TOU tariffs, the capacity and constraints within CHP operation, the operating condition of HVAC, and the indoor air temperature comfortable range. Efficient CHP operation and optimal HVAC scheduling are determined through optimization. The improved performance of the optimization route is discussed in case studies by comparing with two existing optimal strategies, which consider CHP optimal control and DSR separately.

This chapter is arranged as follows. In Section 4.1, the basic configuration of the proposed optimization framework is introduced. In Section 4.2, the modeling of CHP unit and HVAC system is presented. In Section 4.3, the energy cost minimization problem is formulated. In Section 4.4, a description of the baseline system is illustrated. In Section 4.5, the case study optimizations are implemented under different scenarios, and the results are discussed. Finally, conclusions are drawn in Section 0.

4.1. Model Configuration

A typical S.E. Hub configuration is illustrated in Fig. 4.1, which consists of two energy sources (electricity and gas), a CHP unit, an EMS, and two types of energy demands, namely the electricity demand and the thermal demand. The HVAC load, P_{HVAC}, is purposely separated from the electricity demand since this is taken as the main load in DSR. Apart from the HVAC load, other electricity demands are put into one term, P_L, which are regarded as inflexible loads that cannot be controlled by DSR.

Both P_{HVAC} and P_L are supplied by the power grid, P_{grid}, and the CHP output power, P_1.

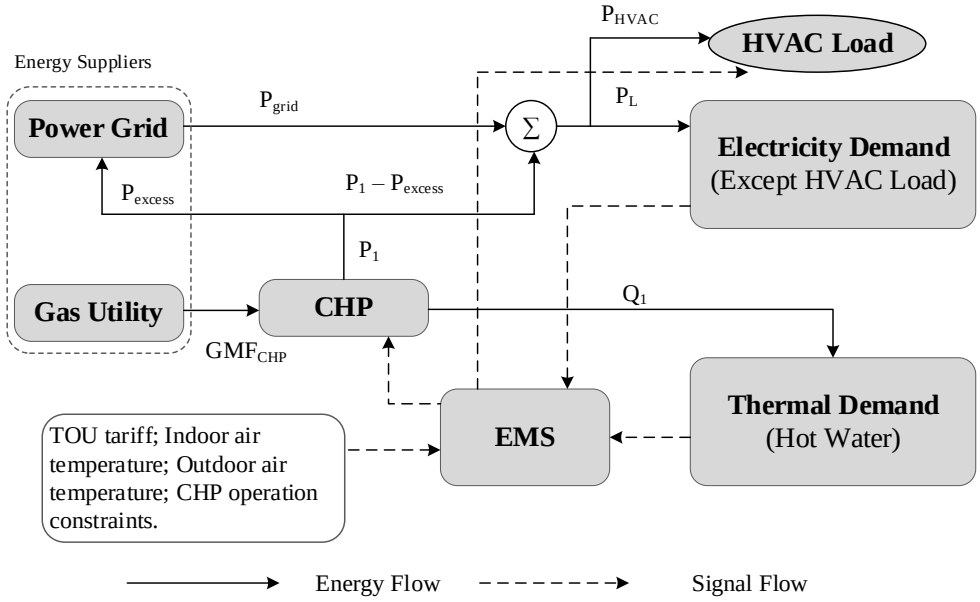

Fig. 4.1 The proposed configuration of an S.E. Hub for optimization.

The fuel of a CHP unit is natural gas and the gas usage within each time slot is represented by gas mass flow, GMF_{CHP}. The excess electricity generated by a CHP unit, P_{excess}, can be exported to the power grid to get profit. The thermal demand in this model is mainly the hot water usage, since the space heating and cooling is supplied by the HVAC system. The thermal demand, Q, is only supplied by the CHP heat output, Q_1. It is assumed that the CHP heat output is sufficient to meet the heat demand and no boiler is required.

The EMS is used to gather information such as energy demands, electricity price, environmental temperature, system operation constraints, etc. The controllable components in this S.E. Hub include a CHP unit and an HVAC system. The EMS controls the power and heat output of CHP unit and the load of HVAC system to achieve optimal economic performance for the whole S.E. Hub.

This proposed model is established on a building system, all of the energy generation, conversion, transmission and consumption are taken place inside the building. Thus, the energy transmission losses among each component can be neglected. It is assumed that all the electricity energy can be fully utilized, where the excess electricity can be sold to be the power grid. However, there may exist thermal heat waste, it can be reduced after considering storage system in Chapter 5.

4.2. Modeling of CHP and HVAC

4.2.1. CHP modeling

The gas consumption of a CHP unit depends on its working conditions, where the power and heat can be produced at different ratios. In order to minimize the operational cost of the CHP unit, the most suitable ratio between power and heat needs to be determined. The cost of natural gas depends on both power and heat generation in CHP. In this thesis, the CHP characteristic operating region is assumed to be convex. Referring to the CHP optimal control in Section 3.1.1, the CHP operating cost ($c_2 \cdot GMF_{CHP}$) and the production of power (P_1) and heat (Q_1) can be represented by vector combination of five characteristic points (u_j, p_j, q_j). Here u_j, p_j and q_j are the cost, power and heat values of the j-th CHP characteristic point. As shown in Fig. 3.1, five characteristic points correspond to 5 extreme CHP operations, then we have

$$c_2 \cdot GMF_{CHP}(t) = \sum_{j=1}^{5} u_j \cdot x_j(t) \tag{4.1}$$

$$P_1(t) = \sum_{j=1}^{5} p_j \cdot x_j(t) \tag{4.2}$$

$$Q_1(t) = \sum_{j=1}^{5} q_j \cdot x_j(t) \tag{4.3}$$

subject to

$$\sum_{j=1}^{5} x_j(t) = 1,\ 0 \le x_j(t) \le 1 \tag{4.4}$$

where $t = 1, 2, \cdots, N$ are the time indices; N is the total sampling number in time horizon; $j = 1, 2, 3, 4, 5$ represent the five characteristic points of CHP; x_j is the decision variable, which encodes the vector combination of the operating.

Constraints on the maximal output power and the power ramping must be considered for real CHP operation and for assuring stability of the whole system.

$$P_1(t) \le P_{CHP}^{\max} \tag{4.5}$$

$$\left| \sum_{j=1}^{5} p_j \cdot \left(x_j(t) - x_j(t-1) \right) \right| \le P_{CHP}^{rate} \tag{4.6}$$

where $P_{CHP}^{\max}$ is the maximal power limit; P_{CHP}^{rate} is the CHP power ramping rate.

The constraint in Eq. (4.6) restricts how much the power production of a CHP unit may increase or decrease between two consecutive time steps. In this work, hourly time step is used in optimization, which is a general set in building energy systems. For the heat generation, the hourly heat output, Q_1, must meet the thermal demand, Q, with consideration of the heat utilization efficiency, η_1^{heat}.

$$\eta_1^{heat} \cdot Q_1(t) \ge Q(t) \tag{4.7}$$

4.2.2. HVAC modeling

To achieve optimal energy utilization, the main electricity consumption appliance, HVAC system, needs to be scheduled. The HVAC system can be controlled to have *n* operating power levels, denoted by $P_{l_{HVAC}}$, where each operating level can be manipulated as on/off by a binary variable, $b_{l_{HVAC}}$. The HVAC operating power at time t is written as

$$P_{HVAC}(t)=\sum_{l_{HVAC}=1}^{n} b_{l_{HVAC}}(t)\cdot P_{l_{HVAC}} \tag{4.8}$$

subject to

$$\sum_{l_{HVAC}=1}^{n} b_{l_{HVAC}}(t)=\begin{cases}1, \text{ HVAC is on}\\ 0, \text{ HVAC is off}\end{cases} \tag{4.9}$$

where $b_{l_{HVAC}}$ is a 0/1 binary decision variable indicating on/off status of the HVAC; l_{HVAC} ($l_{HVAC}=1,\cdots,n$) represents the index of operating levels; n is the number of HVAC working levels, which is taken to be five in this work balancing the effectiveness of the operation strategy and the computational load for the optimization algorithm.

Equation (4.9) assures that, at each time *t*, HVAC can only work at one operating level. The HVAC system is off when all binary variables $b_{l_{HVAC}}$ are zeros. In this work, the objective of HVAC load management is to shape the system load to achieve cost reduction during the period of peak tariff, where the indoor air temperature T^i is kept within an acceptable and comfortable range. The indoor air temperature is affected by multiple factors including the HVAC power transformation efficiency η^{HVAC}, the heat capacity of the building $C_{building}$, the outdoor ambient air temperature, T^o, the ground temperature, T^g, the ventilation temperature, T^v, and their conductance with the indoor air temperature (H^{io}, H^{ig}, H^{iv}). T^g, and T^v are considered as constant in this thesis. The multiplication term $\eta^{HVAC}\cdot P_{HVAC}$ is the HVAC power output used to keep the indoor air temperature. According to the indoor temperature balance function in [179], the indoor air temperature balance function related to the HVAC load can be formulated as

$$\begin{aligned}\eta^{HVAC}\cdot P_{HVAC}(t)=C_{building}\cdot\left(T^i(t)-T^i(t-1)\right)+H^{io}\cdot\left(T^i(t)-T^o(t)\right)\\ +H^{ig}\cdot\left(T^i(t)-T^g\right)+H^{iv}\cdot\left(T^i(t)-T^v\right)\end{aligned} \tag{4.10}$$

The following constraint is applied to keep the indoor temperature within a given range. $T^i_{\min}$ and $T^i_{\max}$ denote the lower and upper indoor temperature bounds, respectively.

$$T_{\min}^{i} \le T^{i}(t) \le T_{\max}^{i} \tag{4.11}$$

4.3. Energy Cost Minimization with Combined CHP and HVAC Optimal Control

For an S.E. Hub, the total energy cost, c_{total}, consists of three parts: electricity cost $c_{electricity}$, natural gas cost c_{gas}, and the income from selling excess electricity c_{income}, i.e.,

$$c_{total} = c_{electricity} + c_{gas} - c_{income} \tag{4.12}$$

$c_{electricity}$ is the sum of purchased electricity multiplying the TOU tariff c_1, which is formulated as

$$c_{electricity} = \sum_{t=1}^{T} c_1(t) \cdot P_{grid}(t) \cdot \Delta t \tag{4.13}$$

where the sample time interval, Δt, is one hour, and T is the total number of sampling hours.

According to the power flow chart in Fig. 4.1, the purchased power from power grid at each time slot can be formulated as

$$P_{grid}(t) = P_{HVAC}(t) + P_L(t) - P_1(t) + P_{excess}(t) \tag{4.14}$$

The cost of natural gas purchased from the gas utility, c_{gas}, can be formulated as

$$c_{gas} = \sum_{t=1}^{T} c_2 \cdot GMF_{CHP}(t) \cdot \Delta t \tag{4.15}$$

where the natural gas price, c_2, is considered as constant; GMF_{CHP} is the gas mass flow of the CHP unit, which is described by Eq. (4.1) in the CHP model.

Besides, when the CHP generates excess electricity, it can be sold to the power grid for income c_{income}.

$$c_{income} = \sum_{t=1}^{T} c_3 \cdot P_{excess}(t) \cdot \Delta t \tag{4.16}$$

where c_3 is the excess electricity sale price from CHP to the grid; and the P_{excess} can be written as

$$P_{excess}(t) = \max\{P_1(t) - (P_{HVAC}(t) + P_L(t)), 0\} \tag{4.17}$$

Referring to the logic correlation modeling methodology in Section 3.2, to denote that P_{excess} and P_{grid} are not able to exist simultaneously, the following constraint is given as

$$P_{excess}(t) \cdot P_{grid}(t) = 0 \tag{4.18}$$

Thus, the mathematical energy cost model of the S.E. Hub is summarised as

$$c_{total} = \sum_{t=1}^{T} \left(c_1(t) \cdot P_{grid}(t) + c_2 \cdot GMF_{CHP}(t) - c_3 \cdot P_{excess}(t) \right) \cdot \Delta t \tag{4.19}$$

In this model, there are two controllable components, namely CHP unit and HVAC system. When considering five operating points for CHP and five power levels for HVAC, the total number of decision variables in these two components is ten and they are denoted as follows.

Table 4.1 Decision variables in optimization

Components	Decision variables	Values
CHP	x_1, x_2, x_3, x_4, x_5	Real numbers between 0 and 1
HVAC	b_1, b_2, b_3, b_4, b_5	Binary numbers 0 or 1

Denote the 10 decision variables in a vector ϕ. The feasible domain of ϕ is denoted as Φ.

$$\phi = \left[x_1, x_2, x_3, x_4, x_5, b_1, b_2, b_3, b_4, b_5 \right]^{\mathrm{T}} \tag{4.20}$$

The energy cost minimization problem for a typical S.E. Hub is formulated as follows

$$\begin{aligned} & \phi^* = \arg\min_{\phi \in \Phi} \left(c_{total}\left(\phi\right) \right) \\ & s.t. \\ & P_{excess}\left(t\right) \cdot P_{grid}\left(t\right) = 0 \\ & \sum_{j=1}^{5} x_j(t) = 1 \\ & P_1\left(t\right) \le P_{CHP}^{\max} \\ & \left| P_1\left(t\right) - P_1\left(t-1\right) \right| \le P_{CHP}^{rate} \\ & \eta_1^{heat} \cdot Q_1\left(t\right) \ge Q\left(t\right) \\ & \sum\nolimits_{l_{HVAC}=1}^{5} b_{l_{HVAC}}\left(t\right) \le 1 \\ & T_{\min}^{i} \le T^{i}(t) \le T_{\max}^{i} \end{aligned} \tag{4.21}$$

The decision variables include real numbers and integers; thus the overall optimization is a mixed-integer programming problem. An advanced global optimization method, Genetic Algorithm (GA) [180], is selected to solve this problem. GA simulates the biological processes of reproduction and the natural selection to find the optimal solution. It has a good convergence rate, low computational time and high robustness with satisfactory precision [181]. GA is conceptually simple without the requirement of gradient information. Furthermore, GA has the ability to deal with various optimization problems, such as stationary or non-stationary, linear or non-linear, continuous or discontinuous objective functions [182].

4.4. Baseline Model Assessment

The initial energy hub without optimization is assumed as the baseline system, which will be presented in this section. In this work, the S.E. Hub model is established using data collected from a smart hotel building in Miami State, USA [183]. The TOU

tariff for grid power is taken from [184] and the outdoor air temperature used is the historical Miami State air temperature data in November 2016 [185], as shown in Fig. 4.2 (a) and (b), respectively. The original S.E. Hub model is established using survey data from USA. In order to make this work more meaningful to the UK, all price data including TOU tariff, gas price and excess electricity sell price, are taken form the UK grid. The settings of all constant parameters are provided in Table 4.2. Both the gas price c_2 and the feedback tariff c_3 are considered as constant, which are set as $0.03\ £/kW\cdot h$ and $0.05\ £/kW\cdot h$, respectively [52].

Table 4.2 Setting of constant parameters

Parameters	Values	Parameters	Values
c_2	$2.83\ p/kw\cdot h$	H^{iv}	$12.5\ kW/^{\circ}C$
c_3	$5\ p/kw\cdot h$	H^{ig}	$2.5\ kW/^{\circ}C$
μ_j (£)	$(10,10,45,35,34)$	η^{HVAC}	0.85
p_j (kw)	$(80,80,250,400,400)$	$C_{building}$	$22.92\ kW/^{\circ}C$
q_j (kw)	$(10,200,500,350,10)$	T^g	$12^{\circ}C$
$P_{CHP}^{\max}$	$400\,kW$	T^v	$12^{\circ}C$
P_{CHP}^{rate}	$100\,kW$	$T^i(t=0)$	$16^{\circ}C$
$P_1(t=0)$	0	$T^i_{\min}$	$16^{\circ}C$
η_1^{heat}	0.85	$T^i_{\max}$	$24^{\circ}C$
H^{io}	$16\ kW/^{\circ}C$	T	360h

The simulation period is set to be 15 days (360 hours) and this length will reflect the practical situation and test the reliability of the algorithm. Each sampled time slot is 1 hour. In this 15-days period, the TOU tariff, the outdoor temperature, the original load of HVAC system without DSR, the sum of inflexible power demands, and the total power demands of the baseline system are illustrated in Fig. 4.2 and Fig. 4.3.

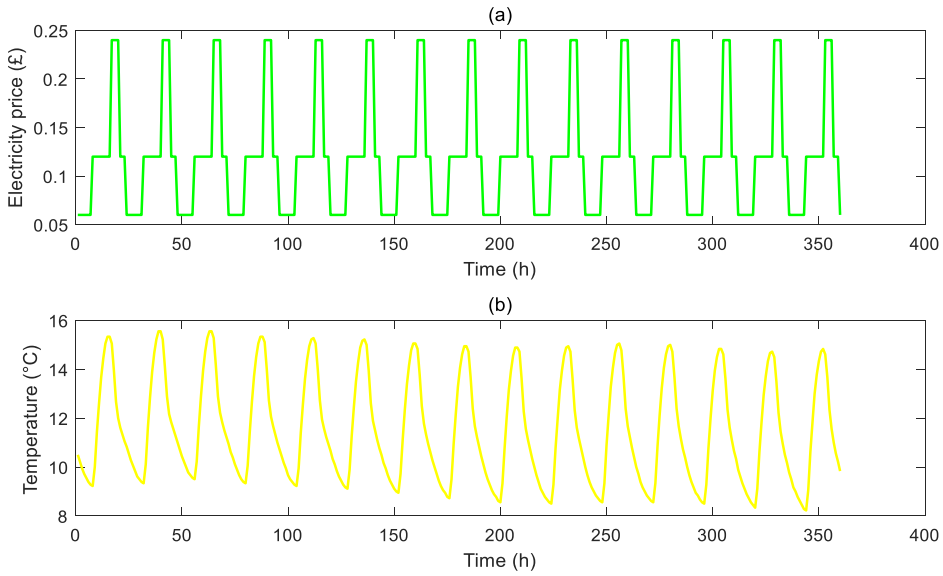

Fig. 4.2 (a) The TOU tariff and (b) the outdoor temperature

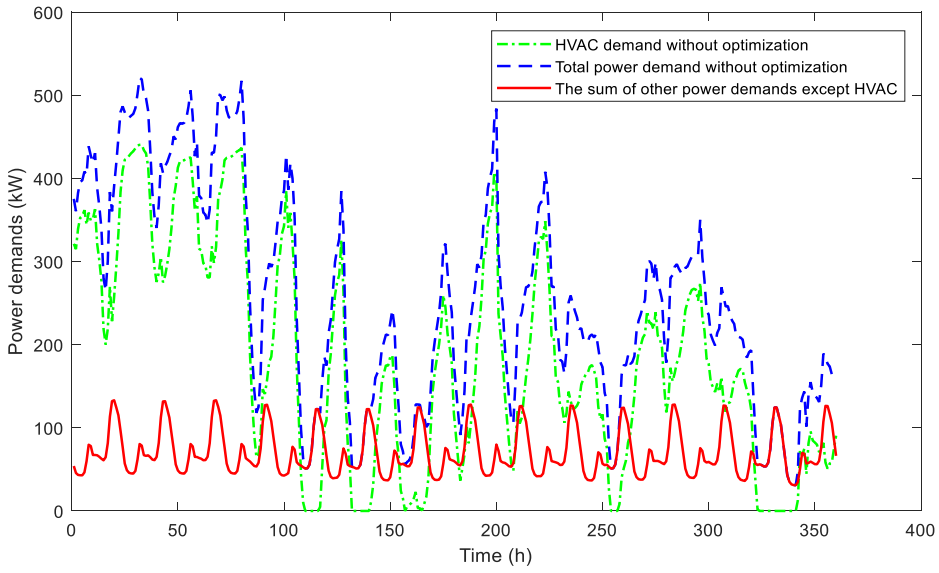

Fig. 4.3 The power demands of the baseline system

All model simulations are implemented with MATLAB software.. In the original operation of this hotel building system, there is no CHP unit, instead a centralized gas boiler is used for thermal supply to hot water usage. Also no load management is applied to the HVAC system. All the electricity demands are supplied by the power grid. In all the simulations in this thesis, it is assumed that there is no loss of electricity transmission from the power grid to appliances. The power balance function of the baseline system is

$$P_{grid}(t) = P_L(t) + P_{HVAC}(t) \tag{4.22}$$

where the data for P_{HVAC} and P_L are shown in Fig. 4.3. The thermal demand data $Q(t)$ are also taken from survey data, as illustrated in Fig. 4.4 (a). The hourly costs of electricity and gas are calculated by $\Delta t \cdot c_1(t) \cdot P_{grid}(t)$ and $\Delta t \cdot c_2 \cdot Q(t)/\eta^{boiler}$, respectively, where the TOU tariff data $c_1(t)$ are shown in Fig. 4.2 (a); the gas price c_2 is $0.03£/kW \cdot h$; and η^{boiler} is the energy efficiency of the centralized gas boiler, which is taken to be 0.85.

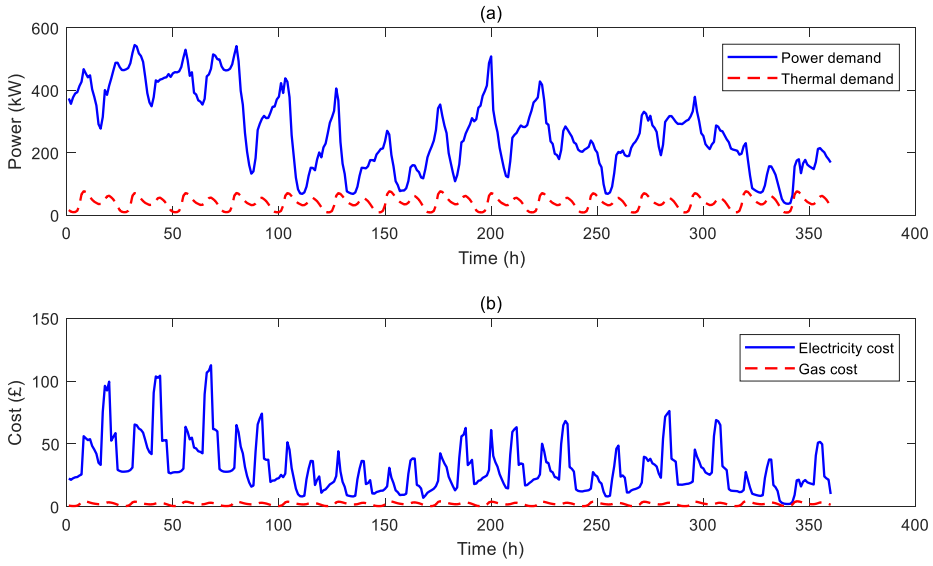

Fig. 4.4 (a) The energy demands and (b) the energy cost of the baseline system

The results from the survey data are taken as the baseline results, which will be used for comparison with different control strategies presented later. The thermal and

power demands and the energy cost for the baseline system are shown in Fig. 4.4, from which it can be seen that the electricity power demand is much higher than the thermal demand for hot water. This is because the space heating is supplied by the HVAC system. The indoor temperature managed by HVAC consumes power from grid, and the gas is only used for thermal demand. Correspondingly, the electricity cost is much higher than the gas cost. The total energy cost of the baseline system is £12,040 over the 15 days.

4.5. Optimization under Different Scenarios

In this section, the strength of the proposed optimization strategy will be examined by comparing with two existing micro-grid optimizations. In Section 4.5.1, the system operates only with CHP optimal control. Section 4.5.2 simulates an optimization scheme with only HVAC load management, where a centralized gas boiler is used to replace the CHP unit for thermal demand. Section 4.5.3 presents the simulation results of the proposed optimization method that combines both CHP operation and HVAC load management.

4.5.1. Scenario 1: Optimization with only CHP control implemented

Scenario 1 is designed to examine the control effect of CHP unit under the TOU tariff. There's no load management of HVAC. Both P_{HVAC} and P_L are taken as inflexible loads and the storage systems are not considered, as in the baseline system. The system configuration of Scenario 1 is shown in Fig. 4.5. The performance of this CHP control strategy will be studied by comparison with the baseline system.

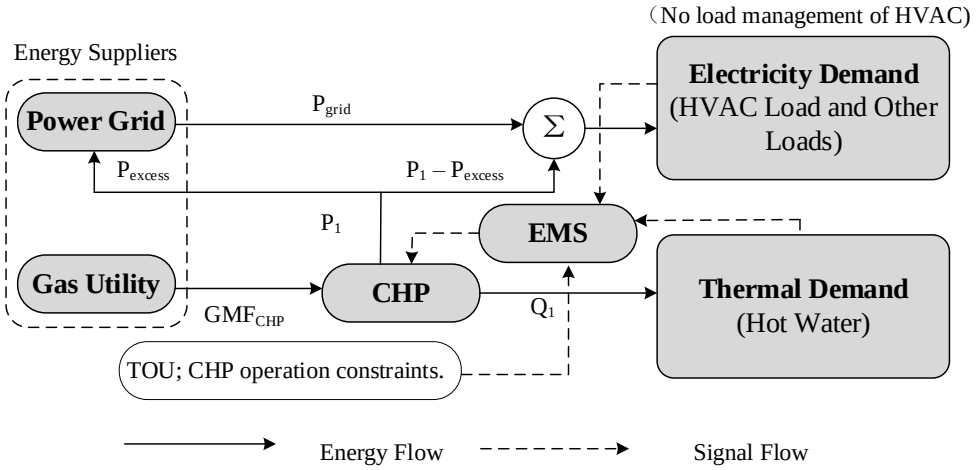

Fig. 4.5 System configuration of Scenario 1 with only CHP control.

In this scenario with only CHP control, the power balance function is

$$P_1(t)+P_{grid}(t)=P_L(t)+P_{HVAC}(t)+P_{excess}(t) \tag{4.23}$$

The CHP unit is modeled by Eq. (4.1)-(4.3) under the constraints in (4.4)-(4.6). The heat generated from CHP unit needs to cover the thermal demand, i.e., $\eta_1^{heat}\cdot Q_1(t)\geq Q(t)$. The hourly energy cost, c_{s1}, in Scenario 1 is formulated as

$$c_{s1}(t)=\Delta t\cdot\left(c_1(t)\cdot P_{grid}(t)+c_2\cdot GMF_{CHP}(t)-c_3\cdot P_{excess}(t)\right) \tag{4.24}$$

The five decision variables in CHP control are denoted as ϕ_1. Φ_1 is the feasible domain for ϕ_1.

$$\phi_1=\left[x_1,x_2,x_3,x_4,x_5\right]^{\mathrm{T}} \tag{4.25}$$

Hence, in Scenario 1, the objective function is formulated as

$$\phi_1^* = \arg\min_{\phi_1 \in \Phi_1} \left(c_{total}\left(\phi_1\right) \right)$$

s.t.

$$\begin{aligned} & P_{excess}(t) \cdot P_{grid}(t) = 0 \\ & \sum_{j=1}^{5} x_j(t) = 1 \\ & P_1(t) \le P_{CHP}^{\max} \\ & \left| P_1(t) - P_1(t-1) \right| \le P_{CHP}^{rate} \\ & \eta_1^{heat} \cdot Q_1(t) \ge Q(t). \end{aligned} \tag{4.26}$$

The calculated results of the decision variable set ϕ_1 is plotted in Fig. 4.6. The five characteristic points of power generation are $[p_1, p_2, p_3, p_4, p_5] = [80,80,250,400,400]$ kW. In this simulation, the decision variable x_3 mostly equals zero, it implies that the CHP unit always generates electricity at a lower or higher output level.

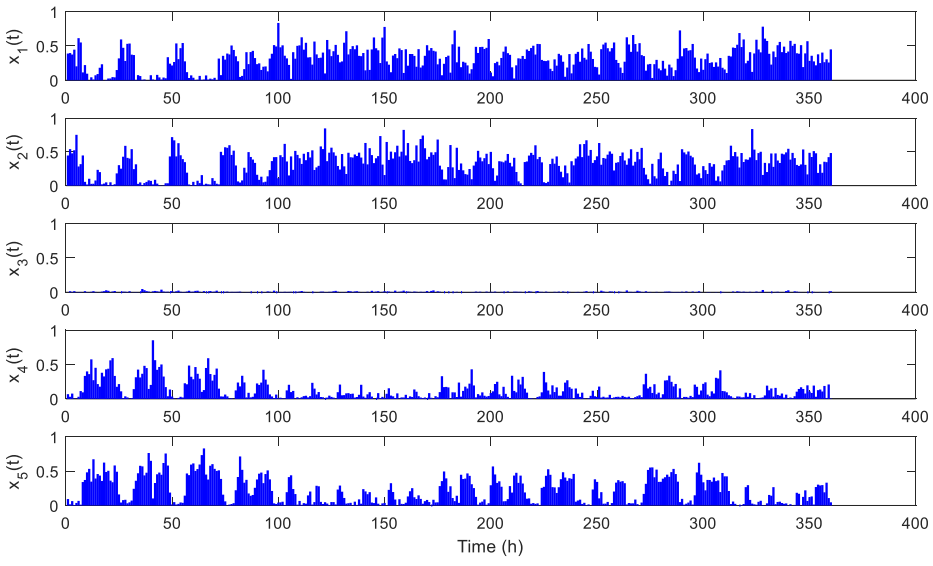

Fig. 4.6 Decision variables x_1 to x_5 for the CHP unit in Scenario 1

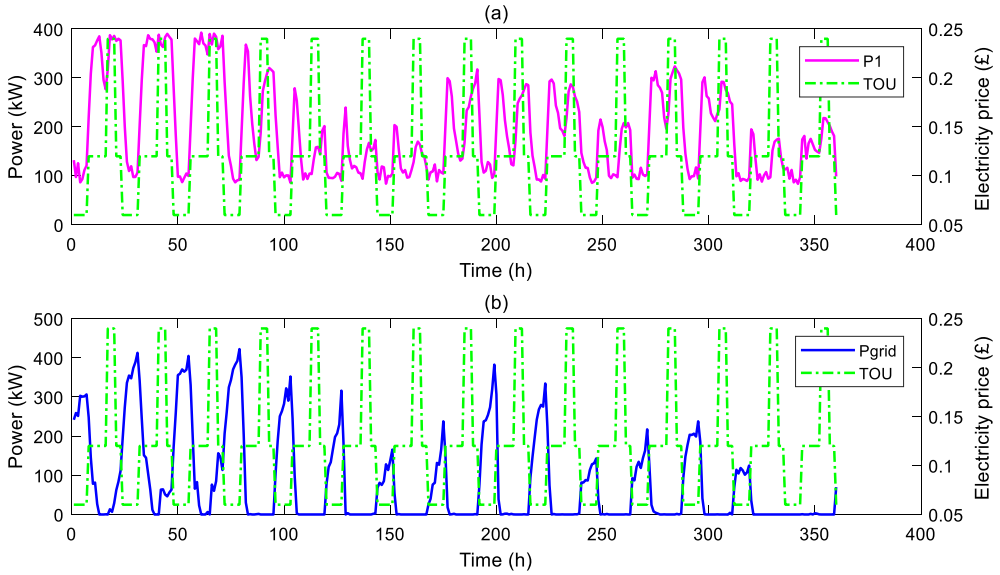

Fig. 4.7 (a) Power output of the CHP unit and (b) power purchased from the grid in Scenario 1.

The calculated power generation and the power purchased from the grid are shown in Fig. 4.7(a) and (b), in both the TOU tariff is provided as a reference. It can be seen that the control of CHP unit has been effective over the whole time period under the TOU tariff, because in this scenario the CHP unit is the sole hot water supplier. From the survey data in Fig. 4.4 (a), the thermal demand of the building system is relative low compared to the electricity demand, this implies that excessive heat generation from CHP may lead to more heat losses without energy storage system. Due to the high coupling characteristic of power and heat production in CHP generation, it is more economical to purchase electricity from the power grid, especially at the time of low electricity price. It can be seen from Fig. 4.7 that when the electricity price is high, the CHP system tends to generate more power (Fig. 4.7 (a)); and when the electricity price is low, the S.E. Hub purchases electricity from the power grid (Fig. 4.7 (b)).

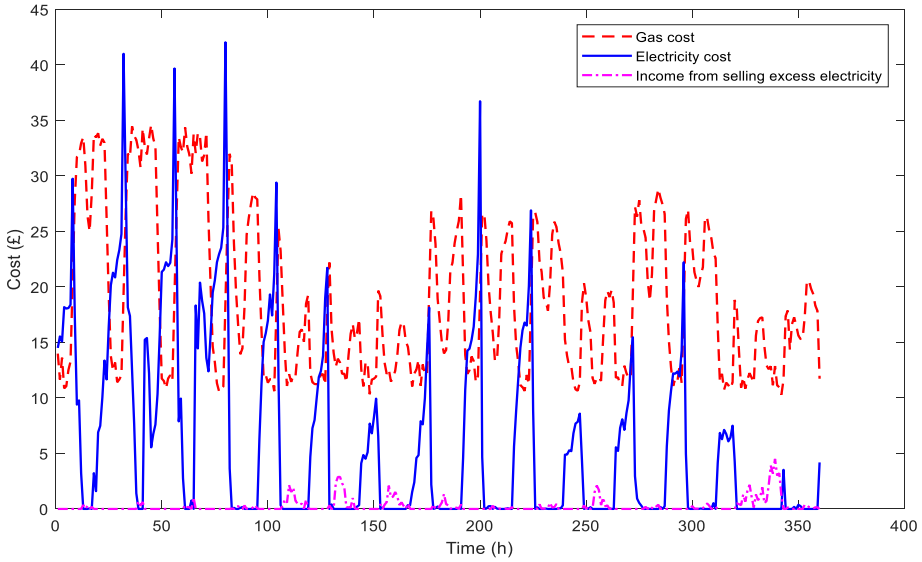

Fig. 4.8 Electricity cost, gas cost, and income in Scenario 1.

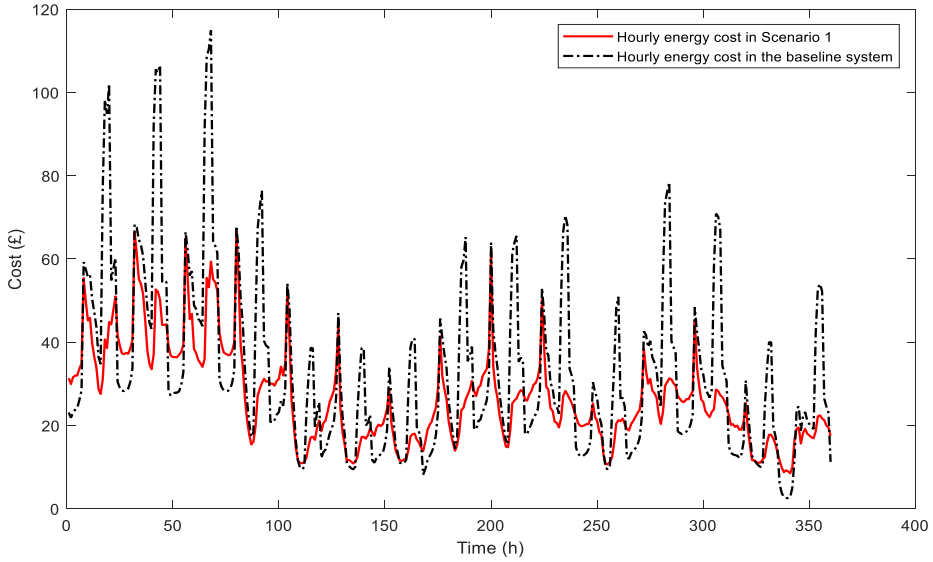

Fig. 4.9 Energy costs under CHP control (Scenario 1) and baseline settings

The costs of gas and electricity in Scenario 1 is shown in Fig. 4.8. Comparing Fig. 4.8 with Fig. 4.4 (b), it can be seen that the gas cost is increased when CHP is included in the S.E. Hub, but the electricity cost from grid supply is reduced. The total energy costs from the grid and gas together, under CHP control and baseline settings, are compared in Fig. 4.9, from which the cost reduction by CHP optimal control can

be clearly seen. The sum of the total energy cost over 15 days is £9,718 with CHP control (Scenario 1), while the sum of the total cost for the baseline system is £12,040. Therefore, the optimal CHP control strategy has achieved a reduction of 19.3% of the total energy cost over 15 days compared to the baseline system.

4.5.2. Scenario 2: Optimization with only HVAC scheduling implemented

In this scenario, we consider only the HVAC load management in optimization of S.E. Hub. The CHP optimal control is not included. Similar to the baseline system, a centralized gas boiler system is used to replace the CHP unit to supply thermal demand $Q(t)$. Without CHP, the electricity supply is purely purchased from power grid. The load demand HVAC system is controlled at on/off status of each HVAC power level, via the decision variables, $b_{l_{HVAC}}$. The system configuration of this scenario is shown in Fig. 4.10.

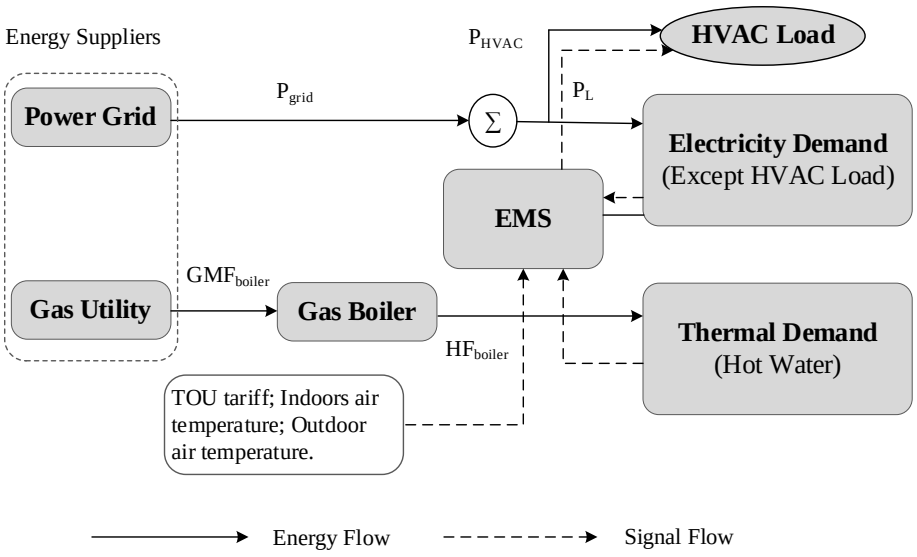

Fig. 4.10 System configuration in Scenario 2 with only HVAC control

The grid power formulation is the same as the baseline system in Section 4.4, i.e., $P_{grid}(t) = P_L(t) + P_{HVAC}(t)$. The heat demand is supplied by the heat flow, HF_{boiler}, generated by the gas boiler.

$$HF_{boiler}(t) = Q(t) \tag{4.27}$$

$$HF_{boiler}(t) = \eta^{boiler} \cdot GMF_{boiler}(t) \tag{4.28}$$

where η^{boiler} is the operating efficiency of the gas boiler; GMF_{boiler} is the gas mass flow of boiler input.

The hourly energy cost for Scenario 2, c_{s2}, is calculated by

$$c_{s2}(t) = \left(c_1(t) \cdot P_{grid}(t) + c_2 \cdot Q(t)/\eta^{boiler}\right) \cdot \Delta t \tag{4.29}$$

The five decision variables in HVAC load management are denoted as ϕ_2, its feasible domain is Φ_2.

$$\phi_2 = \left[b_1, b_2, b_3, b_4, b_5 \right]^{\mathrm{T}} \tag{4.30}$$

The energy cost minimization model is established as

$$\begin{aligned} &\phi_2^* = \arg\min_{\phi_2 \in \Phi_2} \left(c_{total}\left(\phi_2\right)\right) \\ &s.t. \\ &\eta^{boiler} \cdot GMF_{boiler}\left(t\right) = Q\left(t\right) \\ &\sum\nolimits_{l_{HVAC}=1}^{5} b_{l_{HVAC}}\left(t\right) \le 1 \\ &T_{\min}^{i} \le T^{i}(t) \le T_{\max}^{i} \end{aligned} \tag{4.31}$$

The optimized decision variables are illustrated in Fig. 4.11. The optimal scheme for HVAC system and the corresponding indoor air temperature in 360 hours are shown in Fig. 4.12. Again the TOU tariff is provided in Fig. 4.12 to provide the background of variation of electricity price.

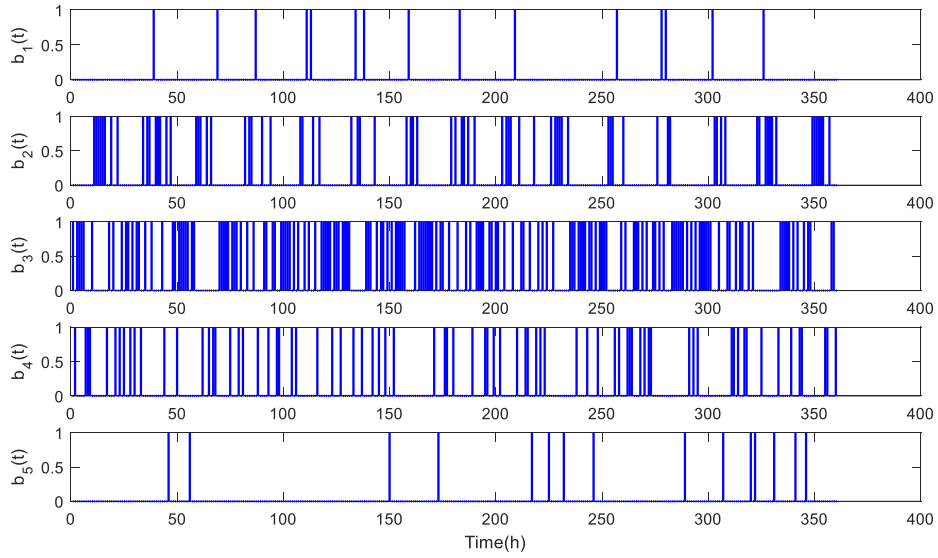

Fig. 4.11 Decision variables b_1 to b_5 for HVAC operation in Scenario 2.

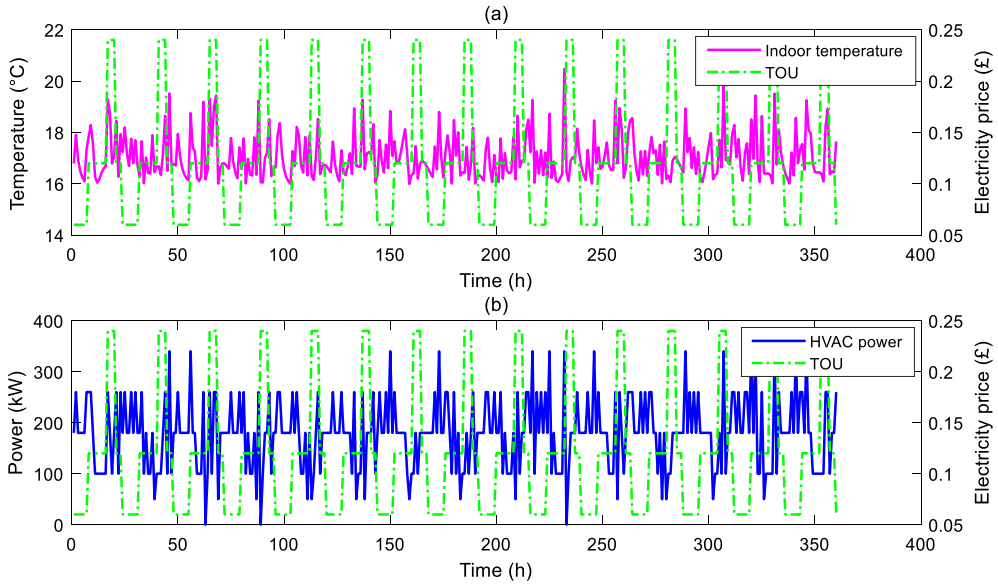

Fig. 4.12 (a) Indoor air temperature and (b) HVAC load under the TOU tariff in Scenario 2.

As can be seen from the optimized results in Fig. 4.12 (a), the hotel building's indoor air temperature was kept within the range of $[16, 24]$℃ as expected. When the HVAC system is on, its power is controlled at 5 levels (50, 100, 180, 260, 340) kW (Fig. 4.12 (b)), which is affected by the TOU tariff. The HVAC system is in off status

in a few occasions. In order to reduce the load demand at the period of peak electricity price, the controlled HVAC system increases its load demand before the peak price occurs so as to increase the indoor air temperature in advance before the peak price. In this way the HVAC load is lowered while the internal temperature can still be kept within the desired range; the total system operational cost is thus reduced.

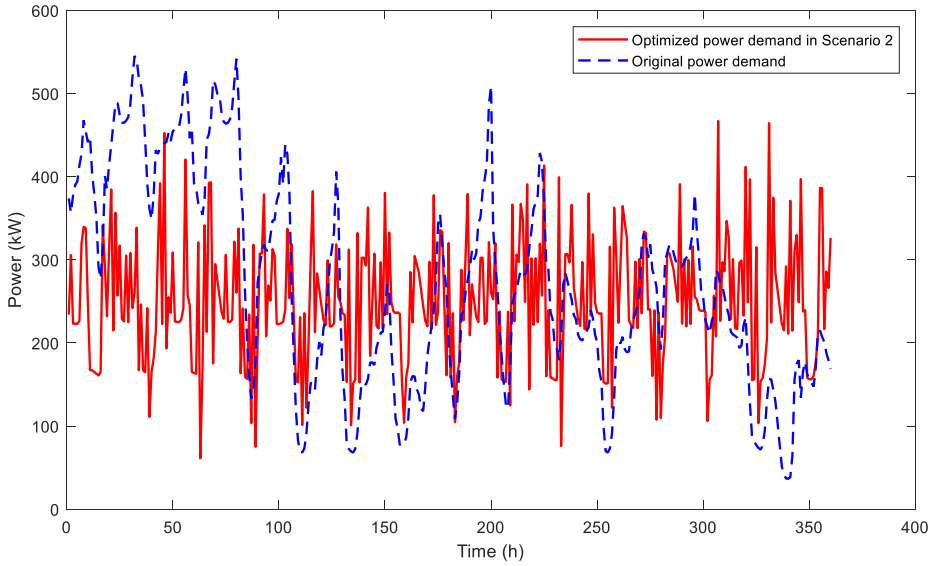

Fig. 4.13 The optimized power demand in Scenario 2 and the power demand in baseline system

In Fig. 4.13, it is shown that the optimized total power demand in Scenario 2 is lower than the baseline power demand most of the time during the 15 days. In the baseline system with survey data, there were times when the hotel was loosely occupied and that reduced power demand, e.g. the temperature control was off for empty rooms. With the HVAC control in Scenario 2, it is assumed that all rooms are occupied and the temperature in all rooms are always kept within the desired range. Thus, the optimized power and total cost of Scenario 2 is higher than the baseline system at some specific time slots as shown in Fig. 4.13 and Fig. 4.14. With the optimal HVAC operation, the sum of total energy cost in Scenario 2 is £11,305, which brings a reduction of 6.1% in the total energy cost from the baseline system's £12,040.

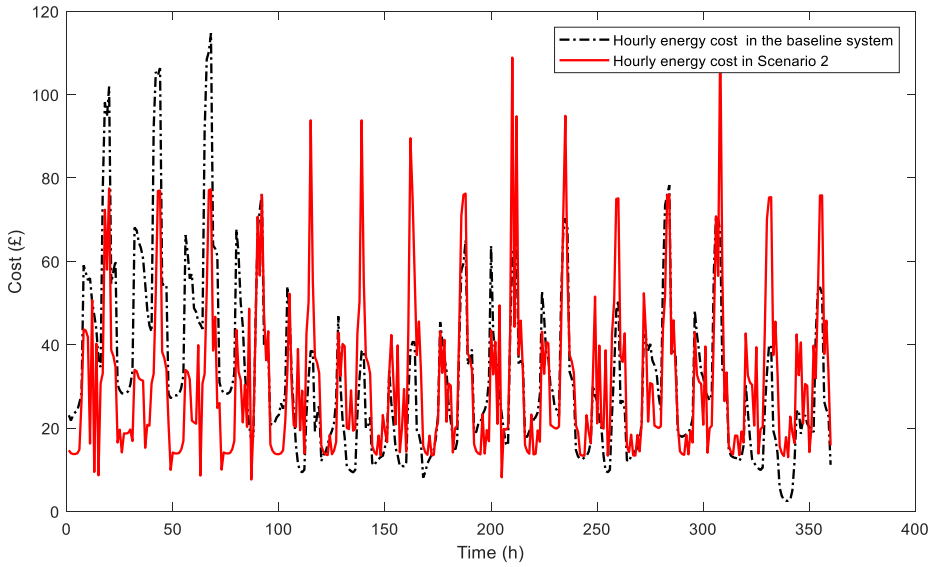

Fig. 4.14 Energy costs under optimal HVAC operation (Scenario 2) and baseline settings

4.5.3. Scenario 3: CHP optimal control combined with HVAC optimal scheduling

In this section, the energy hub operates following the proposed operational strategy in Section 4.3, which is formulated in Eq. (4.21). The system operates with CHP optimal control and HVAC load management together, the latter is also called DSR. The system configuration is shown in Fig. 4.1, which is not repeated here.

The optimized results for the five decision variables in CHP operation and five for HVAC load management are plotted in Fig. 4.15 and Fig. 4.16, respectively.

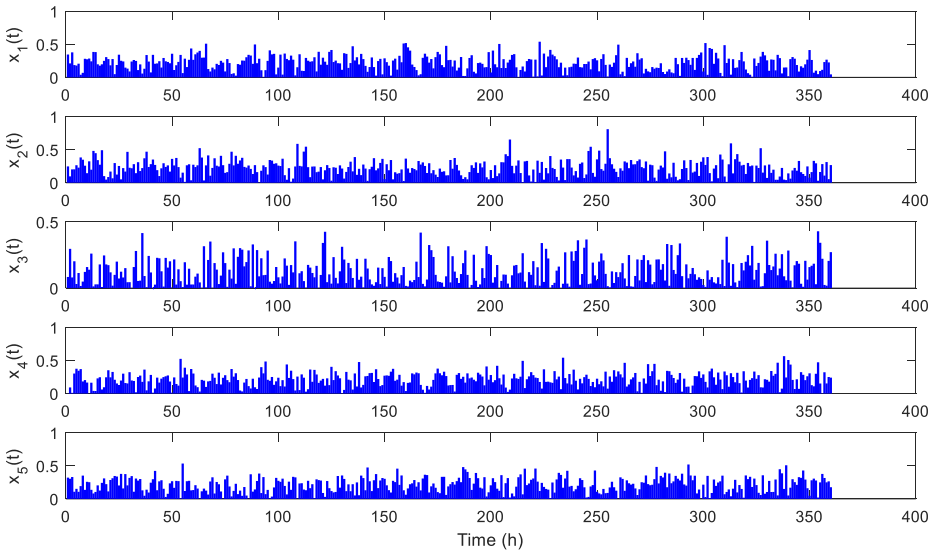

Fig. 4.15 Decision variables x_1 to x_5 for the CHP unit in Scenario 3

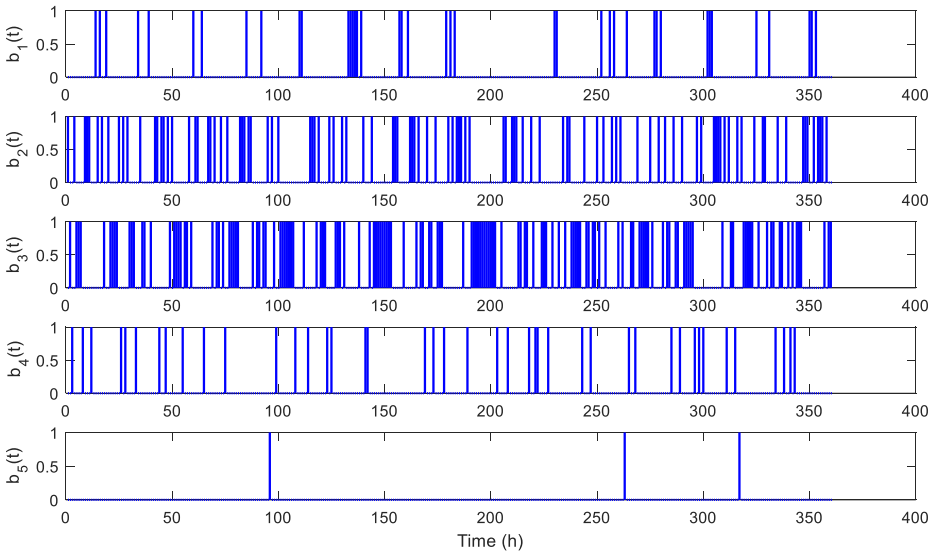

Fig. 4.16 Decision variables b_1 to b_5 for the HVAC system in Scenario 3

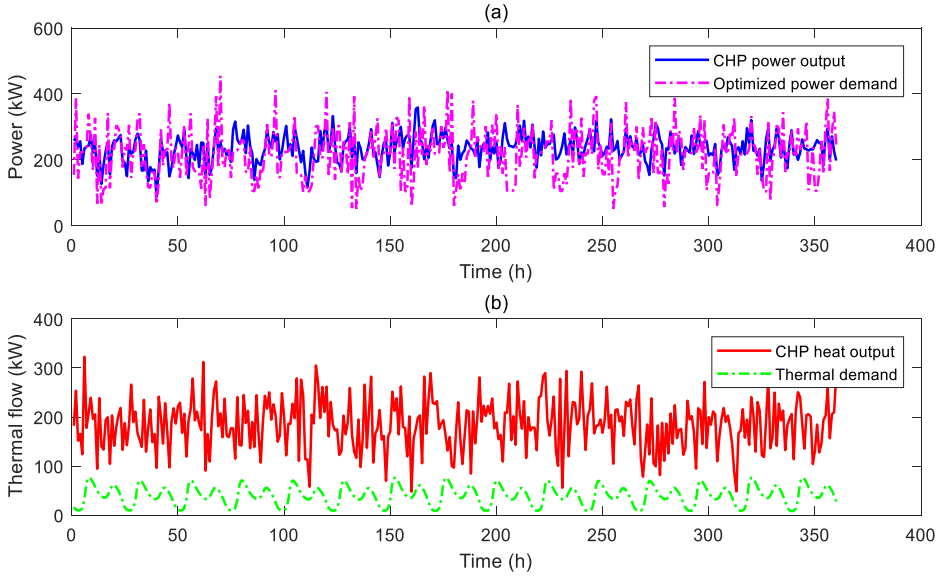

Fig. 4.17 (a) CHP power output and power demand; and (b) CHP heat output and thermal demand in Scenario 3

In Fig. 4.17 (a), the optimized HVAC load and the inflexible loads constitute the optimized power demand. Comparing Fig. 4.7 (a) with Fig. 4.17 (a), it can be seen that the peak value of CHP output power in Scenario 3 is lower than that in Scenario 1 (CHP control only), but the CHP power output in Scenario 3 has smaller variation, which can help to extend the lifecycle of CHP units. In Scenario 3, the power demands are supplied by both the CHP unit and the power grid, among them the CHP provides the majority of electricity demand.

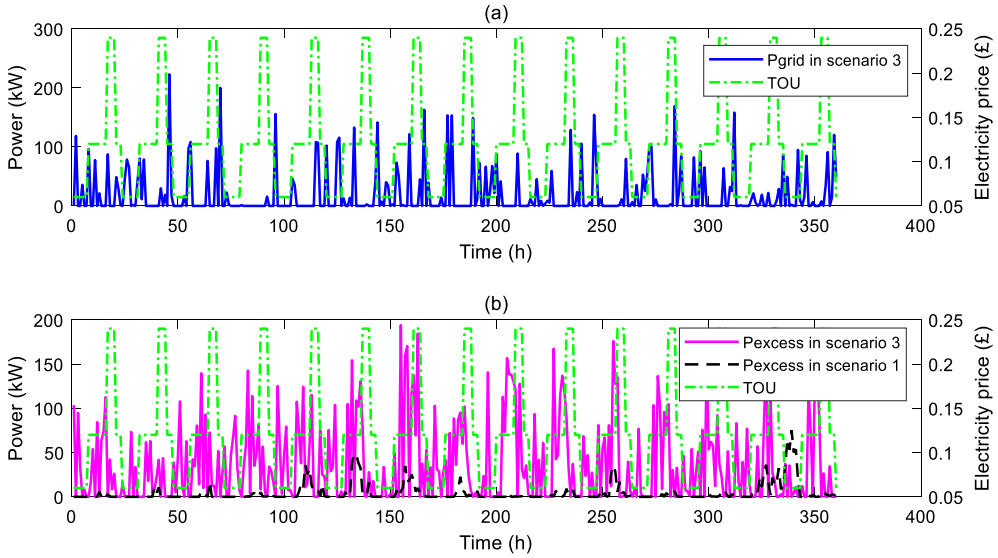

Fig. 4.18 (a) Power purchased from the power grid and (b) power sold to the power grid in Scenario 3

The grid power is shown in Fig. 4.18(a) and the excessive power in Scenario 1 and Scenario 3 are shown in Fig. 4.18(b). It can be seen that in Scenario 3, the Hub system successfully avoids purchasing electricity from the grid during the peak electricity price period. On the other hand, the excess power sold back to the power grid is much more than Scenario 1. Therefore, the system flexibility has been improved through the combination of CHP optimal control and HVAC load management.

The indoor temperature profile is shown in Fig. 4.19 (a) and the HVAC power operation levels are given in Fig. 4.19 (b). It can be seen that the indoor air temperature is kept within the expected range and the HVAC powers operates at 5 levels. The combined strategy in Scenario 3 can not only shift the HVAC load, but also optimize CHP generation under the TOU tariff. With the help of CHP dynamic operation, the DSR program is less dependent on TOU tariff.

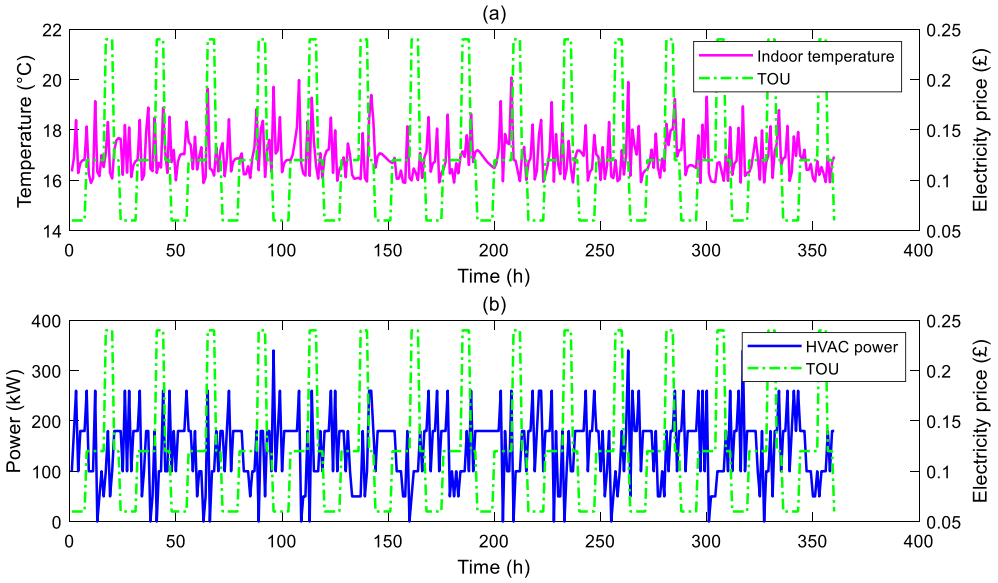

Fig. 4.19 The response of (a) indoor air temperature and (b) HVAC load under the TOU tariff in Scenario 3

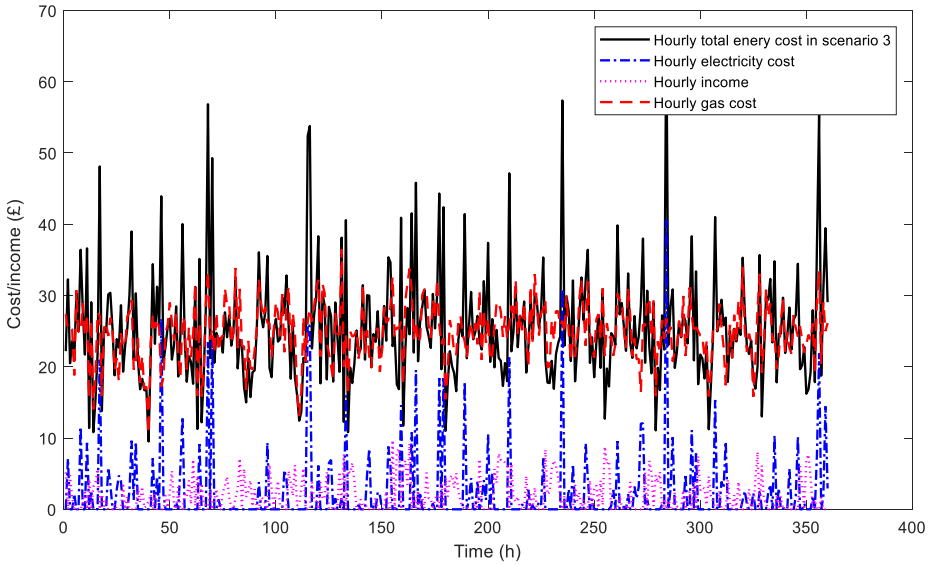

Fig. 4.20 Energy costs and income in Scenario 3.

The energy cost details of Scenario 3 are expressed in Fig. 4.20. Within the 15 days, the main cost of the S.E. Hub is the cost of natural gas, which always keeps at a relatively high level. The electricity cost is much lower in Scenario 3 compared to the that in the baseline system.

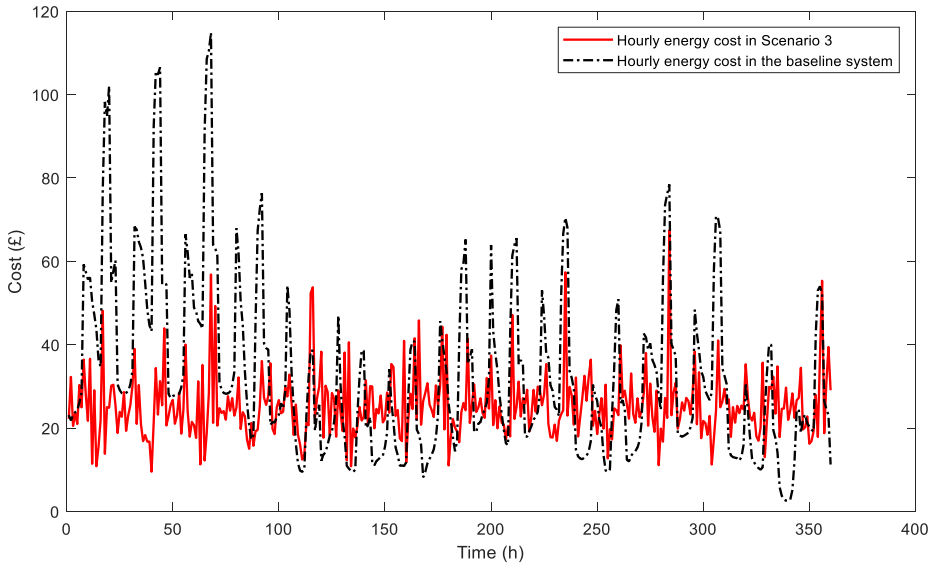

Fig. 4.21 Energy costs under combining CHP optimal control and HVAC load management (Scenario 3) and the baseline system

The total energy cost of Scenario 3 is compared to the baseline system in Fig. 4.21. It can be seen that the optimized total energy cost with the proposed control scheme is significantly lower than that in the baseline system. The total energy cost in Scenario 3 is £9,133 which is a reduction of 24.1% of total energy cost of the baseline system (£12,040). The performance of Scenario 3 is also better than separate CHP control (£9,718) and HVAC load management (£11,305) in Scenarios 1 and 2, respectively, in that the total cost is reduced and the system flexibility is enhanced.

Table 4.3 Statistics on total costs in different scenarios

	Grid cost	Gas cost	Income	Total cost
Baseline system	£11,223	£817	0	£12,040
Scenario 1 – CHP only	£2,414	£7,408	£104	£9,718
Scenario 2 – HVAC only	£10,760	£545	0	£11,305
Scenario 3 – combined CHP and HVAC control	£845	£8,950	£662	£9,133

The optimization results are listed in Table 4.3. The total energy cost in Scenario 3 is lower than both Scenarios 1 and 2. It demonstrates that the combination of CHP optimal control and load management on HVAC system has better performance than CHP or HVAC control alone. In order to achieve the overall S.E. Hub energy cost minimization under varying electricity price, the energy hub system in Scenario 3 can not only shift HVAC load to reduce the electricity usage in peak tariff period, but also modify the CHP operation to reduce the electricity purchase and increase excess electricity sales. The combination of hourly modulating CHP operation and demand responds enhances the system's flexibility under a TOU tariff.

4.6.Summary

In this chapter, an energy cost minimization model for an S.E. Hub is established, based on which the CHP optimal control is integrated with the HVAC load management. The development in this work suggests the possibility to combine the optimal operation of an S.E. Hub with DSR programs. It is revealed that a clear reduction of total energy cost can be achieved with the use of the proposed optimization strategy. Through the comparison among different scenarios, the superiority of the proposed optimization strategy is demonstrated against existing optimization strategies, which separate CHP optimal control and DSR. In the next chapter, further investigation will be focused on system promotion by considering energy storage system.

5. OPTIMAL OPERATION OF CHP AND ENERGY STORAGES INTEGRATED WITH DSR

In an S.E. Hub, an energy storage system is required for the wider and more extensive applications of DSR. In Chapter 4, the proposed optimization framework including CHP optimal control and optimal scheduling of HVAC is established; the EMS can reduce the energy hub's energy cost by adjusting CHP operation and shift the demand load of the HVAC system. However, the economic performance of the CHP unit is not fully explored due to the wasted heat and the DSR performance of HVAC is potential to be further improved. In this regard, it is indispensable to employ energy storage systems as buffer components under a TOU tariff.

In this chapter, the deployment of controllable storage systems for improving the effectiveness of the S.E. Hub's optimization is examined. Safe and economic available range of ESS and TSS, and SOC and DOD-related degradations of ESS are taken into consideration in the optimization problem. Different capacity sizes and charging/discharging power levels of TSS and ESS are tested for a better understanding of optimization performance. The function of ESS and TSS for system flexibility, CHP generation efficiency and the interaction with DSR are investigated in the case study. Moreover, two types of storage modeling methods are investigated in this Chapter. The description of the energy storage system ranges from simple to complex modeling; the simple one doesn't consider the charging/discharging efficiency while the complex one does.

This chapter is arranged as follows. The basic configuration of the upgraded optimization model is introduced in Section 5.1. The model methodology of the storage system and the expanded optimization problem are presented in Section 5.2. The assessment of capacities and charging/discharging power levels of ESS and TSS are performed in Section 5.3. After the most suitable capacities and power levels are

determined, the optimization results of Scenario 4 are obtained in Section 5.4. Subsequently, a new energy storage system method is proposed considering charging/discharging efficiency, which is taken as Scenario 5 in Section 5.5. Finally, a summary is given in Section 5.6.

5.1. S.E. Hub Model Configuration with Energy Storage Systems

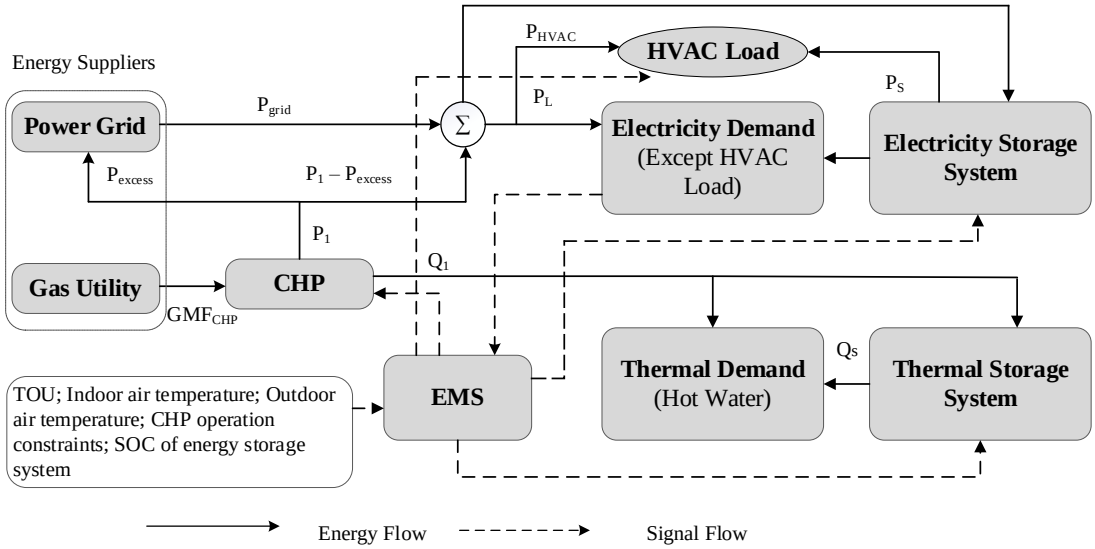

Fig. 5.1 S.E. Hub configuration with energy storage systems

Fig. 5.1 represents a typical S.E. Hub which consist of two energy sources (electricity and gas), a CHP unit, an EMS, an ESS, a TSS, and two types of energy demands, namely the electricity demand and the thermal demand. With the use of ESS and TSS, electricity power and thermal energy can be stored in ESS and TSS and used when required. Most terms are the same as shown in Fig. 4.1. The thermal demand in this system is mainly hot water usage, and the space heating and cooling is supplied by the HVAC system. The thermal demand, Q, is supplied by the CHP heat output, Q_1, and the TSS discharging energy flow, Q_s. The electricity demand is supplied by the CHP output, P_1, the grid power, P_{grid}, and the ESS discharging power, P_s.

EMS is used to gather information such as energy demands, electricity price, environmental temperature, system operation constraints, SOC of ESS and TSS. The

controllable components in this S.E. Hub include CHP unit, HVAC system, ESS and TSS. The EMS controls the power and heat output of CHP unit, the load of HVAC system and the charging/discharging of ESS and TSS to achieve optimal economic performance of the whole S.E. Hub.

5.2. Scenario 4: Optimal Control with ESS and TSS with a Simple Model

The modeling of energy storage systems and the expanded energy cost model will be presented in this section. Referring to the S.E. Hub optimization methodologies in Section 3.1.2, the ESS and TSS operations and self-discharging rates are considered in this chapter. To start with, the charging/discharging efficiencies are not considered which will simplify the modeling. A more complex modeling method of ESS and TSS will be presented later in Section 5.5.

5.2.1. Storage system modeling

The energy storage systems include ESS and TSS. The energy stored in ESS and TSS are denoted as S_P and S_Q, and the SOC of ESS and TSS are respectively described as [186]

$$SOC_{ESS}(t) = \frac{S_P(t)}{C_{ESS}} \tag{5.1}$$

$$SOC_{TSS}(t) = \frac{S_Q(t)}{C_{TSS}} \tag{5.2}$$

where C_{ESS} and C_{TSS} are the storage capacities of ESS and TSS respectively.

Considering the storage efficiencies [187], the time-varying energy stored in ESS and TSS are described by

$$S_P(t) = \eta_P \cdot S_P(t-1) - P_s(t) \tag{5.3}$$

$$S_Q(t) = \eta_Q \cdot S_Q(t-1) - Q_s(t) \tag{5.4}$$

where η_P and η_Q are the storage efficiencies of ESS and TSS considering their self-discharging rates, which are set as 0.99 and 0.95 respectively.

In order to maintain the stability of the whole system, the charging/discharging power levels of each cycle are assumed to be fixed. The charging/discharging power of ESS and TSS are formulated as on/off models without charging/discharging efficiencies, which are formulated as

$$P_s(t)=\begin{cases}+e, & \text{if ESS is discharging}\\ -e, & \text{if ESS is charging}\\ 0, & \text{otherwise}\end{cases} \tag{5.5}$$

$$Q_s(t)=\begin{cases}+a, & \text{if TSS is discharging}\\ -a, & \text{if TSS is charging}\\ 0, & \text{otherwise}\end{cases} \tag{5.6}$$

where e and a (kW) are the charging/discharging powers of ESS and TSS respectively, they are two positive constants.

The energy stored in ESS and TSS are subject to equipment limitations [120].

$$S_P^{\min} \le S_P(t) \le S_P^{\max} \tag{5.7}$$

$$S_Q^{\min} \le S_Q(t) \le S_Q^{\max} \tag{5.8}$$

where $S_P^{\min}$ and $S_P^{\max}$ are the minimum and the maximum energy stored in ESS; and $S_Q^{\min}$ and $S_Q^{\max}$ for minimum and maximum energy stored in TSS.

The storage capacity of TSS equipped with unpressurized water tanks is calculated by Eq. (5.9), which considers water temperatures at the top and at the bottom of the tank. A drop of $5℃$ of water temperature is assumed in the district heating network at its inlet and outlet [187]. Moreover, the maximum temperature is set to be $98℃$ for an unpressurised TSS.

$$S_Q^{\max} = \frac{1}{3600}\rho \cdot V \cdot C_{water} \cdot \left\{ \min\left[\left(t_g - 5\right), 98 \right] - \left(t_h + 5\right) \right\} \tag{5.9}$$

where ρ is the water density; V is the water volume in the TSS; C_{water} is the specific heat capacity of water, $C_{water} = 4.2kJ/\left(kg \cdot °C\right)$; t_g and t_h are the supply and return water temperatures in the district heating network, respectively.

After employing TSS, the new thermal demand constraint is formulated as

$$\eta_1^{heat} \cdot Q_1(t) + Q_s(t) \geq Q(t) \tag{5.10}$$

- **ESS's cost of SOC-related degradation**

The SOC-related degradation cost of ESS can be formulated as

$$c_{SOC}^{ESS}(t) = c_{con}^{ESS} \cdot \frac{\alpha \cdot SOC(t) - \beta}{CF_{\max} \cdot 15 \cdot 365 \cdot 24} \tag{5.11}$$

where c_{con}^{ESS} is the construction cost of the battery, which is assumed as $£15000/100kW \cdot h$ [63]; α and β are determined by linear regression from the battery's measured data, which is set as $1.59 \cdot 10^{-5}$ and $6.41 \cdot 10^{-6}$, respectively [188]; CF_{max} is the maximum capacity fade constant, which is set as 20% in this work, it represents the lifetime of battery will end when the SOC of the battery cannot charge up to 80%. And the lifetime of the ESS is set as 15 years in this work.

- **ESS's cost of DOD-related degradation**

The DOD of ESS in each time slot can be expressed as

$$DOD(t) = 1 - SOC(t) \tag{5.12}$$

Each discharging cycle cost related to DOD degradation can be expressed by a polynomial function, which is proposed in [189, 190]. The corresponding lifecycle number of the battery is related to the DOD variation (ΔDOD). The number of life cycles is denoted as *Z*, which is formulated as

$$Z = f(\Delta DOD) = \left(1.06 \cdot (\Delta DOD)^4 - 2.80 \cdot (\Delta DOD)^3 + 2.66 \cdot (\Delta DOD)^2 - 1.07 \cdot (\Delta DOD) + 0.17\right) \cdot 10^5 \tag{5.13}$$

The cost of DOD-related degradation can be calculated as

$$c_{DOD}^{ESS}(t) = c_{con}^{ESS} \cdot \frac{\Delta DOD(t)}{f\left(\Delta DOD(t)\right)} \tag{5.14}$$

5.2.2. Energy cost minimization model

In order to reduce the total energy cost of the S.E. Hub, an expanded energy cost minimization model is established in this section. The total energy cost, c_{total}, consists of four parts: electricity cost, $c_{electricity}$, natural gas cost, c_{gas}, the cost of storage system, $c_{storage}$, and the income from selling surplus electricity, c_{income}. Thus, the energy cost model can be formulated as

$$c_{total} = c_{electricity} + c_{gas} + c_{storage} - c_{income} \tag{5.15}$$

$$c_{electricity} = \sum_{t=1}^{T} c_1(t) \cdot P_{grid}(t) \cdot \Delta t \tag{5.16}$$

In Eq. (5.16), the power purchased from power grid, P_{grid}, can be formulated as

$$P_{grid}(t) = P_{HVAC}(t) + P_L(t) - P_s(t) - P_1(t) + P_{excess}(t) \tag{5.17}$$

The cost of natural gas, c_{gas}, can be formulated as

$$c_{gas} = \sum_{t=1}^{T} c_2 \cdot GMF_{CHP}(t) \cdot \Delta t \tag{5.18}$$

where the gas price c_2 is considered as constant; GMF_{CHP} is the gas mass flow of CHP input, which is described by Eq. (4.1) in CHP modeling.

The operational cost of the storage system $c_{storage}$ mainly considers the cost of ESS. The operational cost of TSS is negligible in this study because of its relatively

low construction cost and simple working principle. The heat losses in TSS due to storage time is formulated in Eq. (5.4). In this section, the charging/discharging efficiencies of ESS and TSS are not considered to allow a simple model for storage systems. The cost of ESS typically includes SOC-related degradation cost, c_{SOC}^{ESS}, DOD-related degradation cost, c_{DOD}^{ESS}, and the temperature related degradation cost. The temperature related degradation is usually caused by the fluctuations in charging or discharging. It is negligible for ESS in this thesis, because the charging/discharging current and voltage of batteries are assumed to be stable. The $c_{storage}$ can be formulated as

$$c_{storage}=\sum_{t=1}^{T}\left(c_{SOC}^{ESS}(t)+c_{DOD}^{ESS}(t)\right) \tag{5.19}$$

c_{SOC}^{ESS} and c_{DOD}^{ESS} can be calculated by Eq. (5.11) and (5.14). Thus, the total cost of the energy system is formulated as

$$c_{storage}=\sum_{t=1}^{T}c_{con}^{ESS}\cdot\left(\frac{1.59\cdot10^{-5}\cdot SOC(t)-6.41\cdot10^{-6}}{CF_{\max}\cdot15\cdot365\cdot24}+\frac{\Delta DOD(t)}{f(\Delta DOD(t))}\right) \tag{5.20}$$

Besides, the CHP may generate excess electricity, P_{excess}, which can be sold to the power grid to get profit c_{income}.

$$c_{income}=\sum_{t=1}^{T}c_3\cdot P_{excess}(t)\cdot\Delta t \tag{5.21}$$

$$P_{excess}(t)=\max\left\{P_1(t)-\left(P_{HVAC}(t)+P_L(t)-P_s(t)\right),0\right\} \tag{5.22}$$

$$P_{excess}(t)\cdot P_{grid}(t)=0 \tag{5.23}$$

Referring to the correlation constraints introduced in Section 3.2, Eq. (5.23) indicates that P_{excess} and P_{grid} do not exist at the same time. P_{grid} and P_{excess} are

both affected by CHP operation, optimal scheduling of HVAC system and storage system operation.

The energy cost model of the S.E. Hub is summarized as

$$c_{total} = \sum_{t=1}^{T}\left(c_1(t)\cdot P_{grid}(t) + c_2\cdot GMF_{CHP}(t) - c_3\cdot P_{excess}(t)\right)\cdot \Delta t + \sum_{t=1}^{T}\left(c_{SOC}^{ESS}(t) + c_{DOD}^{ESS}(t)\right) \tag{5.24}$$

In this proposed S.E. Hub operation control model, there are four controllable components namely CHP unit, HVAC system, ESS and TSS. The total number of decision variables of these four components is twelve and they are listed in Table 5.1.

Table 5.1 Decision variables in S.E. Hub optimization of Scenario 4

Components	Decision variables	Values
CHP	x_1, x_2, x_3, x_4, x_5	Real numbers between 0 and 1
HVAC	b_1, b_2, b_3, b_4, b_5	Binary numbers 0 or 1
ESS	$P_s(t)$	Integers $a, -a, 0$
TSS	$Q_s(t)$	Integers $e, -e, 0$

The decision variables are denoted as ϕ_4, and its feasible domain is donated as Φ_4.

$$\phi_4 = \left[x_1, x_2, x_3, x_4, x_5, b_1, b_2, b_3, b_4, b_5, P_s, Q_s \right]^T \tag{5.25}$$

All the components in the energy cost model are included in Eq. (5.24). The constraint functions are established via Eq. (4.4)-(4.6), (5.10), (4.9), (4.11), (5.7)-(5.8), (5.23), for all operations. The complete model for the total energy cost minimization of the S.E. Hub can be established as Eq. (5.26).

$$\phi_4^* = \arg\min_{\phi_4 \in \Phi_4} \left(c_{total}\left(\phi\right) \right)$$

s.t.

$$\begin{aligned}
&P_{excess}\left(t\right) \cdot P_{grid}\left(t\right) = 0 \\
&\sum_{j=1}^{5} x_j(t) = 1 \\
&P_1\left(t\right) \le P_{CHP}^{\max}, \quad \left| P_1\left(t\right) - P_1\left(t-1\right) \right| \le P_{CHP}^{rate} \\
&\eta_1^{heat} \cdot Q_1\left(t\right) + Q_s\left(t\right) \ge Q\left(t\right) \\
&\sum\nolimits_{l_{HVAC}=1}^{5} b_{l_{HVAC}}\left(t\right) \le 1 \\
&T_{\min}^{i} \le T^{i}(t) \le T_{\max}^{i} \\
&S_P{}^{\min} \le S_P(t) \le S_P{}^{\max}, \quad S_Q{}^{\min} \le S_Q(t) \le S_Q{}^{\max}
\end{aligned} \tag{5.26}$$

This is also a mixed-integer programming problem, where GA will be selected to solve this problem. Before comparing this expanded optimization including energy storage systems with the optimization in Chapter 4, the most suitable storage capacities and charging/discharging power levels of ESS and TSS need to be investigated first.

5.3. Investigation of Storage Capacities and Power Levels

The operational models of ESS and TSS are established with fixed charging/discharging power levels as mentioned in Section 5.2.1. For a given S.E. Hub system with determined power and thermal demands illustrated in Fig. 5.2, it is crucial to verify different storage capacities and charging/discharging power levels of ESS and TSS for better performance. According to previous studies [141, 143-144], a suitable power range from a backup storage system occupies 20%-50% of the highest demands in building energy systems. According to Fig. 5.2, the highest power demand is 545.2 kW, and the thermal demands are all less than 100 kW. This section attempts 4 cases of storage systems with different proportions, e.g. the ESS and TSS in Case A can supply around 20% of the peak power and thermal heat demand respectively; the ESS and TSS in Case D can supply around 50% of the peak power and thermal heat demand respectively.

In terms of storage capacity, for safety and economy reasons, the available storage range is limited by their lower and upper bounds shown in Eq. (5.7)-(5.8). Thus, the storage capacities of ESS and TSS are set to be five times or more than charging/discharging powers to ensure the continuity of the storage system operation. The corresponding charging/discharging power for ESS and TSS, and their suitable storage capacities are listed in Table 5.2.

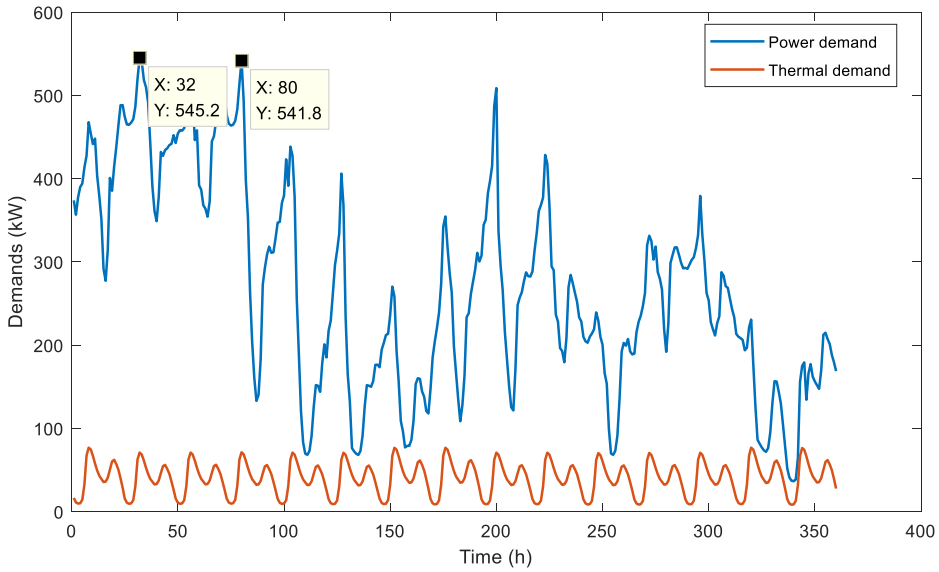

Fig. 5.2 Power and thermal demands in the baseline system

Table 5.2 Charging/discharging power levels and storage capacities of ESS and TSS

	Charging/discharging power of ESS (kW)	Capacity of ESS ($kW \cdot h$)	Charging/discharging power of TSS (kW)	Capacity of TSS ($kW \cdot h$)
Case A	100	500	20	150
Case B	150	750	30	200
Case C	200	1,000	40	250
Case D	250	1,250	50	300

After the storage capacities of ESS and TSS are determined, the corresponding safe storage range in Eq. (5.7)-(5.8). are shown in Table 5.3.

Table 5.3 Available storage range for ESS and TSS

Cases	$S_P^{\min}$	$S_P^{\max}$	$S_Q^{\min}$	$S_Q^{\max}$
Case A	$100kW \cdot h$	$400kW \cdot h$	$15kW \cdot h$	$135kW \cdot h$
Case B	$150kW \cdot h$	$600kW \cdot h$	$20kW \cdot h$	$180kW \cdot h$
Case C	$200kW \cdot h$	$800kW \cdot h$	$25kW \cdot h$	$225kW \cdot h$
Case D	$250kW \cdot h$	$1000kW \cdot h$	$30kW \cdot h$	$270kW \cdot h$

The optimization objective in this work is to minimize the operational cost of the S.E. Hub, the construction cost of TSS is not considered. The construction cost of ESS (c_{con}^{ESS}) is related to the calculation of ESS degradation cost of the storage system by Eq. (5.24). The ESS is lithium-ion battery with $£15000/100kW \cdot h$ [63]. The c_{con}^{ESS} in different cases is valued in Table 5.4.

Table 5.4 Construction costs of ESS in different cases

Cases	c_{con}^{ESS}
Case A	£75,000
Case B	£112,500
Case C	£15,0000
Case D	£187,500

As the same in Chapter 4, the research data are collected from a smart hotel building in Miami State, USA. The system's operating data are collected from [183]. The hotel system in all cases operates under TOU tariffs [184]. And the outdoor air temperature is from the historical Miami State air temperature data in November 2016 [185]. All uncontrollable variables are illustrated in Fig. 5.3. Except for the difference

in storage capacities and charging/discharging powers among the four cases, the setting of the remaining constant parameters related to gas price, feed in tariff, CHP unit, and HVAC system are similar to Table 4.2 in Chapter 4, and the setting of the extra constant parameters about the storage system is listed in Table 5.5.

Table 5.5 Setting of extra constant parameters about ESS and TSS

Parameters	Values	Parameters	Values
η_P	0.99	t_g	$90^{\circ}C$
η_Q	0.95	α	$1.59 \cdot 10^{-5}$
ρ	$997 kg/m^3$	t_h	$40^{\circ}C$
CF_{max}	20%	β	$6.41 \cdot 10^{-6}$

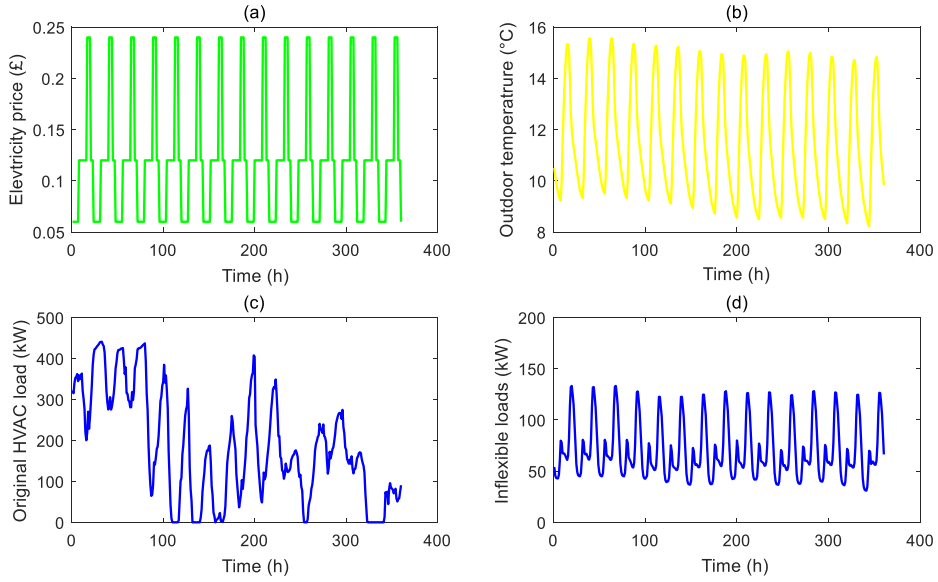

Fig. 5.3 (a) The TOU tariff; (b) Outside air temperature; (c) Original HVAC load without optimization; (d) Sum of inflexible loads

Scenario 4 describes the proposed optimal operational strategy and illustrates the optimization problem formulated in Eq. (5.26). In this scenario, different storage capacities and charging/discharging powers are investigated in four cases, and the setting of related parameters is given in Table 5.2 to Table 5.5. The comparison studies

among the four cases are mainly focused on the working conditions of ESS and TSS, the degradation cost of ESS and the total energy cost in 360 hours.

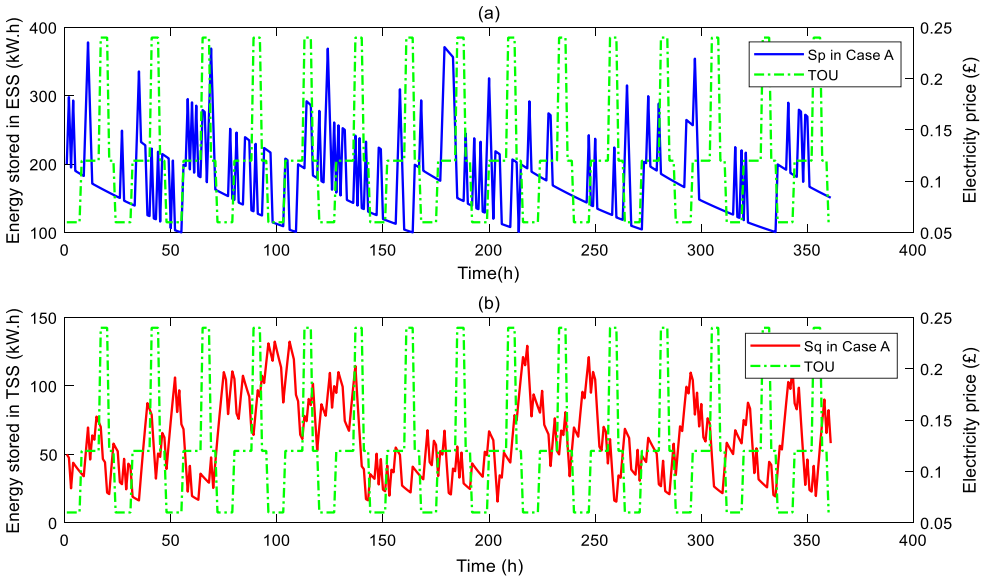

Fig. 5.4 The operating conditions of (a) ESS and (b) TSS in Case A

The electricity power in ESS and thermal energy in TSS in Case A are illustrated in Fig. 5.4(a) and Fig. 5.4 (b), respectively. With the controlled charging/discharging operations, ESS can improve the S.E. Hub system in two aspects. One is to purchase electricity from the power grid during the valley tariff periods through charging. The other one is to support CHP generation with a more economic performance, for example, ESS can share the electricity load with CHP unit at the peak tariff periods. TSS can be used to enhance the CHP performance in response to thermal demand and improve the system stability. TSS help CHP to reduce the impact from thermal demand and to operate at a highly efficient power level for operational cost reduction. Considering safety and economic requirements, the energy stored in ESS and TSS are limited between $100-400\,kW\cdot h$ and $15-135\,kW\cdot h$, respectively in Case A.

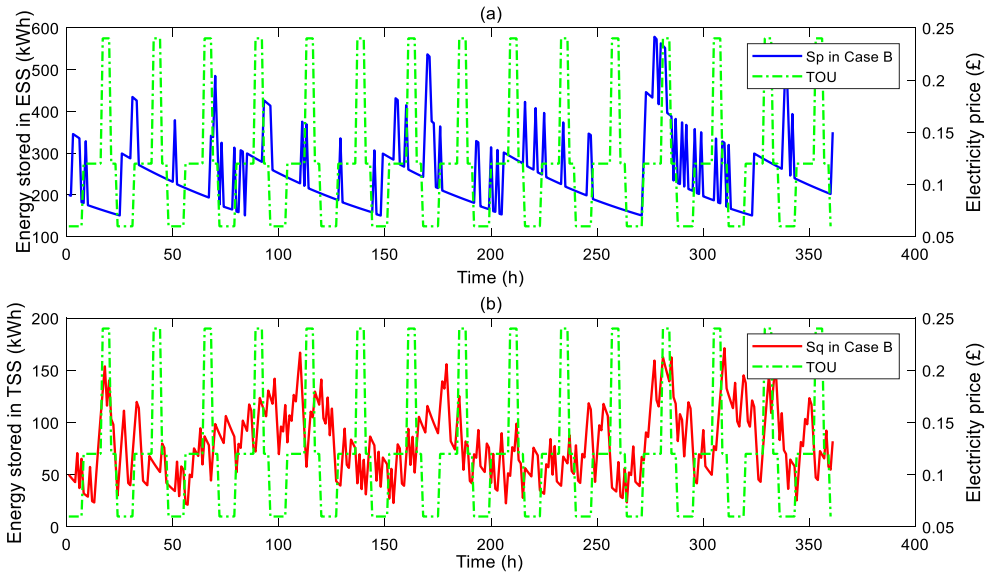

Fig. 5.5 The operating conditions of (a) ESS and (b) TSS in Case B

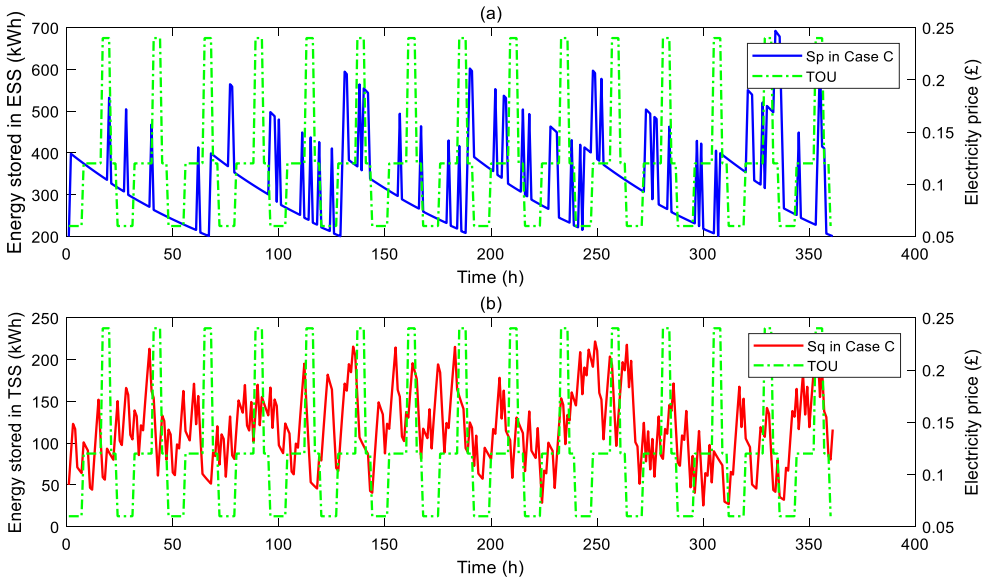

Fig. 5.6 The operating conditions of (a) ESS and (b) TSS in Case C

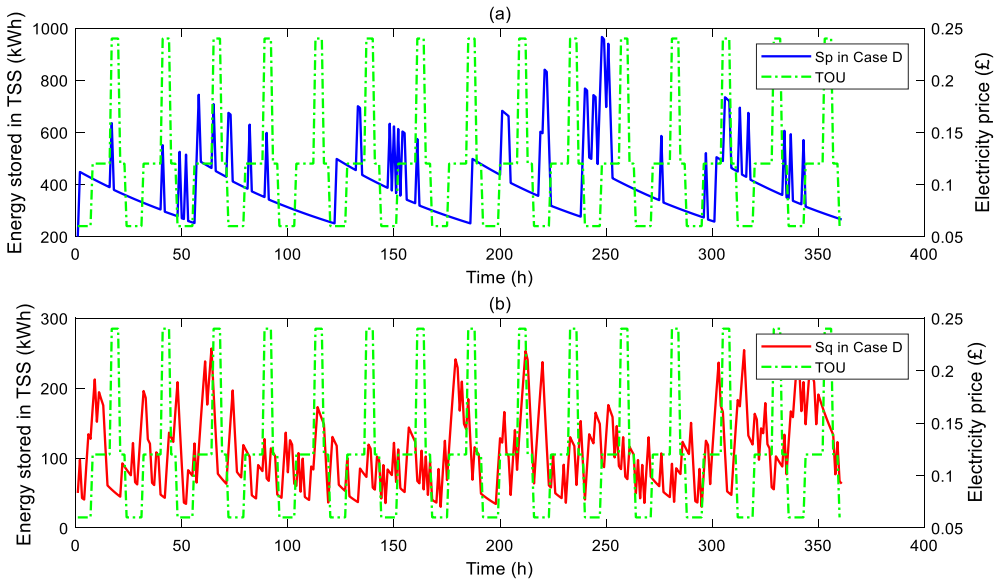

Fig. 5.7 The operating conditions of (a) ESS and (b) TSS in Case D

The operating conditions of TSS and ESS in another three cases are illustrated in Fig. 5.4-Fig. 5.7. The charging/discharging frequency of ESS is decreased when the ESS capacity and charging/discharging powers are increased. The charging/discharging times of ESS and TSS in all four cases are shown in Table 5.6. The change of storage capacities and charging/discharging powers among 4 cases does not impact the operating frequency of TSS, this is because the thermal demand of this S.E. Hub is much lower than the power demand. The main function of TSS is to reduce the thermal impact for full-power generation. The setting of TSS for 4 cases does not change much. Hence, the frequency of TSS operation is not affected.

Table 5.6 Charging/discharging times of ESS and TSS

	ESS charging times	ESS discharging times	TSS charging times	TSS discharging times
Case A	66	58	134	86
Case B	48	41	133	84

Case C	40	33	129	83
Case D	37	31	126	84

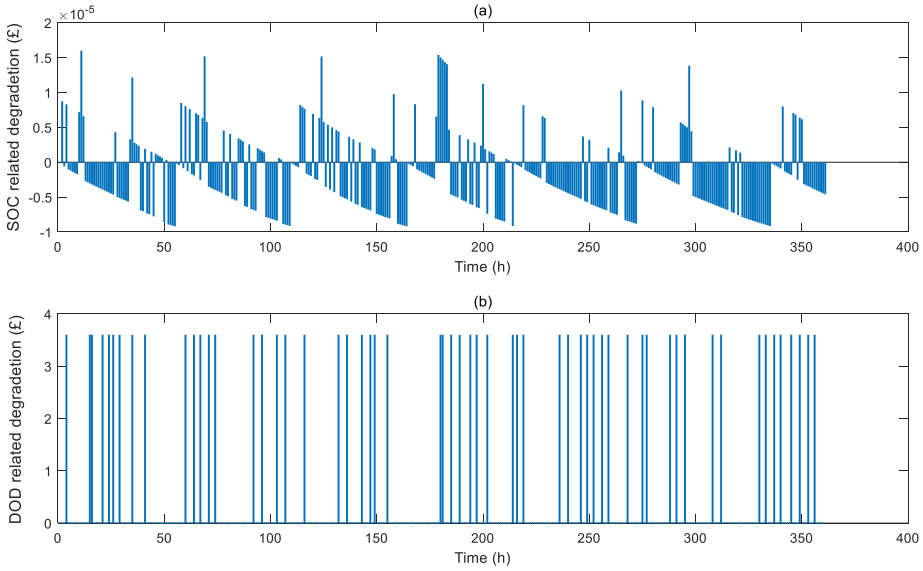

Fig. 5.8 The degradation cost of ESS in Case A: (a) SOC−related degradation and (b) DOD−related degradation

In this work, the degradation cost of ESS is also studied as a part of the S.E. Hub's operational cost. The negative cost of SOC-related degradation in Fig. 5.8(a) means it is beneficial to battery's life. Because the discharging power level is fixed in this model, the DOD variation and the DOD-related degradation cost are both fixed in Fig. 5.8(b). As a result, the SOC-related degradation cost can be ignored, and the sum of DOD-related degradation cost of 58 discharging times in Case A is £208.8. The degradation cost of ESS in the other three cases are illustrated as below.

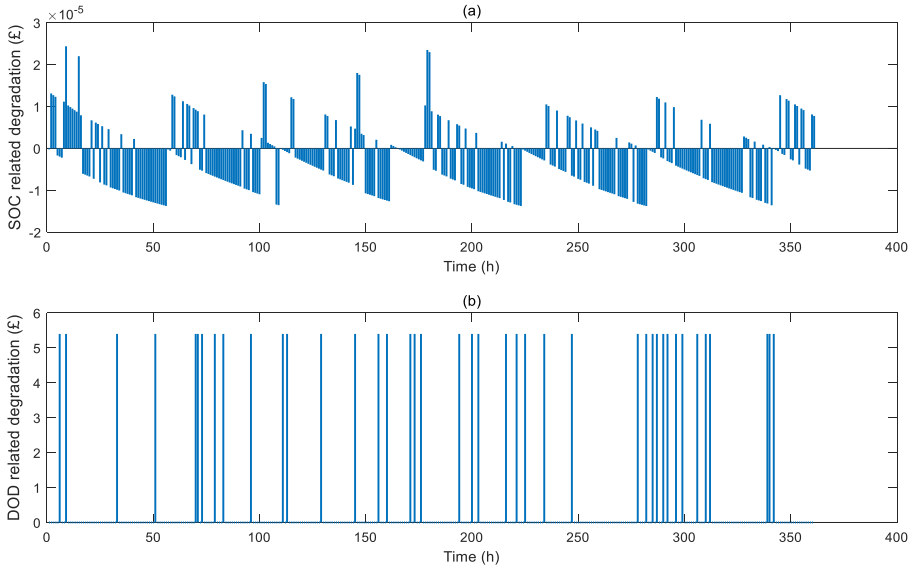

Fig. 5.9 The degradation cost of ESS in Case B: (a) SOC−related degradation and (b) DOD−related degradation

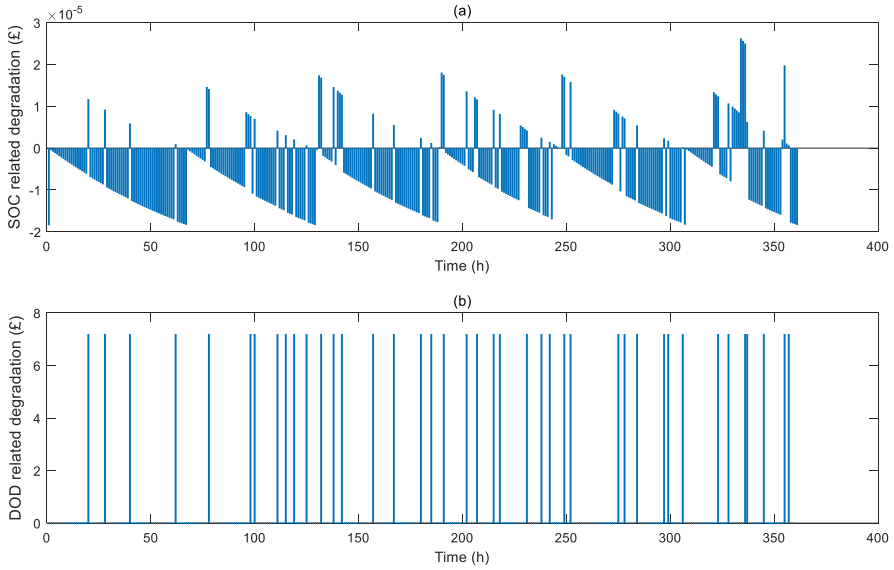

Fig. 5.10 The degradation cost of ESS in Case C: (a) SOC−related degradation and (b) DOD−related degradation

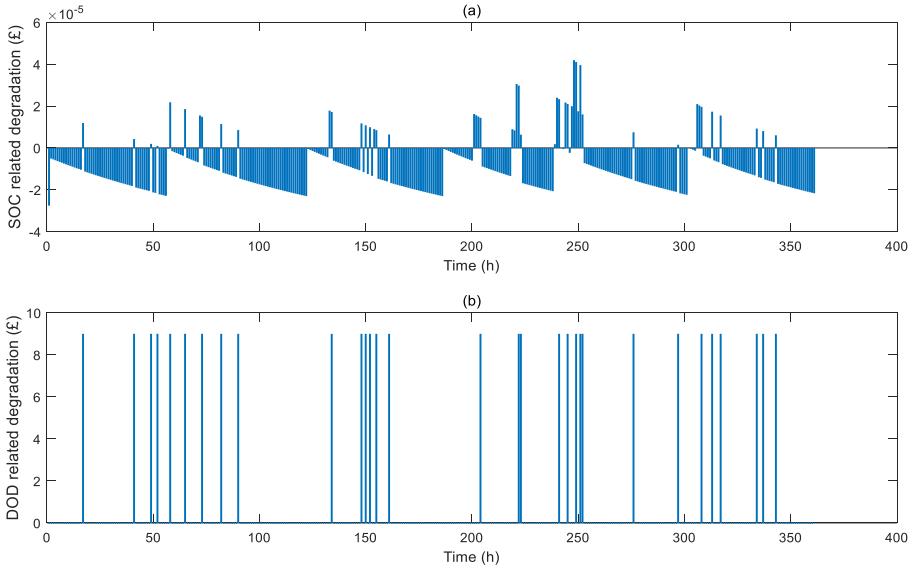

Fig. 5.11 The degradation cost of ESS in Case D: (a)SOC−related degradation and (b)DOD−related degradation

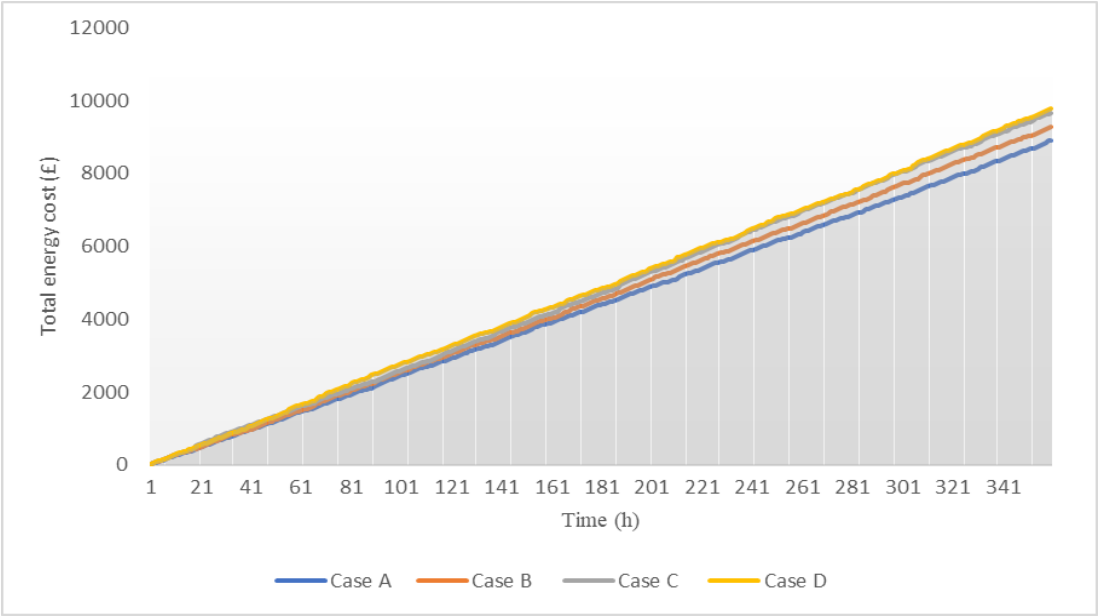

Fig. 5.12 The total energy cost comparison among four cases

According to Fig. 5.9-Fig. 5.11, the SOC−related degradation cost in all four cases can be ignored. Fig. 5.12 shows the total energy costs of 4 cases in 360 hours, where Case A has the lowest total cost and Case D requires the most energy payment. As the storage capacity and charging/discharging powers are higher, the cost of system

operation increases. The total DOD−related degradation cost of ESS and the total operational cost of the S.E. Hub in four cases are listed in Table 5.7.

Table 5.7 Energy cost analysis among 4 cases

	Total DOD-related degradation cost of the ESS	Total operational cost of the S.E. Hub	Total cost without considering degradation cost of ESS
Case A	£208.8	£8,844.3	£8,635.5
Case B	£221.4	£9,279.6	£9,058.2
Case C	£237.3	£9,705.8	£9,468.5
Case D	£279	£9,782.6	£9,503.6

As the storage system capacity increases, the higher construction cost makes the increase of DOD−related degradation cost, even when the number of discharging cycles of ESS decreases. Additionally, the total cost also increases from Case A to Case D without considering the degradation costs of ESS. This indicates that Case A can help the energy hub system operate with a larger benefit. Thus, the storage system capacities and charging/discharging powers in Case A are the best choice for this S.E. Hub system. The following optimization (Scenarios 4 and 5) employs $100kW-500kW\cdot h$ ESS and $20kW-150kW\cdot h$ TSS.

5.4. Optimization Results of Scenario 4

This section shows the results of the proposed optimization scheme in Section 5.2.2. The object of investigating this scenario is to verify whether the optimal operational strategy has better flexibility and optimization effect after adding the energy storage systems. The optimized decision variables ϕ_4 are illustrated in Fig. 5.13-Fig. 5.15.

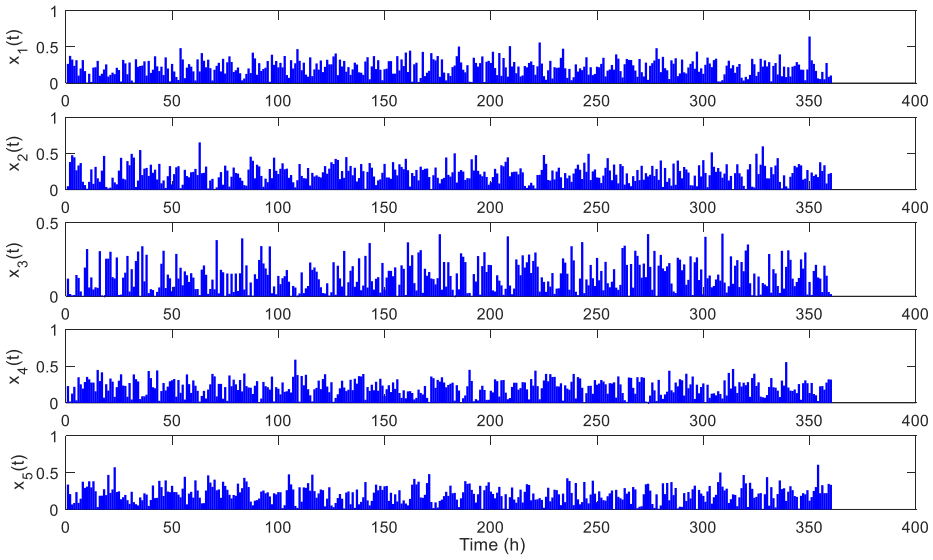

Fig. 5.13 Decision variables x_1 to x_5 for the CHP unit in Scenario 4

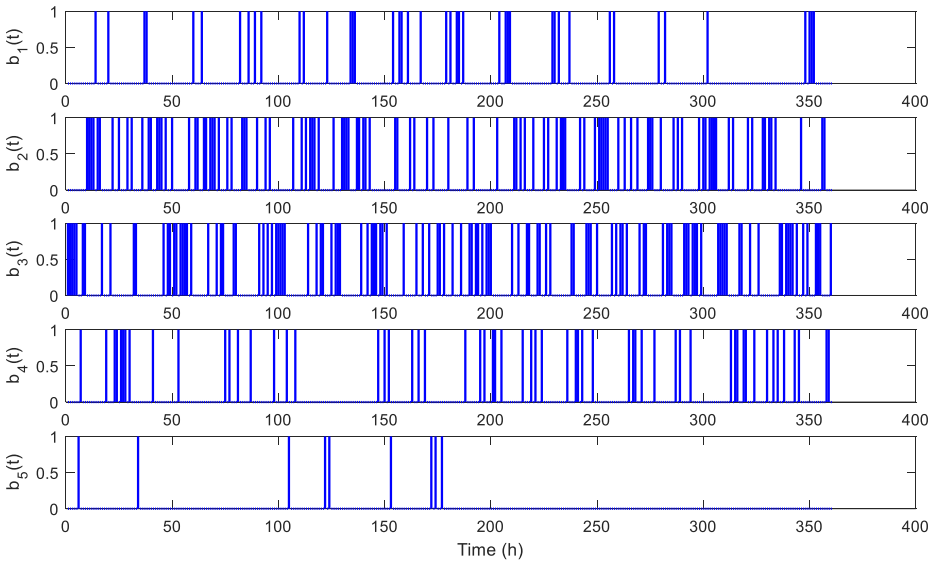

Fig. 5.14 Decision variables b_1 to b_5 for the HVAC system in Scenario 4

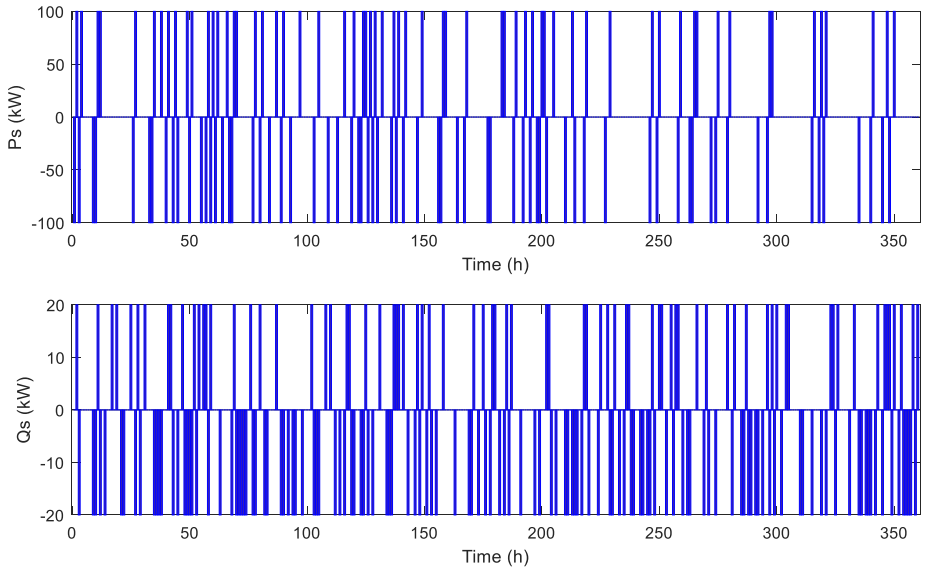

Fig. 5.15 Decision variables P_s and Q_s for the ESS and TSS in Scenario 4

The operation of the storage system is described as Case A in Section 5.3. The energy stored in ESS and TSS and the degradation cost of ESS is illustrated in Fig. 5.4 and Fig. 5.8. In terms of system operation, the CHP power generation and the optimized power demand in Scenario 4 are compared to Scenario 3 in Fig. 5.16. It can be seen that the power generated by the CHP unit can cover the power demand most of the time in Scenario 4, and accompanied with surplus power sold to grid. In Scenario 3, CHP provides the majority of the power demand but rarely beyond 300 kW. The average power generation rate in Scenario 4 is higher than that in Scenario 3, which means a higher power generation can be achieved in the proposed optimal operational strategy taking energy storage systems.

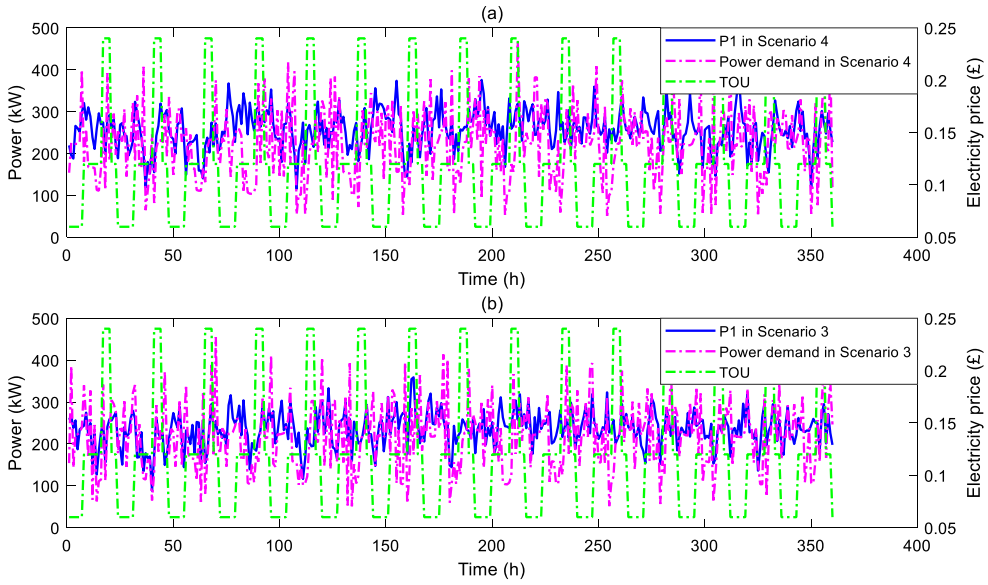

Fig. 5.16 The power generation of CHP and the optimized power demand in (a) Scenario 4 and (b) Scenario 3

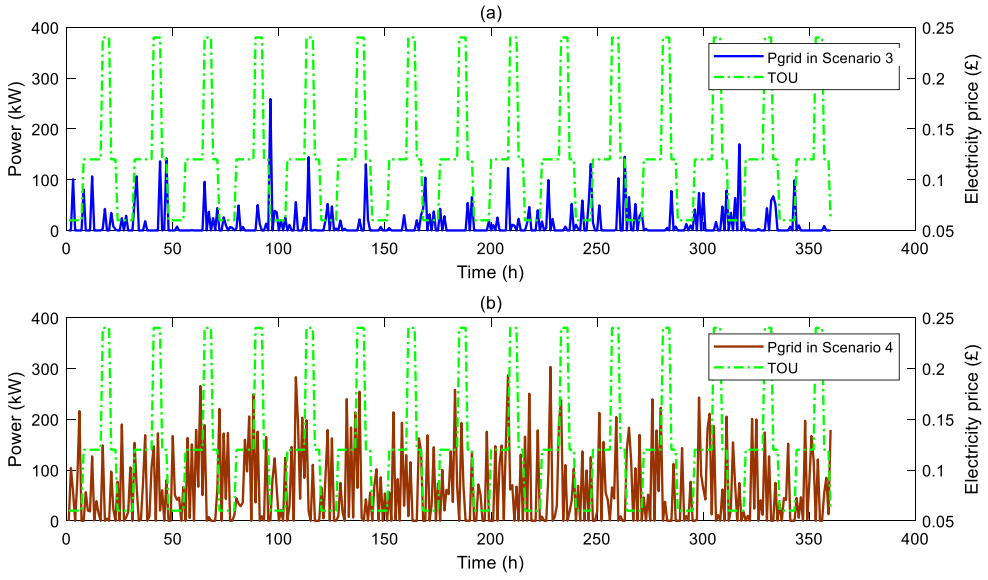

Fig. 5.17 The power purchased from power grid in (a) Scenario 3 and (b) Scenario 4

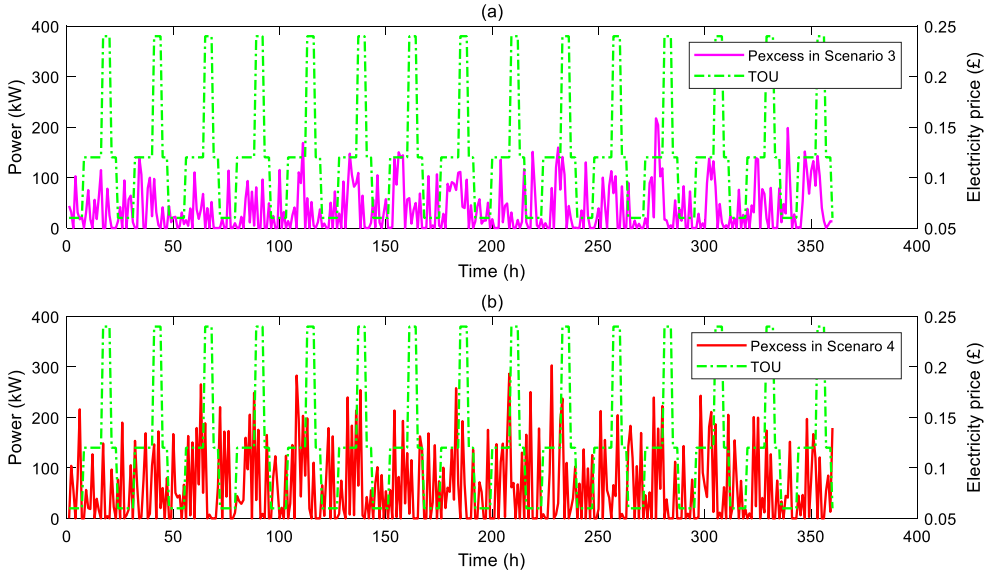

Fig. 5.18 Excess power sold to the power grid in (a) Scenario 3 and (b) Scenario 4

For Scenario 3 and Scenario 4, the purchased power from the grid and the excess power sold back to grid are shown in Fig. 5.17 and Fig. 5.18, respectively. It can be seen that the amount of power purchased from the power grid and the selling back power in Scenario 4 are much higher than those in Scenario 3. The ESS gives more flexibility to the hub system in response to a varying electricity price. The S.E. Hub can purchase more power from the grid during low price region to store in ESS. The combination of ESS and TSS also reduces influence from thermal demand variations. Instead of increasing the indoor air temperature and modifying CHP generation before the peak value of electricity price as in Scenario 3, the system has the alternative to save energy to storage systems. Thus, the proposed strategy implemented in Scenario 4 can further reduce the overall energy cost of an S.E. Hub.

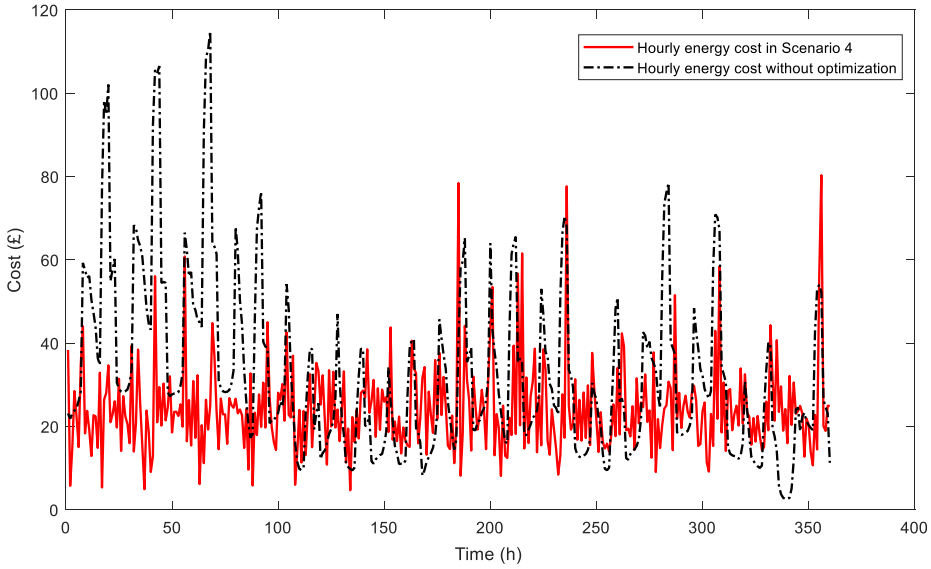

Fig. 5.19 Energy costs in Scenario 4 compared to the baseline system

The sum of energy cost in Scenario 4 is £8,844 including the degradation cost of ESS. It saves 26.5% of total operational cost when compared to the baseline system (£12,040) in Chapter 4. The optimization performance of the proposed strategy in this Section is better than the previous three scenarios in Chapter 4 without energy storage systems. The function of the controllable storage systems in the S.E. Hub system is indicated by comparing Scenarios 3 and 4. The latter further enhances the system's flexibility, assist CHP unit into a better operation to maximize the optimal effect.

5.5. Alternative Modeling of Storage System Considering Charging/discharging Efficiencies

The optimization in Scenario 4 mainly focuses on the function of the energy storage systems and their cooperation with the CHP optimal operation and scheduling of the HVAC system. For simplification, the model employed in Section 5.2 does not consider charging/discharging efficiencies of ESS and TSS. In fact, the charging/discharging of ESS causes energy conversion losses, and the charging/discharging of TSS causes thermal losses in energy transmission. To include

these two factors into optimization, an alternative model for ESS and TSS is employed as in Scenario 5.

The charging/discharging power of ESS and TSS are formulated as on/off models with charging/discharging efficiencies in this section, which are formulated as

$$P_s(t)=\begin{cases}+e\cdot\varphi, & \text{if ESS is discharging}\\ -e\cdot\varphi, & \text{if ESS is charging}\\ 0, & \text{otherwise}\end{cases} \tag{5.27}$$

$$Q_s(t)=\begin{cases}+a\cdot\psi, & \text{if TSS is discharging}\\ -a\cdot\psi, & \text{if TSS is charging}\\ 0, & \text{otherwise}\end{cases} \tag{5.28}$$

where φ is the ESS charging/discharging efficiency, which represents the energy conversion loss. ψ is the TSS charging/discharging efficiency, which covers the transmission loss.

After considering φ and ψ, the system's operation is formulated under four conditions.

- If ESS is discharging, P_s is positive:

The power balance function is

$$P_{grid}(t)=P_{HVAC}(t)+P_L(t)-P_s(t)-P_1(t)+P_{excess}(t) \tag{5.29}$$

The excess power generated by the CHP unit is formulated as

$$P_{excess}(t)=\max\left\{P_1(t)-\left(P_{HVAC}(t)+P_L(t)-P_s(t)\right),0\right\} \tag{5.30}$$

The ESS operation with time-based power storage efficiency is described as

$$S_P(t)=\eta_P\cdot S_P(t-1)-\frac{P_s(t)}{\varphi} \tag{5.31}$$

- If ESS is charging, P_s is negative:

The power balance function is

$$P_{grid}(t) = P_{HVAC}(t) + P_L(t) - \frac{P_s(t)}{\varphi} - P_1(t) + P_{excess}(t) \tag{5.32}$$

The excess power generated by the CHP unit is formulated as

$$P_{excess}(t) = \max\left\{P_1(t) - \left(P_{\mathrm{HVAC}}(t) + P_L(t) - \frac{P_s(t)}{\varphi}\right), 0\right\} \tag{5.33}$$

The ESS operation with time-based power storage efficiency is described as

$$S_P(t) = \eta_P \cdot S_P(t-1) - P_s(t) \tag{5.34}$$

- If TSS is discharging, Q_s is positive:

The TSS operation with time-based thermal storage efficiency is described as

$$S_Q(t) = \eta_Q \cdot S_Q(t-1) - \frac{Q_s(t)}{\psi} \tag{5.35}$$

The thermal demand constraint is formulated as

$$\eta_1^{heat} \cdot Q_1(t) + Q_s(t) \geq Q(t) \tag{5.36}$$

- If TSS is charging, Q_s is negative:

The TSS operation with time-based thermal storage efficiency is described as

$$S_Q(t) = \eta_Q \cdot S_Q(t-1) - Q_s(t) \tag{5.37}$$

The thermal demand constraint is formulated as

$$\eta_1^{heat} \cdot Q_1(t) + \frac{Q_s(t)}{\psi} \geq Q(t) \tag{5.38}$$

The energy cost model of the S.E. Hub in Scenario 5 is the same as in Scenario 4, which is summarized as Eq. (5.24). And similar to Scenario 4, the controllable

components in Scenario 5 are CHP unit, HVAC system, ESS and TSS with 12 controllable variables, which are listed in Table 5.1.

At any time slot t, there are totally 12 decision variables denoted as ϕ_5. The feasible domain of ϕ_5 is donated as Φ_5.

$$\phi_5 = \left[x_1, x_2, x_3, x_4, x_5, b_1, b_2, b_3, b_4, b_5, P_s, Q_s \right]^{\mathrm{T}} \tag{5.39}$$

Hence the complete model for the total energy cost minimization of the S.E. Hub can be established as Eq. (5.40).

$$\begin{aligned}
&\phi_5^* = \arg\min_{\phi_5 \in \Phi_5} \left(c_{total} \left(\phi_5 \right) \right) \\
&s.t. \\
&P_{excess}(t) \cdot P_{grid}(t) = 0 \\
&\sum_{j=1}^{5} x_j(t) = 1 \\
&P_1(t) \le P_{CHP}^{\max}, \quad \left| P_1(t) - P_1(t-1) \right| \le P_{CHP}^{rate} \\
&\eta_1^{heat} \cdot Q_1(t) + Q_s(t) \ge Q(t) \quad \text{when TSS is charging} \\
&\eta_1^{heat} \cdot Q_1(t) + \frac{Q_s(t)}{\psi} \ge Q(t) \quad \text{when TSS is discharging} \\
&\sum\nolimits_{l_{HVAC}=1}^{5} b_{l_{HVAC}}(t) \le 1 \\
&T_{\min}^i \le T^i(t) \le T_{\max}^i; \\
&S_P{}^{\min} \le S_P(t) \le S_P{}^{\max}, \quad S_Q{}^{\min} \le S_Q(t) \le S_Q{}^{\max}
\end{aligned} \tag{5.40}$$

The object of Scenario 5 is to check the performance of the operational strategy by considering charging/discharging efficiency of ESS and TSS. Scenario 5 is a supplementary investigation to Scenario 4. The setting of storage systems in Scenario 5 is shown in Table 5.8.

Table 5.8 Setting of storage system in Scenario 5

	TSS	ESS

Capacity	$500\ kW \cdot h$	$150\ kW \cdot h$
Charging/discharging power	100kW	20kW
Initial storage status (t=0)	$200\ kW \cdot h$	$100\ kW \cdot h$
Charging/discharging efficiency	0.85	0.8

The optimized controllable variables are plotted in Fig. 5.20-Fig. 5.22.

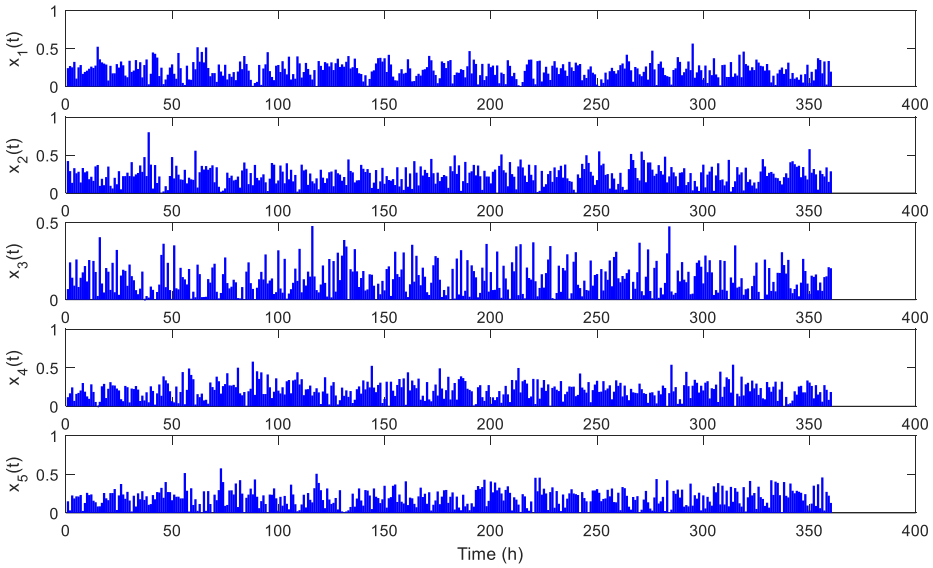

Fig. 5.20 Decision variables x_1 to x_5 for the CHP unit in Scenario 5

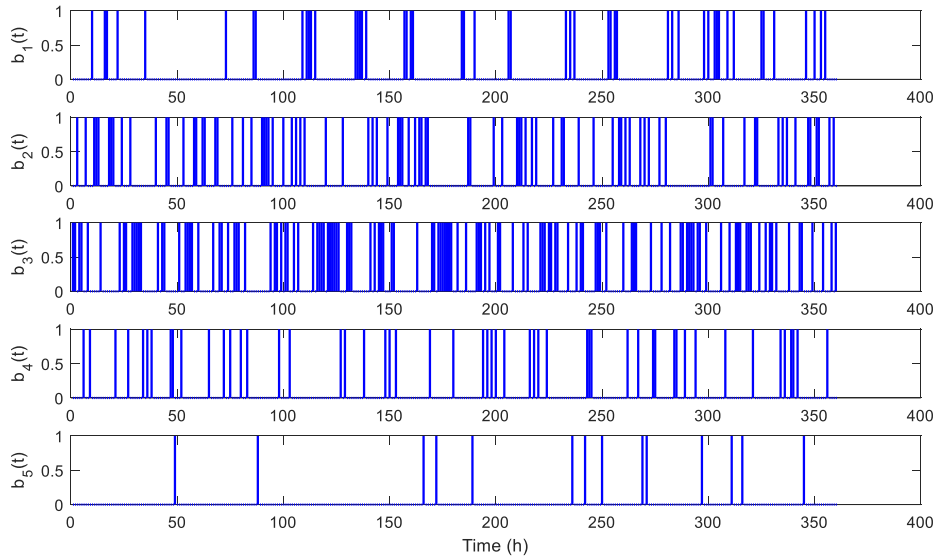

Fig. 5.21 Decision variables b_1 to b_5 for the HVAC system in Scenario 5

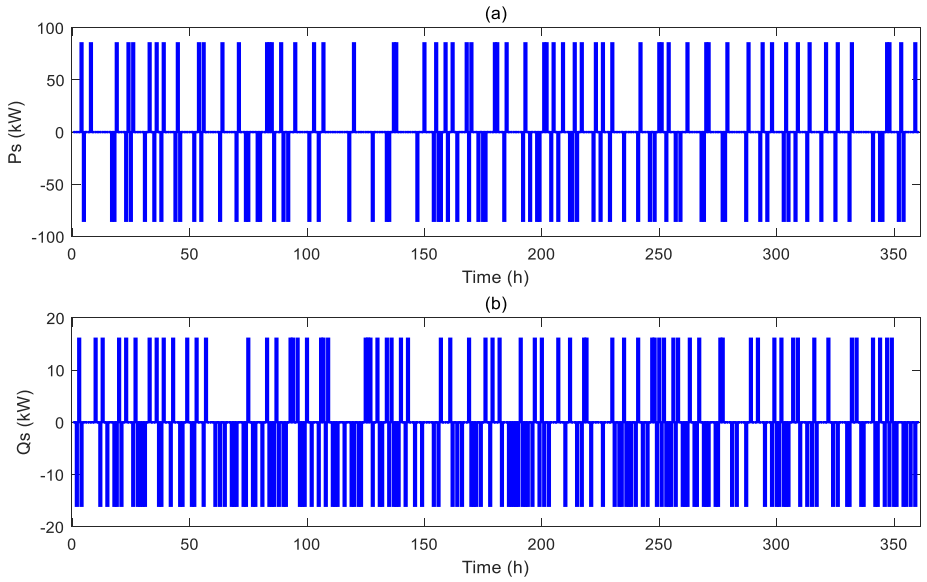

Fig. 5.22 Decision variables (a) $P_s(t)$ and (b) $Q_s(t)$ for the ESS and TSS in Scenario 5

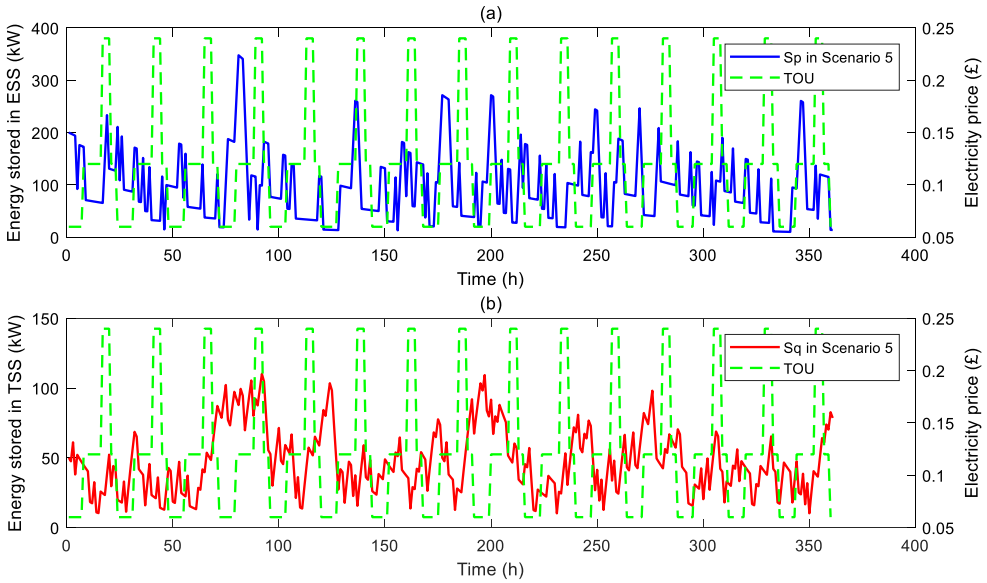

Fig. 5.23 The operation of (a) ESS and (b) TSS in Scenario 5

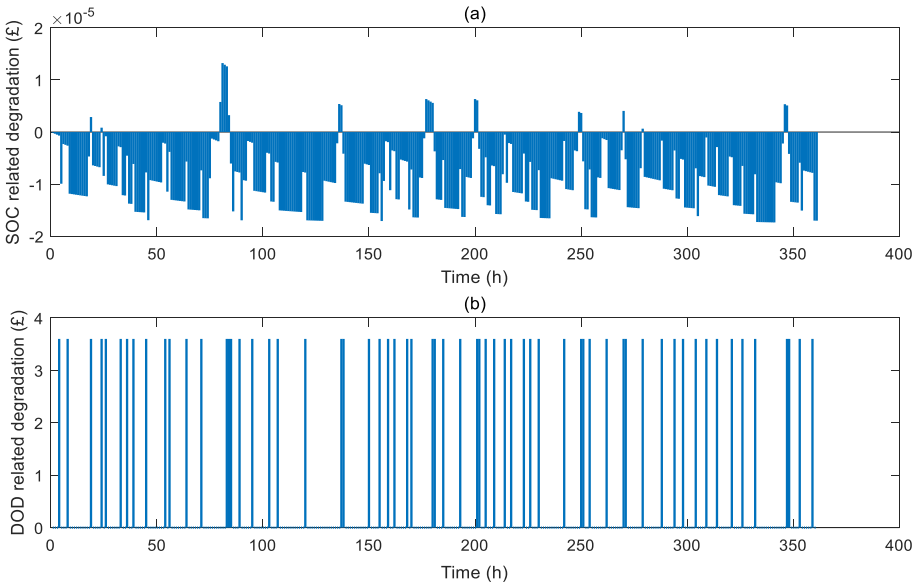

Fig. 5.24 The (a) SOC and (b) DOD−related degradation cost in Scenario 5

Comparing Fig. 5.23 with Fig. 5.4, the ESS in Scenario 5 appears to have weaker storage performance than that in Scenario 4. In order to be practical, the energy stored in ESS in Scenario 5 increases only 85 kW during charging, and decreases 100kW during discharging. And the energy losses due to storage time are also considered,

even when there is no charging/discharging operation. To ensure power balance of charging and discharging, the ESS in Scenario 5 requires more charging times, which means higher cost. The ESS charges 76 times and discharges 63 times in Scenario 5, both of which are higher than the numbers in Scenario 4. The SOC and DOD−related degradation costs are illustrated in Fig. 5.24(a) and Fig. 5.24(b), respectively. As can be observed, the SOC−related degradation costs can be ignored, and the sum of DOD−related degradation cost from 63 discharging activities in Scenario 5 is £226.8.

Next the system flexibility in Scenario 5 is investigated by comparing with Scenario 3. The characteristic of the system flexibility can be reflected by electricity purchased in the valley tariff and the excess electricity sold back to the power grid, which are illustrated in Fig. 5.25 and Fig. 5.26 respectively.

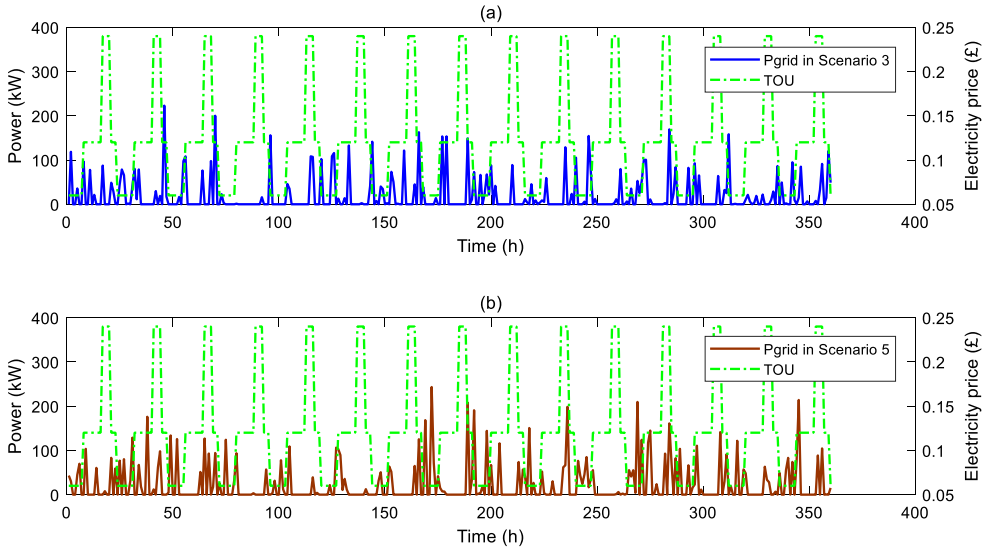

Fig. 5.25 The power purchased form grid in (a) Scenario 3 and (b) Scenario 5

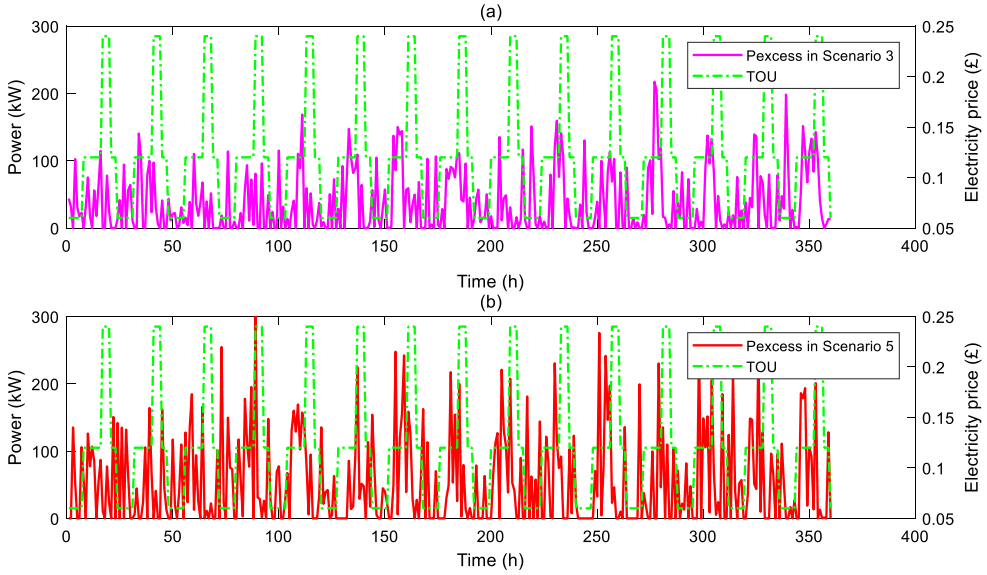

Fig. 5.26 The excess power sold to the grid in (a) Scenario 3 and (b) Scenario 5

In Fig. 5.25, the distribution of purchasing power from the power grid in Scenario 5 shows better performance than that in Scenario 3; it is mainly concentrated on the valley tariff period. This indicates that the average electricity payment to the power grid in Scenario 5 is cheaper than that in Scenario 3. According to Fig. 5.26, the amount of excess power in Scenario 5 is more than that in Scenario 3, which means more profit can be obtained in Scenario 5. All these results indicate that the use of energy storage systems can help to improve the whole system's operation flexibility. The higher degree of system flexibility enhances the system's adjusting ability under varying electricity prices and improves the optimization effect of the S.E. Hub. Comparing with Fig. 5.17 and Fig. 5.18, the system flexibility in Scenario 5 is lower than that in Scenario 4, this is because the charging/discharging efficiencies are considered in Scenario 5.

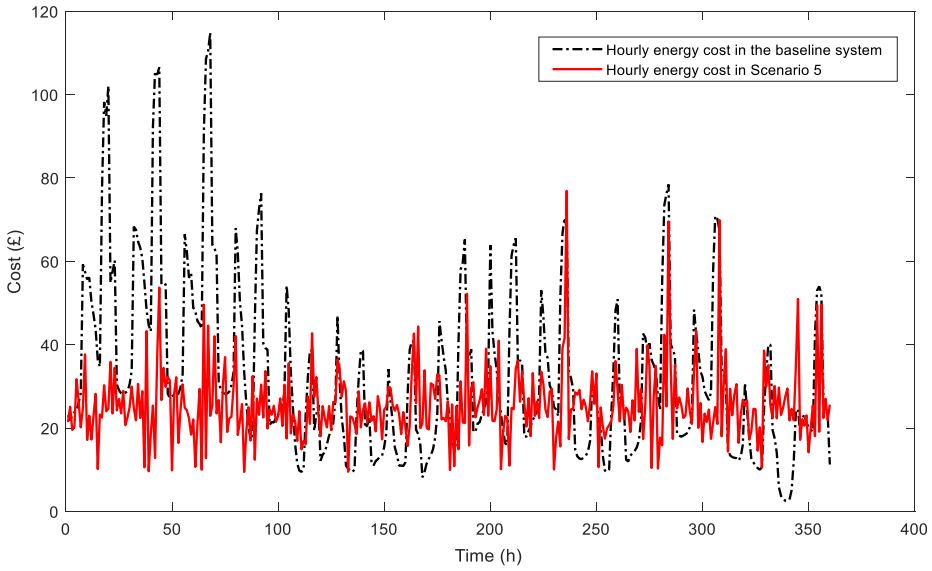

Fig. 5.27 Energy costs in Scenario 5 and the baseline system

As a result, the total operational cost in 360 hours in Scenario 5 is £9,104 including £226.8 degradation cost of ESS. This represents a saving of 24.4% of the total energy cost from the baseline system ((£12,040)). Comparing with Scenario 3 without energy storage systems, the optimization performance is improved when the TSS and ESS are included.

5.6. Summary

In this chapter, an expanded modeling framework has been established for the operational energy cost minimization of an S.E. Hub with added energy storage systems. An operational strategy for EMS is developed to optimally control the CHP unit, ESS and TSS together with optimal scheduling of the HVAC system. System operation requirements and environmental factors are considered in the optimization, including those on CHP's power generation rate, indoor/outdoor/ground/ventilation's temperatures, safe and economic charging/discharging range of ESS and TSS, and two types of degradation cost of ESS.

Different storage capacities and charging/discharging powers of ESS and TSS are investigated to ensure a better understanding of their impacts on the optimization performance. Two modeling methods of ESS and TSS are explored as Scenarios 4 and 5 in this chapter. In Scenario 4, the modeling of ESS and TSS and corresponding calculations are simplified without considering charging/discharging efficiencies. The optimization in Scenario 5 considers the energy conversion losses of ESS and the energy transmission losses of TSS by their charging/discharging efficiencies. The optimization performance in Scenario 5 is slightly lower than that in Scenario 4, but the results from Scenario 5 is more practical.

Table 5.9 Statistics on total costs in different scenarios

Scenarios	Grid cost	Gas cost	Income	ESS cost	Total cost
Baseline system	£11,223	£817	0	0	£12,040
Scenario 1	£2,414	£7,408	£104	0	£9,718
Scenario 2	£10,760	£545	0	0	£11,305
Scenario 3	£845	£8,950	£662	0	£9,133
Scenario 4	£1,679	£7,893	£936	£208	£8,844
Scenario 5	£999	£8,813	£935	£227	£9,104

The optimization results including Scenarios 1-5 are listed in Table 5.9. The total operational cost in both Scenarios 4 and 5 are lower than in Scenario 3. This demonstrates that the combination of the optimal control on the CHP unit, ESS, TSS and HVAC system has better optimization performance than any previous operational strategies without considering ESS and TSS. The function of the storage systems in this chapter is not only to reduce electricity usage at the peak tariff period, but also to enhance the CHP's power generation. The ESS can charge or discharge power to ensure that the CHP unit keeps operating at a higher power-output efficiency. The TSS

can reduce the impact of thermal demand and enable CHP's full-power operation to save electricity cost or increase profits form electricity sales. In a word, ESS and TSS enhance the system's flexibility, assist CHP unit into better performance to maximize the optimal effect, and reduce the side impact of DSR on consumer energy usage.

The results in this chapter demonstrate a new way to improve microgrid operational efficiency through integrated optimal operation of CHP, ESS and TSS under DSR. By comparing with the optimization results of Chapter 4, the superiority of the optimal operational strategy and the function of storage systems for S.E. Hub optimization are demonstrated. Indeed, Scenario 5 reveals that 24.4% of the total energy cost can be saved under the proposed strategy. The DSR in the S.E. Hub system is represented by the optimal scheduling of the HVAC system under TOU in this chapter.

In the next chapter, further investigation will be made on optimal sizing of CHP for investment decision.

6. OPTIMAL SIZING OF CHP CONSIDERING DSR

In this chapter, decision making is discussed through optimization on investing a CHP unit in building retrofit. The objectives are to reduce the building's operational cost and the payback period for a given investment budget. The building's operational cost is minimized by the proposed operational strategy in Chapter 4, where optimal control of the new installing CHP is integrated with HVAC load management. The payback period refers to the simple payback of the CHP investment which is calculated by the quotient of investment and the annual cost savings from the CHP installation.

The optimization problem in this chapter is addressed by combing the two objectives into one scalar fitness function. Subsequently it can be solved by GA, and the optimal sizing of the CHP unit and its investment can be determined by the building owner's priority among the two objectives.

This chapter is arranged as follows. The optimization model for a smart building's operation cost minimization and payback period minimization is proposed in Section 6.1. Following this, the baseline (without HVAC load management) and benchmark system (prior to installing the new CHP unit, but HVAC load is optimized using same scheme as Scenario 2) is described in Section 6.2. Section 6.3 discusses the optimal sizing of the CHP based on different weighting factors. Finally, conclusions are drawn in Section 6.4.

6.1. Optimization Model for Operational Cost Minimization and Payback Minimization

From the perspective of the building owner or building designer, both operational cost and investment payback period should be considered in energy-efficient building retrofit. An optimization model is proposed to reduce operational cost of the whole system as well as the CHP payback period.

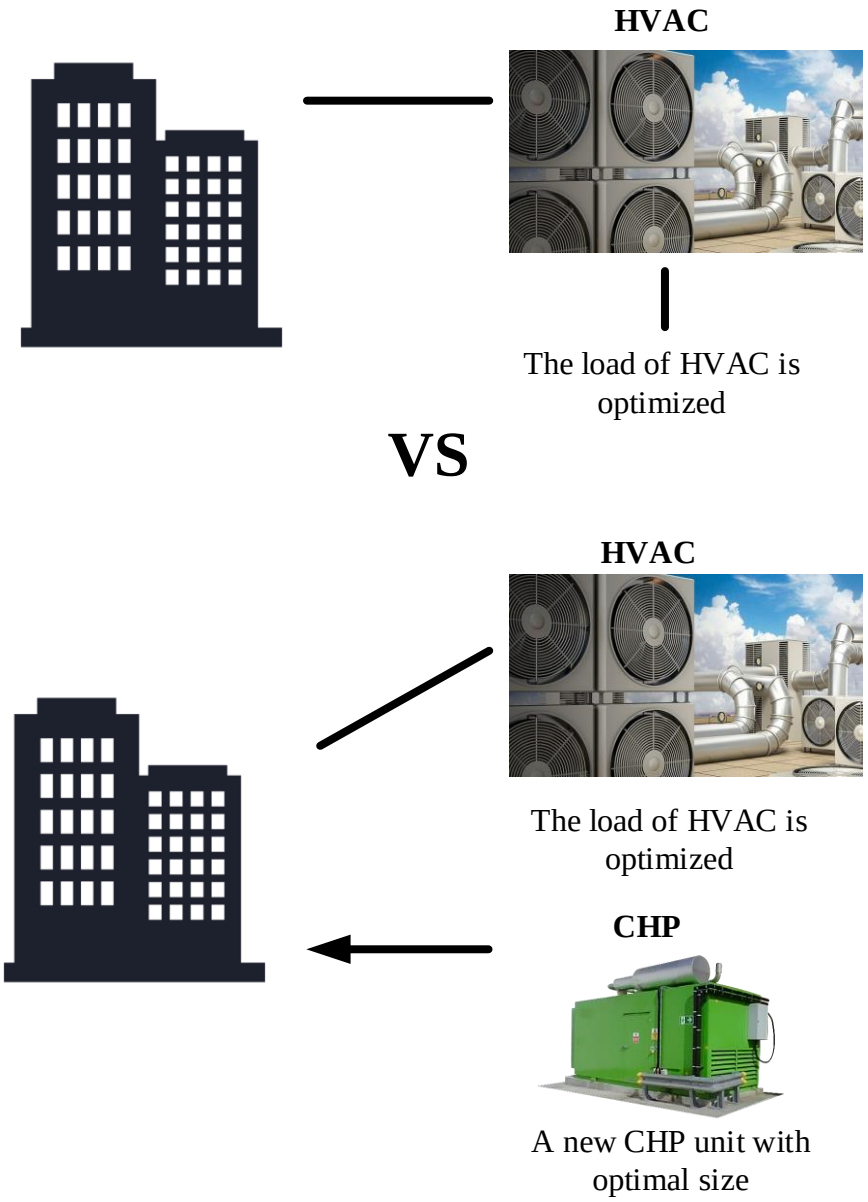

Fig. 6.1 Schematic of the operational cost comparison

To meet the first objective of reducing operational cost of the smart building, optimal power and heat ratio of the CHP unit is dynamically selected and the HVAC load is scheduled, which is similar to Scenario 3 in Chapter 4. For the second objective of reducing the payback period, cost saving is obtained through comparison with a benchmark system (similar as Scenario 2) which implements the optimal load management of the HVAC, as shown in Fig. 6.1. This comparison may lead to a

conservative estimate on investment payback period, which will be much shorter if the HVAC load is not optimized. In the benchmark building system, neither the CHP unit nor the storage systems are included.

The CHP's capacity and price are assumed to satisfy a linear relationship. The unit price of CHP is approximately valued as £35,000 per 100 kW [191]. Let K be an positive integer multiplier of 100 kW in CHP capacity, e.g. $K = 5$ represents that the CHP capacity is 500 kW. K is limited by investment budget I_{budget} as

$$1 \le K \le \frac{I_{budget}}{35,000} \tag{6.1}$$

Since the peak value of power demand in the benchmark building system is between 400-500 kW, designing a CHP unit exceeding 500 kW is not required.

$$1 \le K \le 5 \tag{6.2}$$

The maximal CHP output power constraint is rewritten as

$$P_1(t) \le 100K \tag{6.3}$$

The CHP model is the same as in Eq. (4.1)-(4.3) in Chapter 4, and the CHP operating constraints are described in Eq. (4.4)-(4.7). The HVAC modeling and operating constraints, including indoor air temperature comfortable range, are the same as in Scenario 2, 3, 4 and 5 in the previous two chapters.

The operational cost minimization model for the first objective is similar to Scenario 3 in Section 4.3. The total energy cost c_{total} consists of three parts: electricity cost, natural gas cost and the income from selling excess electricity. There are two kinds of controllable components (i.e. CHP and HVAC), and for each K there are 10 corresponding controllable variables denoted as ϕ^K and its feasible domain is denoted as Φ^K.

$$\phi^K = \left[x_1, x_2, x_3, x_4, x_5, b_1, b_2, b_3, b_4, b_5 \right]^{\mathrm{T}} \tag{6.4}$$

where $x_1 - x_5$ are the decision variables for CHP dynamic control; $b_1 - b_5$ are the 0/1 binary decision variables for HVAC operation management.

The payback period $f_2(K)$ can be calculated by the CHP investment I_{CHP} and the benefits in one year due to energy cost saving B. Load management of the HVAC system implemented in the benchmark system is similar to Scenario 2. Thus, the energy reduction of the new building system with CHP is compared to $c_{daily}^{S_2}$, which is the average daily energy cost of benchmark building in Scenario 2. The two objectives can be defined as

$$\min f_1\left(K, \phi^K\right) = c_{total}\left(\phi^K, K\right) \tag{6.5}$$

$$\min f_2\left(K, \phi^K\right) = \frac{I_{CHP}}{B} = \frac{35000 \cdot K}{365 \cdot \left(c_{daily}^{S2} - f_1\left(K, \phi^K\right)\right)} \tag{6.6}$$

subject to

$$f_1\left(K, \phi^K\right) \le c_{daily}^{S2} \tag{6.7}$$

$$f_2\left(K, \phi^K\right) \le \xi \tag{6.8}$$

and also other constraints in Eq. (6.1)-(6.3), (4.4)-(4.7), (4.9) and (4.11). $f_1(K, \Phi^K)$ is the operational cost of a typical day; ξ is the allowed maximum payback period in years.

The problems presented in Eq. (6.5) and (6.6) are two separate optimization problems, which can be combined into a single optimization by weighting factors λ_1 and λ_2.

$$K^* = \arg\min\left(\lambda_1 \cdot \frac{f_1\left(K, \phi^K\right)}{c_{daily}^{S2}} + \lambda_2 \cdot \frac{f_2\left(K, \phi^K\right)}{\xi} \right) \tag{6.9}$$

subject to

$$\lambda_1+\lambda_2=1,\ \lambda_1>0,\ \lambda_2>0. \tag{6.10}$$

and other constraints in Eq. (6.1)-(6.3), (6.7)-(6.8), (4.4)-(4.7), (4.9) and (4.11).

The two terms in Eq. (6.9) is normalized by $\frac{f_1\left(K,\phi^K\right)}{c_{daily}^{S2}}$ and $\frac{f_2\left(K,\phi^K\right)}{\xi}$, so that they stay a comparable range. The optimization problem obtained above is a mixed-integer programming problem. It is a global optimization problem, which will be solved by GA.

6.2. System Specifications

This chapter aims to find the optimal sizing of the CHP unit considering CHP hourly operation and HVAC scheduling. The research data are collected from the same hotel building as in Chapters 4 and 5. The established operation model (only with load management of HVAC, but without CHP and storage system) of Scenario 2 in Chapter 4 is assumed as the benchmark system for results comparison in this section. However instead of 360 hours in the previous scenarios, the operational cost of the smart building in a typical day (24h) is adopted to simplify the calculation, and this typical day refers to a day with specific average energy consumption. The settings of constant parameters are the same as in Table 4.2, except the values of characteristic points in CHP modeling.

Table 6.1 The corresponding values for CHP cost, power and heat of five characteristic points

Cost/Power/Heat	Values of each characteristic point
μ_j (£)	$(2, 2, 9, 7, 6.8)\cdot K$
p_j (kW)	$(16, 16, 50, 80, 80)\cdot K$

q_j (kW)	$(2, 40, 100, 70, 2)\cdot K$

The investment budget I_{budget} is set at £175,000, and the allowed maximum payback period ξ is 3.5 years. The given data (including TOU tariff, outside building temperature, HVAC load, the sum of inflexible loads, total power demand and thermal demand) in a typical day are obtained by calculating their average hourly data over 15 days. These obtained daily data are plotted as Fig. 6.2.

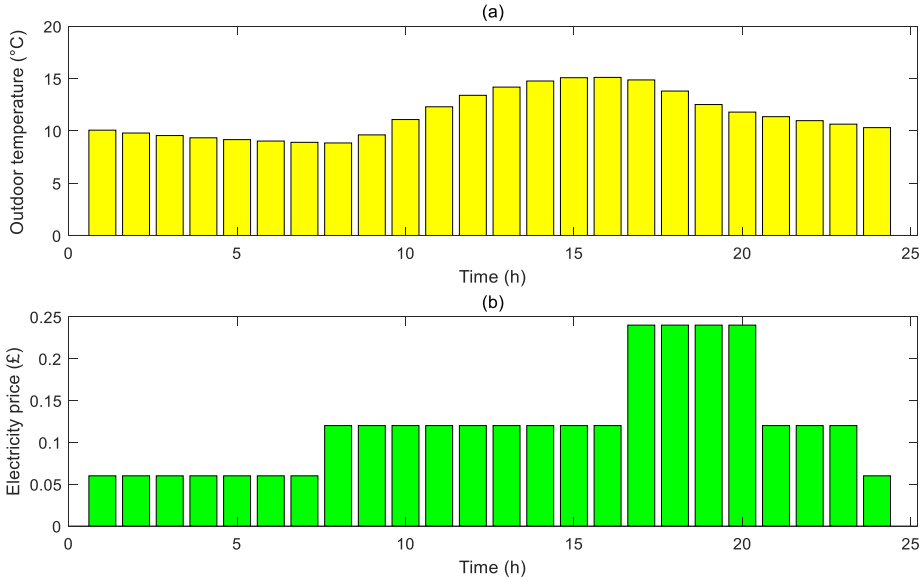

Fig. 6.2 (a) Outdoor temperature and (b) TOU tariff in a typical day

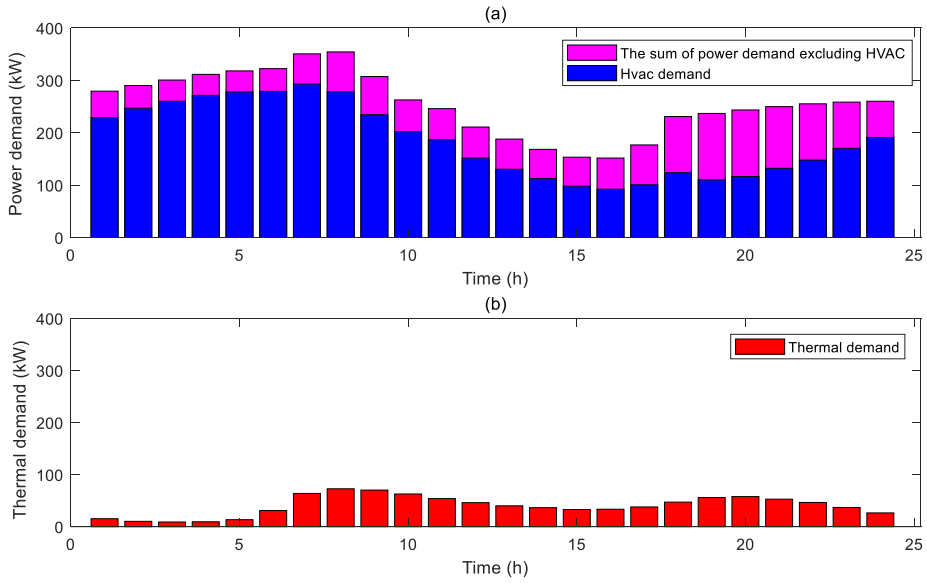

Fig. 6.3 (a) Power and (b) thermal demand of the baseline building system

The power demand of the baseline building system in a typical day without load management of the HVAC is illustrated in Fig. 6.3. Since HVAC consumes the majority of electricity in this hotel building for space heating and cooling, the building's power demand is much higher than thermal demand. For the baseline system without CHP unit, the thermal demand is supplied by a centralized gas boiler and the power demand is totally supplied by the power grid. The total energy payment in this typical day is £803. To achieve a conservative estimate on CHP payback period, the HVAC in the benchmark system is optimally scheduled as Scenario 2. The total operational cost in a half-months in Scenario 2 is £9,133, thus $c_{daily}^{S_2}$ is calculated to be £754.

6.3. Results and Discussion

This case study aims to find the optimal sizing of CHP unit depending on the preference of the building owner/designer with respect to the two objectives, which are represented by λ_1 and λ_2, respectively. The optimal value of *K* can be obtained by Eq. (6.9) among different values of λ_1 and λ_2. The building system's operation

with different CHP capacity is investigated to identify the corresponding minimal operational cost in a typical day and the corresponding minimal payback period.

6.3.1. System operation with a 200 kW CHP unit

The case study starts by analyzing the extreme value of λ_1 and λ_2, where λ_1 is set as 0, and λ_2 is set as 1, which represents that the preference of the building owner/designer is to minimize the investment payback period only while all the load service requirements are maintained unchanged. As the result, a value of $K = 2$ is obtained, indicating that 200 kW CHP installation provides the shortest payback period. The 100 kW CHP is not suitable, because the new building system's operational cost with 100 kW CHP is higher than the benchmark system cost C_{total}^{S2}.

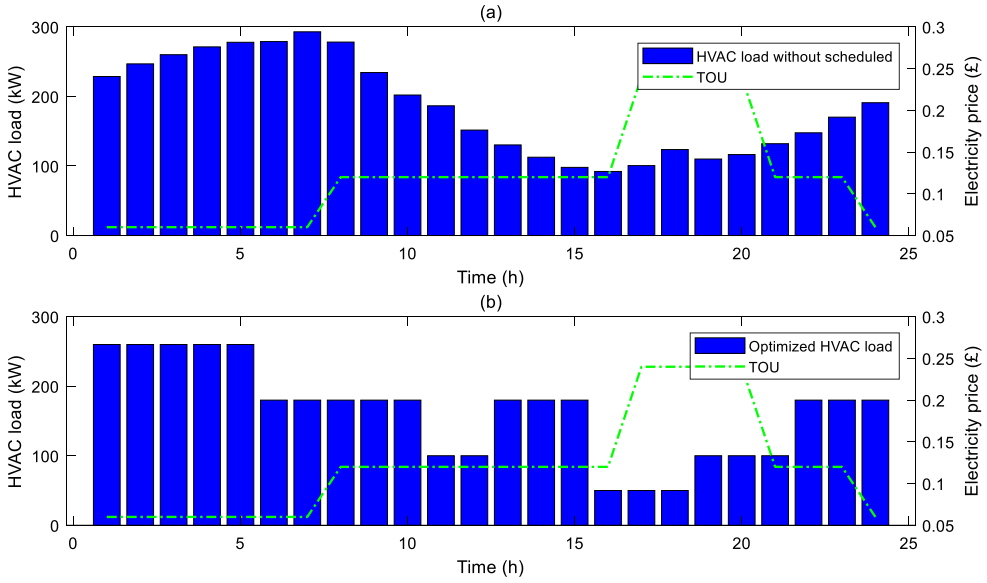

Fig. 6.4 (a) HVAC load in baseline system and (b) optimized HVAC load cooperating with a 200 kW CHP

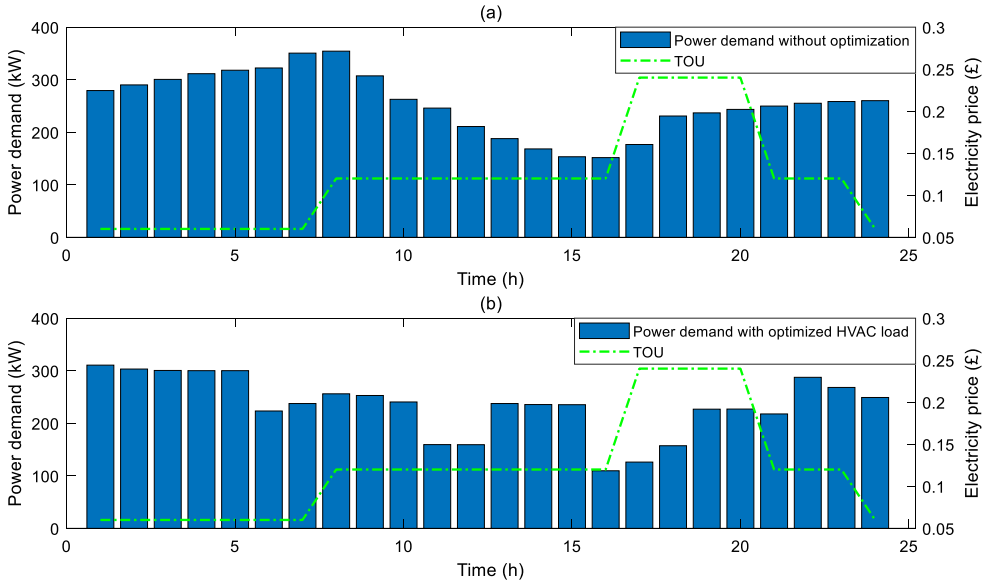

Fig. 6.5 (a) Power demand in the baseline system and (b) optimized power demand with a 200 kW CHP

According to Fig. 6.4, the HVAC load has been scheduled at fixed power levels, and some of the HVAC load in the peak tariff is shifted to reduce the electricity cost. The air-conditioning is initially controlled by guests in the hotel building, but now HVAC is controlled by EMS to keep indoor air temperature at a comfortable range. The building can increase the indoor air temperature in advance of the peak tariff period to reduce the usage at high electricity price. After load management of the HVAC, the total electricity usage of HVAC is reduced compared to the baseline system. Fig. 6.5 illustrates the power demand with optimized HVAC load, which is also lower when compared to the baseline system.

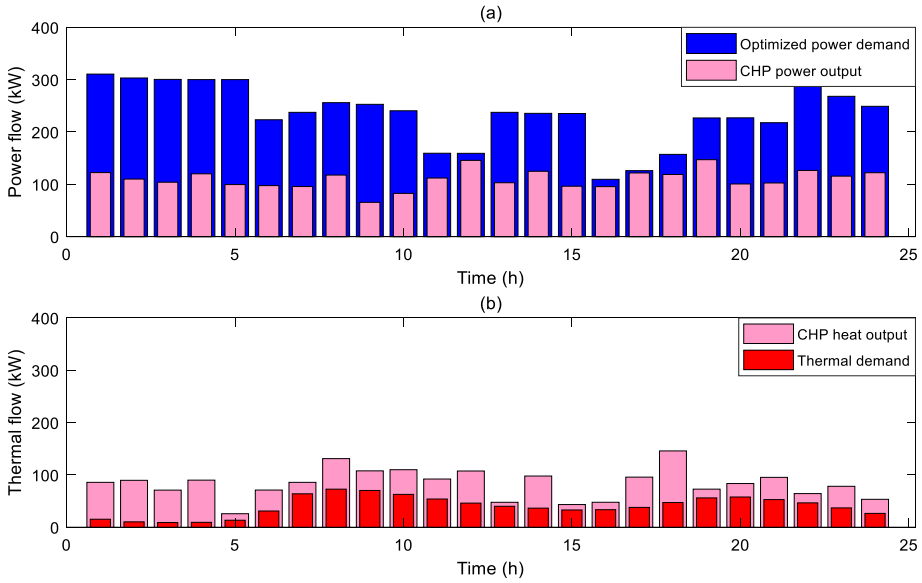

Fig. 6.6 (a) Power and (b) heat production from a 200 kW CHP

Fig. 6.6 shows that a 200 kW CHP unit can meet the building's heat demand and supply nearly half of building's power demand. The CHP power output varies between 100-200 kW most of the time. No excess power is generated by the CHP unit, since all of the power generated is used to supply the power demand.

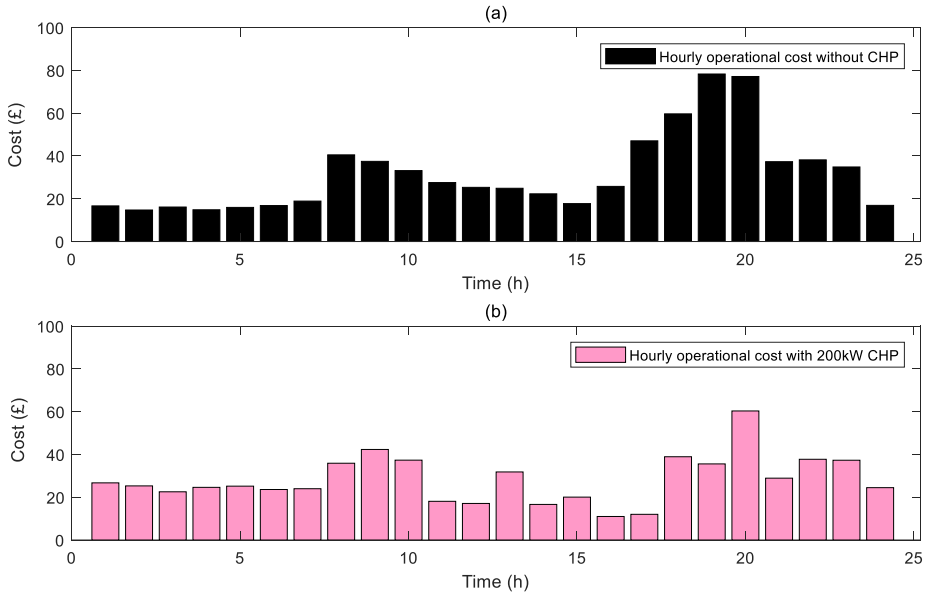

Fig. 6.7 Operational cost from (a) the benchmark system and (b) the building system with a 200 kW CHP

As shown in Fig. 6.7, in the first six hours, the building without CHP has a lower operational cost, since the valley tariff is cheaper than the CHP cost. In Scenario 2, the thermal demand is supplied by a centralized gas boiler. However, this gas boiler is now replaced by the CHP unit, requiring the CHP unit to continually operate to ensure the thermal demand supply, even in the first six hours.

As a result, combining the optimal control on a 200 kW CHP with load management on HVAC, the building's total operational cost in a typical day is £677.46, and the payback period is approximately 2.51 years. The average daily operational cost in Scenario 2 is £753.67, where the HVAC system is also optimally scheduled. Thus, the energy reduction compared to Scenario 2 is caused by CHP's better economic performance in electricity generation. For a smaller value of λ_1, when the building owner/designer prefers the shortest payback period, a 200 kW rated power CHP unit is the optimal selection.

6.3.2. System operation with a 300 kW CHP unit

When the value of λ_1 increases to 0.4 and λ_2 equals 0.6, the optimal sizing of CHP is obtained as $K = 3$. This increased λ_1 implies that more attention is paid to the building's daily operational cost by the building owner/designer, and the corresponding size of CHP is increased to 300 kW.

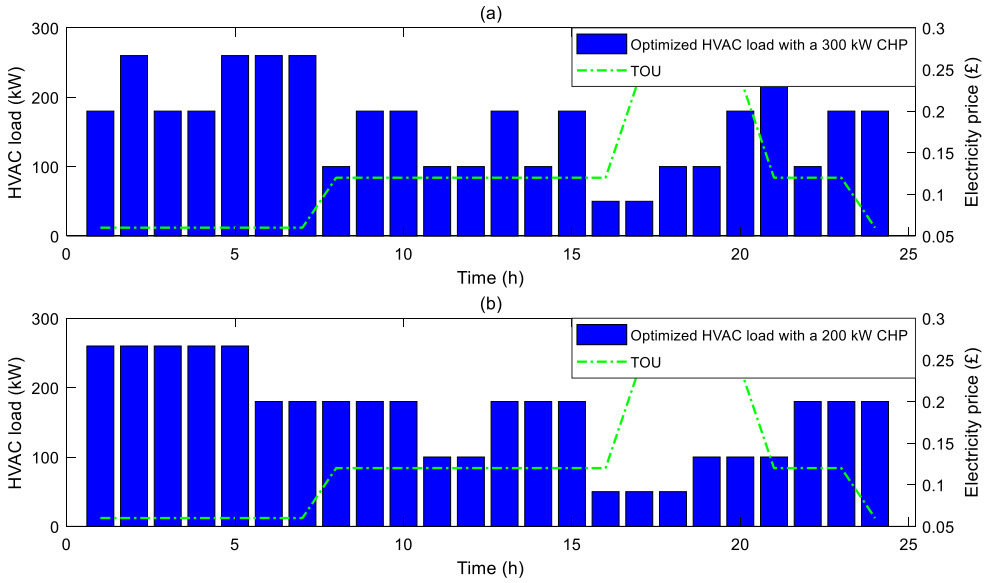

Fig. 6.8 HVAC load comparison between (a) the building with a 300 kW CHP and (b) the building with a 200 kW CHP

From Fig. 6.8, it is evident that the HVAC loads in two buildings are affected by a TOU tariff, especially in the peak tariff period. In both cases, the building systems prevent the electricity usage in the peak tariff through HVAC load management to reduce the total operational cost in 24 hours, where the indoor air temperatures are kept at an acceptable range, as shown in Fig. 6.9.

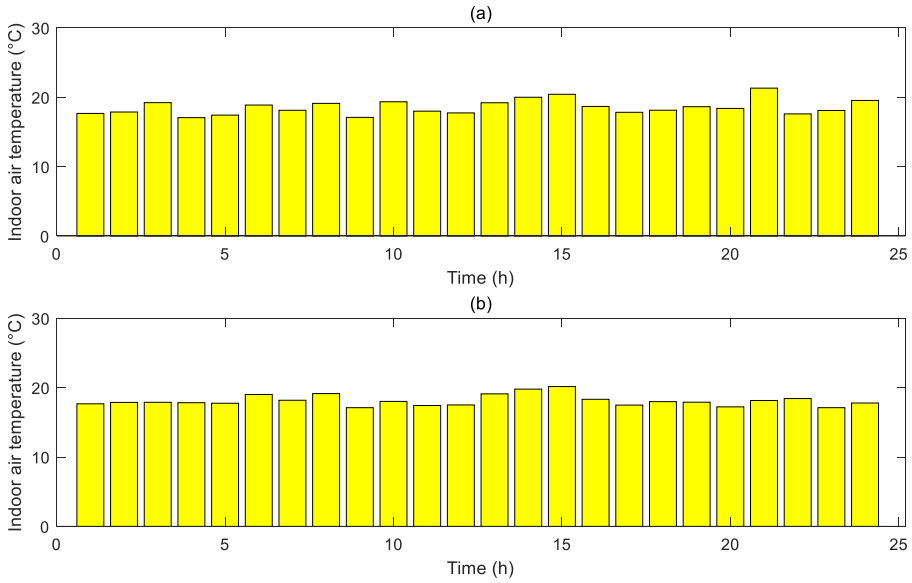

Fig. 6.9 Indoor air temperature of (a) the building with a 300 kW CHP and (b) the building with a 200 kW CHP

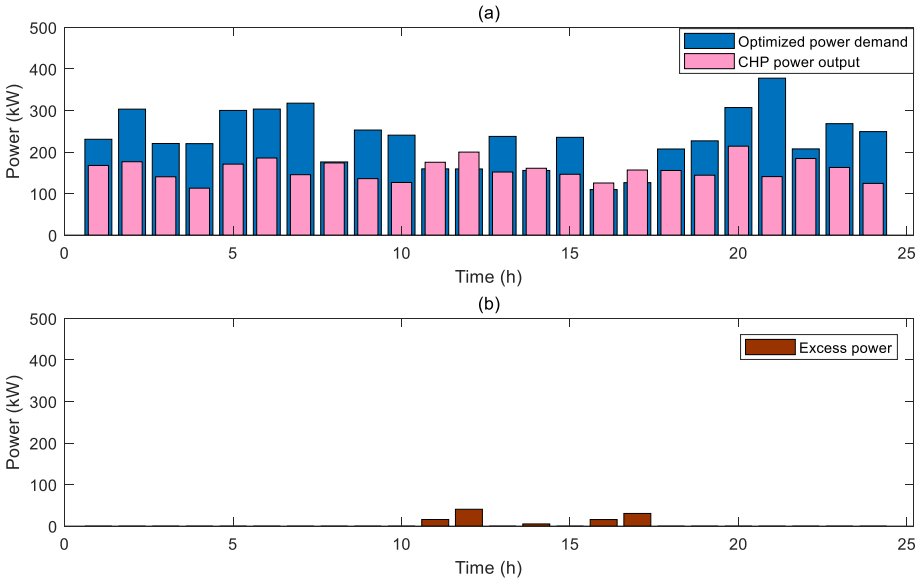

Fig. 6.10 (a) Power output of the CHP compared to the power demand; (b) Excess power generated by a 300 kW CHP

As shown in Fig. 6.10, a 300 kW CHP unit can meet more than half the power demand of the building system. The CHP power output varies between 150-250 kW most of the time. Moreover, in some periods, such as $t = 11$ and $t = 12$, a small

amount of excess power is sold to the power grid for revenue. Thus, the newly installed 300 kW CHP unit can save money not only by providing cheap electricity, but also generate profit from selling excess electricity.

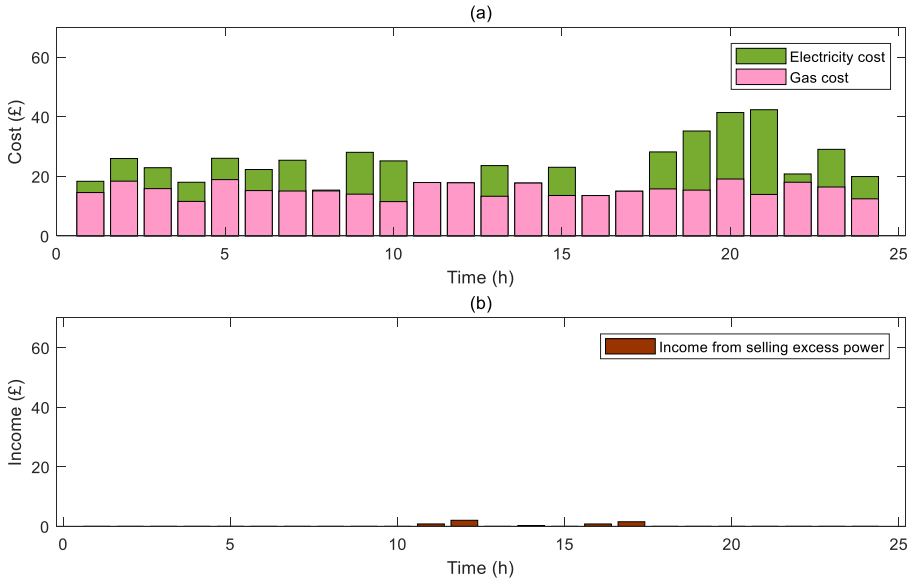

Fig. 6.11 (a) Energy costs and (b) incomes of the building with a 300 kW CHP

Fig. 6.11 shows that the total operational cost of the smart building system with a 300 kW CHP unit consists of three parts: electricity payment to the power grid, natural gas consumption, and the incomes from selling excess power to the power grid. The peak tariff leads to the peak value of building's operational cost, especially in the period from $t = 18$ to $t = 21$. Comparing this with Fig. 6.10, except in the hour $t = 21$, the amount of electricity purchased from the power grid in this period is not large, so the high electricity cost in this period is caused by the expensive tariff. Thus, if the capacity of the CHP unit is larger than 300 kW, where the power supply capability in the peak tariff period is improved, the building system's operational cost can be further reduced.

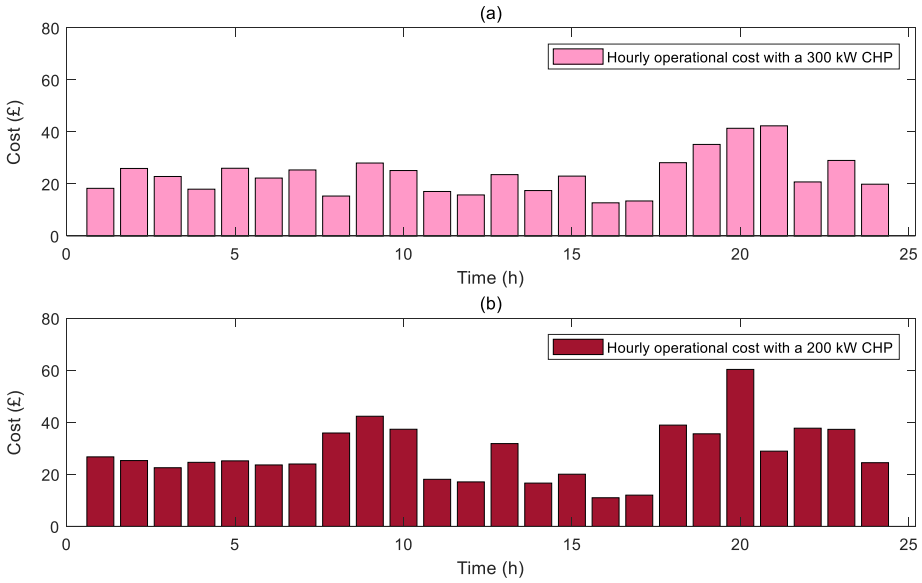

Fig. 6.12 Operational cost of the buildings (a) with a 300 kW CHP and (b) a 200 kW CHP separately

According to Fig. 6.12, the building's operational cost with a 300 kW CHP unit is further reduced than that in the case with a 200 kW CHP unit. Since the incomes illustrated in Fig. 6.11 are very low, this further cost reduction is primarily achieved by more power output from CHP generation. As the result, after a 300 kW CHP installed, the building system's minimal operational cost is £645.14, and the payback period of a 300 kW CHP unit is approximately 2.64 years.

When λ_1 equals 0.4 or 0.5, the solutions of Eq. (6.9) are the same, as $K = 3$. It means that under these preferences on operational cost minimization and payback period minimization, a 300 kW rated power CHP unit is still the optimal selection.

6.3.3. System operation with a 400 kW CHP unit

When the building owner/designer tends to pay more attention to minimizing the building's operational cost than the payback period (λ_1 equals 0.6, 0.7 or 0.8), a 400 kW CHP unit is found as the optimal capacity.

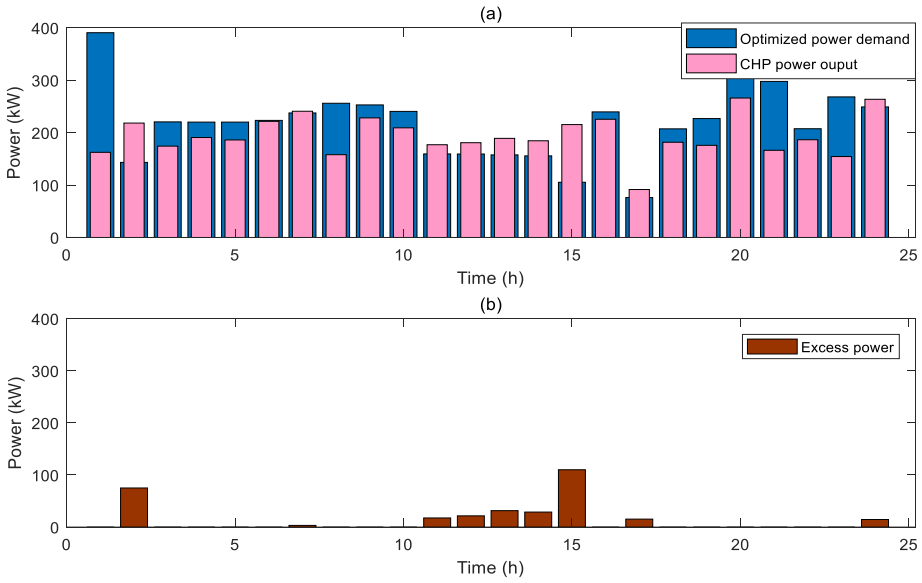

Fig. 6.13 (a) CHP power output compared to the power demand and (b) excess power generated by a 400 kW CHP

According to Fig. 6.13, a 400 kW CHP unit can almost supply the power demand of the building system. The CHP output power varies between 200-300 kW most of the time. Sum of excess electricity is $317.67\ kW \cdot h$, which can be sold to the power grid to make a profit of £15.88 profit in a typical day.

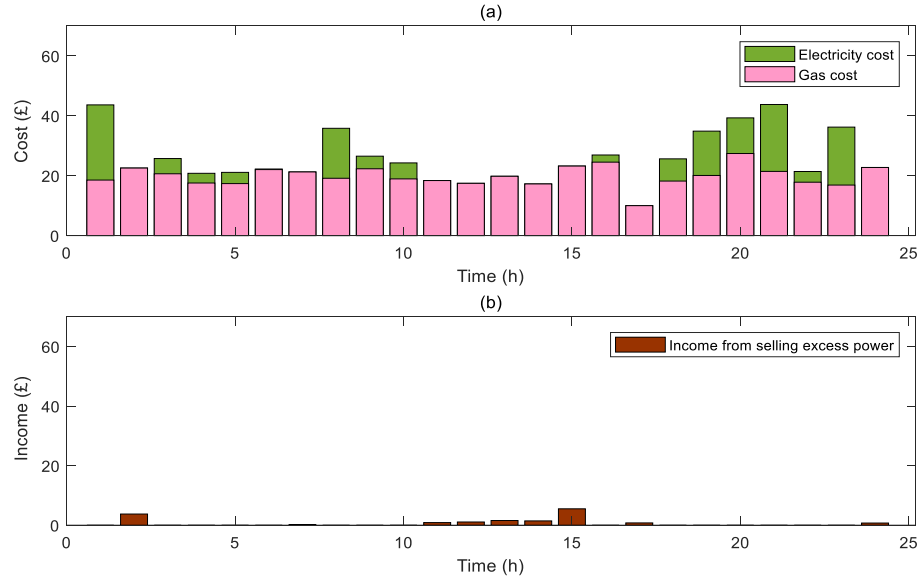

Fig. 6.14 (a) Energy costs and (b) incomes of the building with a 400 kW CHP

From Fig. 6.14, the total operational cost of the building system with a 400 kW CHP unit consists of three parts: electricity payment to the power grid, natural gas payment and the incomes from selling excess power to the power grid. Natural gas replaces electricity as the main energy source, where the electricity cost is £158.55, and the natural gas cost is £475.38. The CHP's generation is limited by the building's lower thermal demand. A 400 kW CHP unit has the ability to generate more excess electricity to get higher profit, however this is accompanied with more thermal losses.

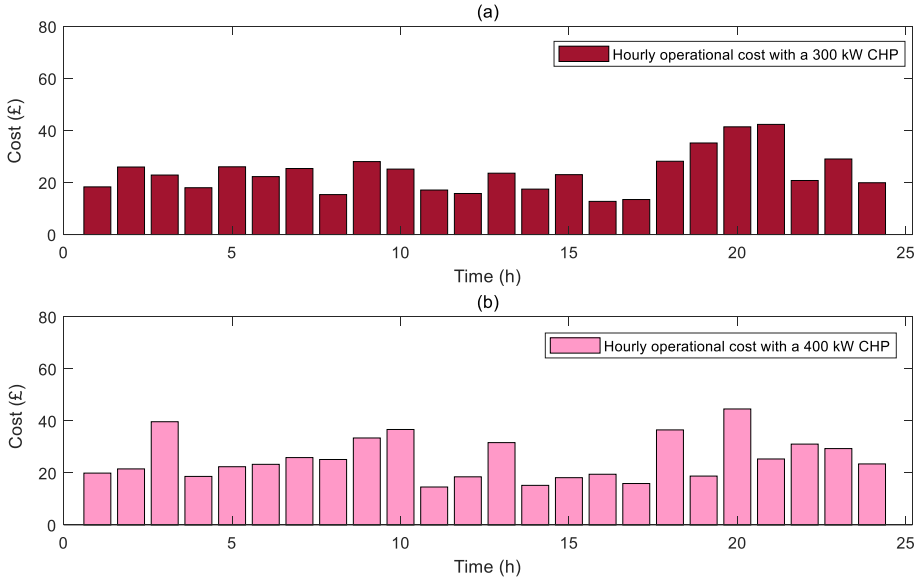

Fig. 6.15 Operational cost of the buildings (a) with a 300 kW CHP and (b) a 400 kW CHP separately

As shown in Fig. 6.15, the 400 kW CHP can decrease operational cost especially at the peak tariff period (from $t = 18$ to $t = 21$), because the CHP with a higher capacity can provide a larger amount of electricity at the peak tariff period. As the result, after the installation of a 400 kW CHP, the building system's minimal operational cost is £618.05, and the payback period of a 400 kW CHP unit is approximately 2.82 years.

When λ_1 equals 0.6, 0.7, and 0.8, the solutions of optimization problem in Eq. (6.9) are the same, as $K = 4$, which means that when the building owner/designer

prefers to have a lower operational cost rather than a shorter payback period, a 400 kW rated power CHP unit is the optimal selection.

6.3.4. System operation with a 500 kW CHP unit

When the value of λ_1 increases to 0,9 and λ_2 equals 0.1, the optimal sizing of CHP is obtained as $K = 5$. In this case, minor consideration of the building owner/designer is given to the payback period, but the minimalization of the operational cost is required. A 500 kW CHP unit is found to be installed. However, this requires a much higher investment of £175,000.

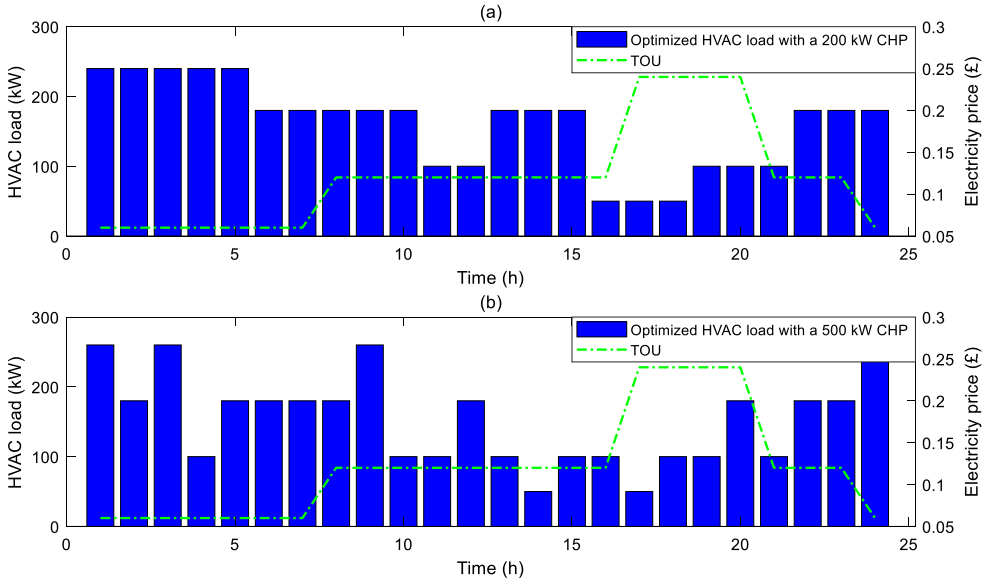

Fig. 6.16 The scheduled HVAC load in buildings with (a) a 200 kW CHP and (b) a 500 kW CHP separately

As shown in Fig. 6.16, the HVAC load is obviously affected by TOU tariff when combined with a 200 kW CHP unit. However, after the installation of the 500 kW CHP, the HVAC load becomes less affected by the changes of electricity tariffs because a 500 kW CHP can almost meet all of the power demand during the peak tariff period.

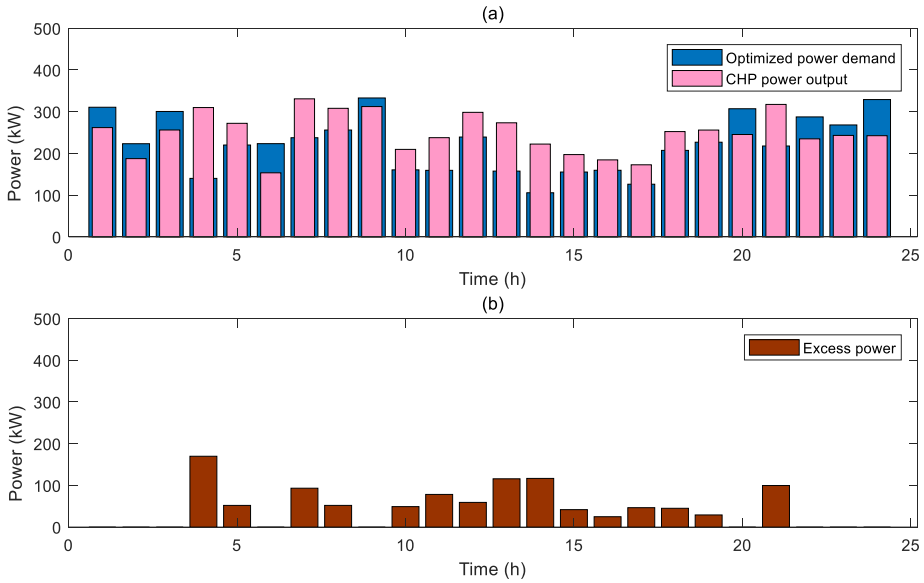

Fig. 6.17 (a) CHP power output compared to the power demand and (b) excess power generated by a 500 kW CHP

According to Fig. 6.17, a 500 kW CHP unit can supply the total power demand of the building system most of the time, and generate a significant quantum excess electricity leading to more revenue. The CHP output power varies between 200-400 kW most of the time. The sum of excess electricity is $1073.34\,kW \cdot h$, which can be sold to the power grid to obtain a profit of £53.67 profit in a typical day.

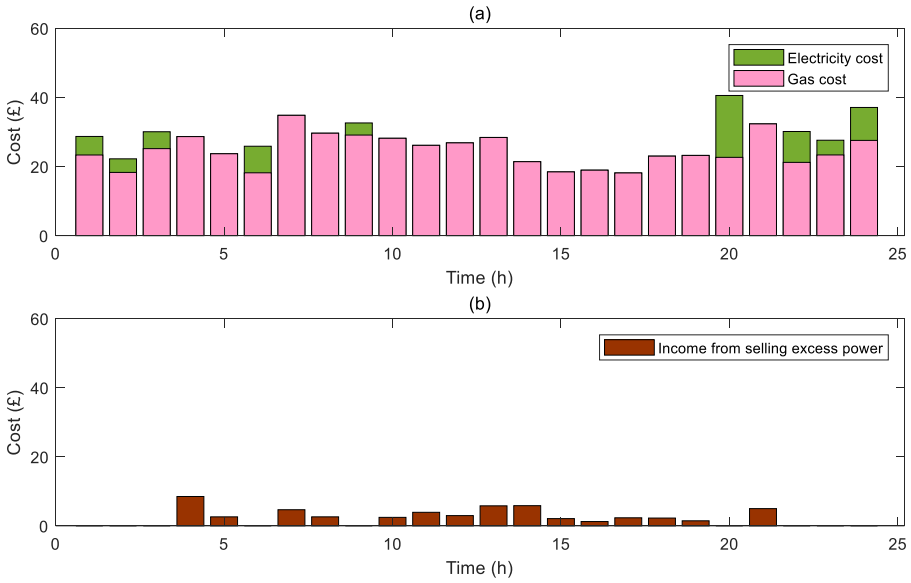

Fig. 6.18 (a) Energy costs and (b) incomes of the building with a 500 kW CHP

From Fig. 6.18, it is observed that natural gas accounts for almost all of the energy costs, at £589.86, while the electricity cost is only £63.73. Resultantly, the building system's minimal operational cost is £599.92 and the payback time of a 500 kW CHP unit is approximately 3.11 years.

When λ_1 equals 0.9 or 1.0, the solutions of Eq. (6.9) are both $K = 5$. This implies that when the main intention of the building owner/designer is to minimize the operational cost of the building regardless of the payback period, a 500 kW rated power CHP unit is the optimal selection.

The optimal sizing of the CHP, the corresponding operational costs after CHP installation, and the payback periods for different values of weighting factors λ_1 and λ_2 are listed in Table 6.2.

Table 6.2 Optimal sizing of the CHP unit depending on the weighting factors

λ_1	λ_2	CHP optimal size	$f_1(K)$ (£)	$f_2(K)$ (year)
0	1.00	$K = 2$	677.46	2.51

0.10	0.90	$K = 2$	677.46	2.51
0.20	0.80	$K = 2$	677.46	2.51
0.30	0.70	$K = 2$	677.46	2.51
0.40	0.60	$K = 3$	645.14	2.64
0.50	0.50	$K = 3$	645.14	2.64
0.60	0.40	$K = 4$	618.05	2.82
0.70	0.30	$K = 4$	618.05	2.82
0.80	0.20	$K = 4$	618.05	2.82
0.90	0.10	$K = 5$	599.92	3.11
1.00	0	$K = 5$	599.92	3.11

6.4.Summary

In this chapter, the problem of CHP optimal sizing is discussed for building retrofit. The two objectives are to reduce the building's operational cost and to reduce the payback period of CHP investment. The investment budget and the preferences of the building owner/designer with respect to these two objectives are considered in the optimization design. The optimization problem has been formed by combing the two objectives into a single function with weighting factors that reflect building owner/designer's preferences. The optimal sizing of the CHP unit has been obtained under different combinations of weighting factors. A 200 kW CHP unit is determined to be the best option for the shortest payback period. When more preference is put on the building's daily operational cost minimization, the optimal capacity of the CHP

increases. Without much consideration on the payback period, a 500 kW rated power CHP unit is found to be the optimal selection to minimize the operational cost of the building system.

CHP is a sustainable and high-efficient distributed generation technology. This case study demonstrates the feasibility to replace the traditional centralized boilers by a CHP unit in commercial buildings. The optimal sizing of a CHP can be obtained through the combined optimization scheme proposed in this chapter.

7. CONCLUSION AND FUTURE WORK

This thesis focuses on optimal operation and sizing of CHP in an S.E. Hub considering demand side response. The main aim is to minimize the total operational cost of the S.E. Hub system that integrates dynamic control of CHP, ESS, TSS and HVAC load management. After obtaining the optimal operational strategies for the S.E. Hub, the optimal sizing problem of the CHP is studied so as to find the proper capacity of CHP within a given budget for cost-saving purpose.

In Chapter 4, an energy cost minimization framework for an S.E. Hub has been established, under which the optimal dynamic control of CHP combined with HVAC load management can be investigated under a TOU tariff. The results in this chapter suggest the benefit to combine the optimal operation of microgrid with a DSR program. The proposed optimization scheme enhances the system's flexibility under varying electricity price. System operational requirements and environmental factors have been considered in the optimization, including CHP's power generation rate and indoor/outdoor/ground/ventilation's temperatures. The economic performance of CHP is optimized, and the best power and heat split ratio is determined through the optimization route. Furthermore, the CHP operation becomes more stable when combined with DSR, which is beneficial to extend lifecycle of a CHP unit.

The case studies in Chapter 4 based on a building system reveals a clear reduction of total energy cost under the proposed optimal solution. Through the comparison among different scenarios, the superiority of the proposed operational strategy has been demonstrated against existing S.E. Hub operational strategies that consider CHP optimal control and DSR separately. The total energy cost has achieved a reduction of 24.1% of the baseline system cost. This performance improvement is achieved without taking into account energy storage systems in the S.E. Hub, which doesn't explore the full potential of the hub system in energy cost saving.

In Chapter 5, the energy operational cost minimization is further expanded to include electrical and thermal energy storage systems. An optimal operational strategy has been developed from the expanded model which controls together the CHP unit, ESS, TSS, and the HVAC system to achieve minimal energy cost. The added components, ESS and TSS, are modeled by considering practical factors such as safe and economic charging/discharging range of ESS and TSS, self-discharging rates and two types of degradation costs of ESS. Meanwhile, the most suitable storage capacities and charging/discharging power flows have been discussed to enhance the optimization performance. Furthermore, the impact of charging/discharging efficiencies of ESS and TSS have been discussed.

Results of case studies in Chapter 5 demonstrate that the deployment of energy storage systems can not only reduce electricity energy demand during the peak tariff period, but also enhance the CHP's power generation. ESS and TSS can be used to share electrical and thermal loads of the system, and keep optimal operation of CHP unit. In this case the total energy cost can be further minimized. With the integration of ESS and TSS, the S.E. Hub has gained a higher supply flexibility and reliability, and also has ensured customer satisfaction on electrical and thermal demands. The case study reveals that 26.5% in Scenario 4 (i.e., the scenario non-considering charging/discharging efficiencies of ESS and TSS) and 24.4% in Scenario 5 (i.e., the scenario considering charging/discharging efficiencies of ESS and TSS) of the total operational cost can be saved over a half-month period.

Chapters 4 and 5 show the significant role of CHP in minimizing the total operational cost of a smart building based S.E. Hub, however, not all the buildings are installed with CHPs, and a high installation cost of CHP usually makes a hard decision for investment. Therefore, the optimal sizing problem for CHP investment has been further investigated in Chapter 6. Two objectives are considered to minimize the building's operational cost and the payback period, respectively. These two objectives

are combined into a single optimization problem using weighting coefficients, which can be solved by GA algorithm.

The optimal sizing of the CHP unit has been obtained under different choices of weighting factors. A 200 kW CHP unit is found to be able to achieve the shortest payback period. When a higher priority is put on the building's daily operational cost minimization, the optimal capacity of the CHP is increased. When the payback period is ignored, a 500 kW CHP unit is found to be the optimal selection to achieve the operational cost minimization of the building system. This case study demonstrates the feasibility to replace the traditional centralized boilers by a CHP unit in commercial buildings.

Potential areas of future research include the following directions.

The DSR strategy for S.E. Hub is developed based on the optimal loading of HVAC system under a TOU tariff in this thesis. Further research can be conducted focusing on the load management under incentive-based DSR programs. Renewable generations and electric vehicles can also be considered in the S.E. Hub system to enable wider applications.

The proposed optimization strategies in this thesis can be further developed to integrate forecasting data, such as future electricity price, power/thermal demand, and outdoor temperature. This will provide predictive feature to the S.E. Hub systems and therefore enhance the operational performance and cost savings.

With the fast development of 5G technology in recent years, increased ability of data transmission and processing techniques can be utilized in the S.E. Hub real time control and management. There's a better chance to generate and regulate operational solutions in smaller time scales that would certainly be more suitable for real-time S.E. Hub operations.

8. APPENDIX

This chapter delivers a short history of CHP and detailed reviews of CHP and ESS technologies. The popular types of CHP generation, such as CCGT, Stirling engine, microturbine system and fuel cell system, are introduced. Suitable types of small-scale CHP system for commercial buildings are recommended. The operating methods, advantages and disadvantages of ESS technologies are discussed, meanwhile recommendations are also made for building energy systems.

8.1. CHP History and Technologies

Since CHP is an important component in microgrid and S.E. Hub, it is helpful to review CHP history and the relevant technologies. The general definition of CHP is a power generation system with capability of using waste heat, which is widely used and can be traced back to late nineteenth century [192]. Due to difficulties to supply thermal energy over a long distance, the traditional power grid is powered by conventional electricity generators (e.g. synchronous generators) instead of CHP. However, with the development of microprocessor-based controller and the increasing requirement of energy-use efficiencies, CHP and micro-CHP systems become popular in microgrids in the early twenty-first century [49, 193].

In the traditional industry, mechanical power is generated by the combustion of coal, which causes huge energy losses during energy conversion between thermal and mechanical power. It was recognized by the Victorian engineers that the wasted thermal energy from power plant can be used to provide heating for workers in winter. In early twentieth century, electricity replaced mechanical power as the main energy source, while the generation of electricity causes significant heat losses. Thus, The earliest CHP plant was formed when workers started to export the waste heat within a factory to surrounding dwellings, offices and shops [49].

The first documented use of CHP in a commercial building is the reconstruction of the Bank of England designed by Oscar Faber [49]. The rebuilt building has its own power generation with a heating system, which utilizes waste heat independently from national grid. From the 1970s, the development of natural gas makes many energy intense industries opt to CHP for cost reduction [194]. As the advent of modern industrial gas turbines and the corresponding control techniques, small-scale CHPs are made possible for business unit. In the twenty-first century, the micro scale CHP emerges to provide power and heat for house hold [195]. This micro scale of CHP is realized based on external combustion engine-Stirling engine. In this type of heat engine, the combustion is separated with the working internal parts, which is also effective at small sizes [196].

Distributed CHP system is very cost efficient in S.E. Hub, if it is proper managed to supply load and sell the surplus electricity to the power grid. In [193], a payback period of less than five years is achievable for the proposed CHP system which can work at least 15 years, indicating that the CHP system produces significant economic benefits in the last 10 years of its life period. In addition, the CHP system provides an eco-friendly solution for the earth's environment [197].

The CHP technologies are categorized and introduced based on the types of generation, such as CCGT, Stirling engines, microturbine system and fuel cell system.

8.1.1. CCGT based CHP

CHP generation is able to be supplied by gas turbine or steam turbine generally, but there is one type of CHP that consists of both two turbines to improve the efficiency of generation, which is called CCGT. In a typical gas turbine [198], which normally consists of a 270 MW primary gas turbine coupled to a 130 MW secondary steam turbine, the temperature of exhaust gas is approximately 600°C. In CCGT plants, the Heat Recovery Steam Generator (HRSG) uses the energy of exhaust gas to raise steam,

which is combined with the original gas turbine to improve the overall energy-utilization efficiency. The typical configuration of CCGT is formed by HRSG and the steam turbine. Depending on the size of steam turbine, more than one HRSG can be installed to absorb the exhaust gas energy. It makes CCGT achieve a thermal efficiency of more than 50% in base-load operation, where the single cycle steam power plant has only around 35% thermal efficiency. The reference [199] describes the benefits and advantages of CCGT plants about the generation efficiency, pollutant emission and operating cost. Moreover, CCGT not only has lower pollution levels, but also can be installed with cheaper cost [200].

Fig. A.1 and Fig. A.2 show the structure of HRSG and the steam turbine respectively. Fig. A.3 shows the connection approaches of HRSG and steam turbine.

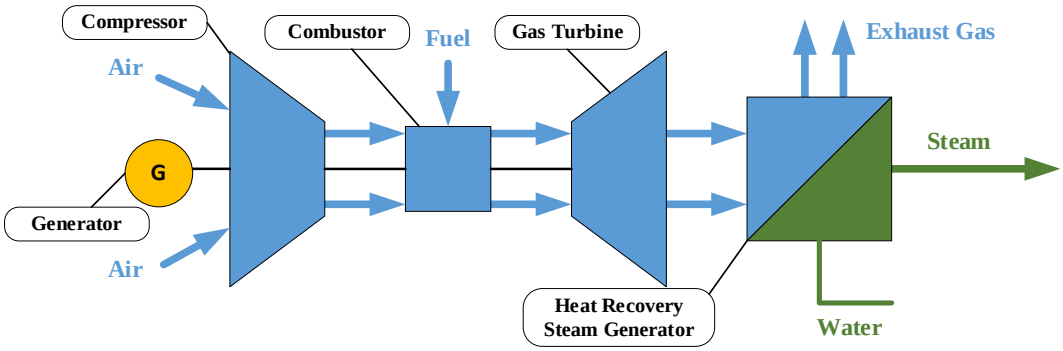

Fig. A.1 Structure of HRSG

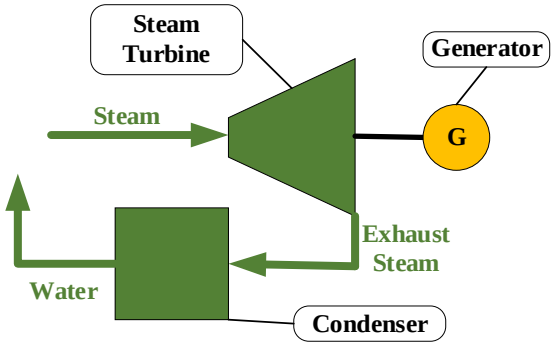

Fig. A.2 Steam turbine with a condenser

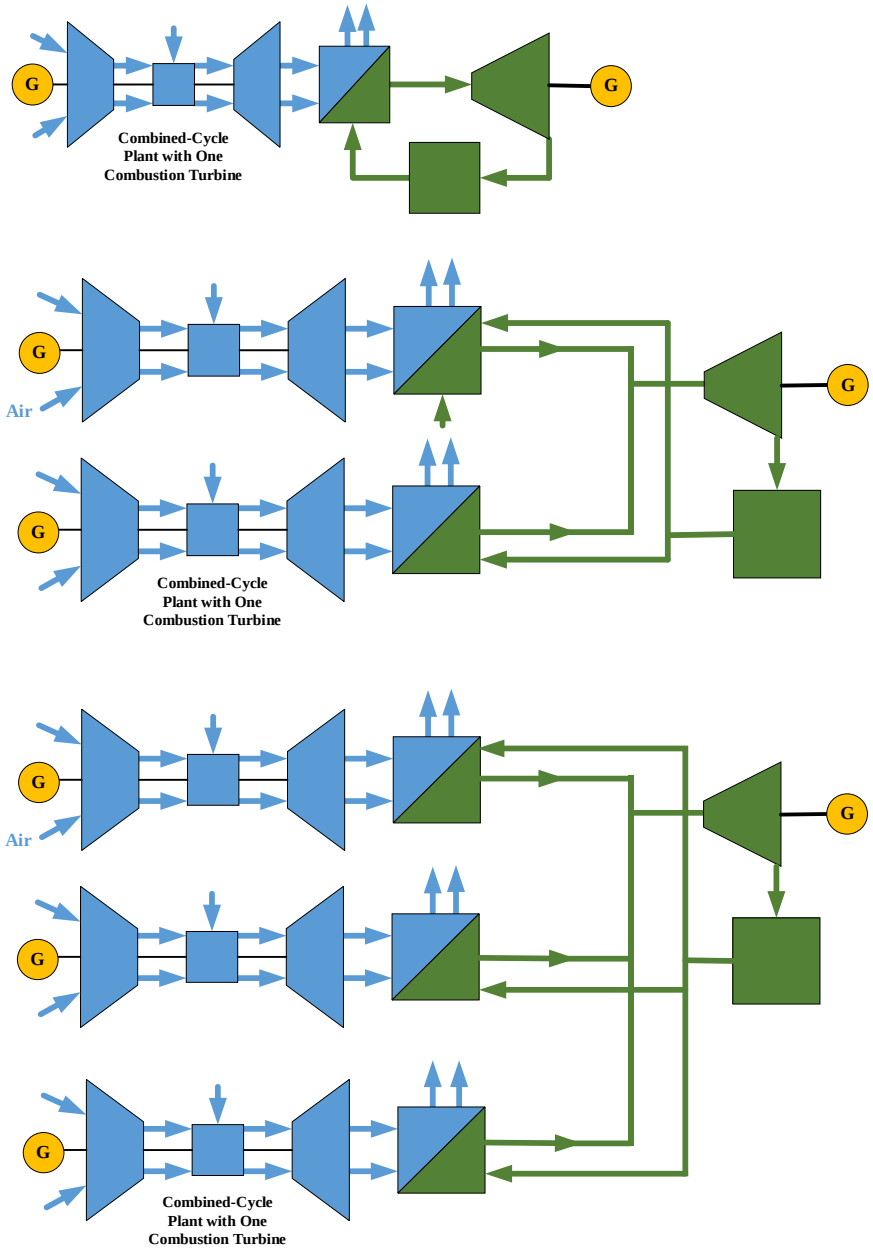

Fig. A.3 Combinations of HRSG and steam turbine

As shown in the above figures, there are two electricity-generation cycles in CCGT systems. One is the gas turbine cycle and the other one is the steam turbine cycle [198]. The energy to heat the cold water in steam turbine cycle is released from the high temperature gas in gas turbine cycle.

The above mentioned CCGT are usually hundreds of MW which is a large-scale CHP system generally adopted in industrial applications. There are also other small CHP systems to be discussed below.

8.1.2. Stirling engine based CHP

Stirling engines are currently used in cooling systems, industrial engines and cogeneration, etc. [49, 201-205] with high efficiency of generation, environment friendly working medium (such as compressed air, helium, nitrogen and hydrogen), and relatively low cost.

Stirling engines are external combustion engines, which work with a closed regenerative thermodynamic cycle. Stirling engines have three typical types: alpha, beta and gamma types, which are differently structured as shown in Fig. A.4.

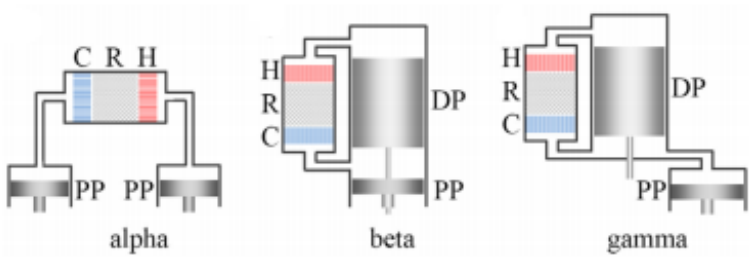

Fig. A.4 Three typical types Stirling engines (H: heater; R: regenerator; C: cooler; DP: displacer; PP: power piston) [202]

- Alpha type Stirling engines have two cylinders with two power pistons, which are installed at cooler side and heater side separately. Both pistons are used to transfer energy caused by different pressure of gas which is sealed within the cylinder. The working gas is forced to move back and forth via the regenerator; hence the thermal efficiency is enhanced by the regenerator. Alpha Stirling engine can work as double-acting configuration by connecting to a serious alpha unit.

- Beta type Stirling engines have one cylinder with one power pistons connecting to one displacer. The inside gas is not allowed to exchange via displacer, the regenerator is the only way for exchanging. The movement of displacer is the unique approach to control the heating gas space, where the cooling gas space is controlled by both the displacer and power piston. For high temperature Stirling engines, the gas between cooler side and the heater side has very large difference of temperatures, where the displacer is even required to have radiation shields inside.
- Gamma type Stirling engines have two cylinders with one power piston and one displacer, which are similar to Beta type Stirling engines. The difference is that the power piston in Gamma unit is installed in other cylinder and connects cooling gas space in main cylinder via a tube. The large void volume of cooling gas space will reduce the efficiency of power transmission. But the Gamma type engines can use two cylinders with different dimensions, which is critical in low temperature differential Stirling engines.

The external combustion system of Stirling engine makes it possible to use the renewable heat resources, such as geothermal and solar energy, despite they are at relatively low and moderate temperature [202]. A large number of previous research focuses on Stirling engines operating at low and moderate temperature, where Kongtragool and Wongwises [206] summarize the general principles and research results of the Stirling cycle engine, solar-powered Stirling engines and low temperature differential (LTD) Stirling engines in 2003. In 2008, Thombare and Verma [207] presents a detailed review on the technical development of Stirling cycle engines, and its potential application in low temperatures.

The typical Stirling engine based CHP can deliver 1 kW to 50 kW power [207]. Thus, it is a micro-scale CHP used in residential area generally.

8.1.3. Microturbine systems based CHP

A microturbine based CHP consists of a compressor, a combustion chamber, a turbine and a generator. The compressor compresses air to a greater pressure (3-5 bars), the combustion chamber, by taking advantage of part of the compressed air and the combustion gases entering the chamber, is able to burn the fuel. The turbine expands gases to produce greater power than what the compressor could consume. The extra power is transformed into shaft power to motivate the generator (Fig. A.5). The gases exhausted from the turbine can be of a higher temperature. Then a recuperator is used (Fig. A.6) to recover some of the energy. The power generation efficiency of the current microturbines with recuperated configuration is at nearly 30 per cent, which, however, would be halved without the recuperator. In this CHP, the overall efficiency to generate power and heat is generally between 75 and 85 percent based on the applications [49].

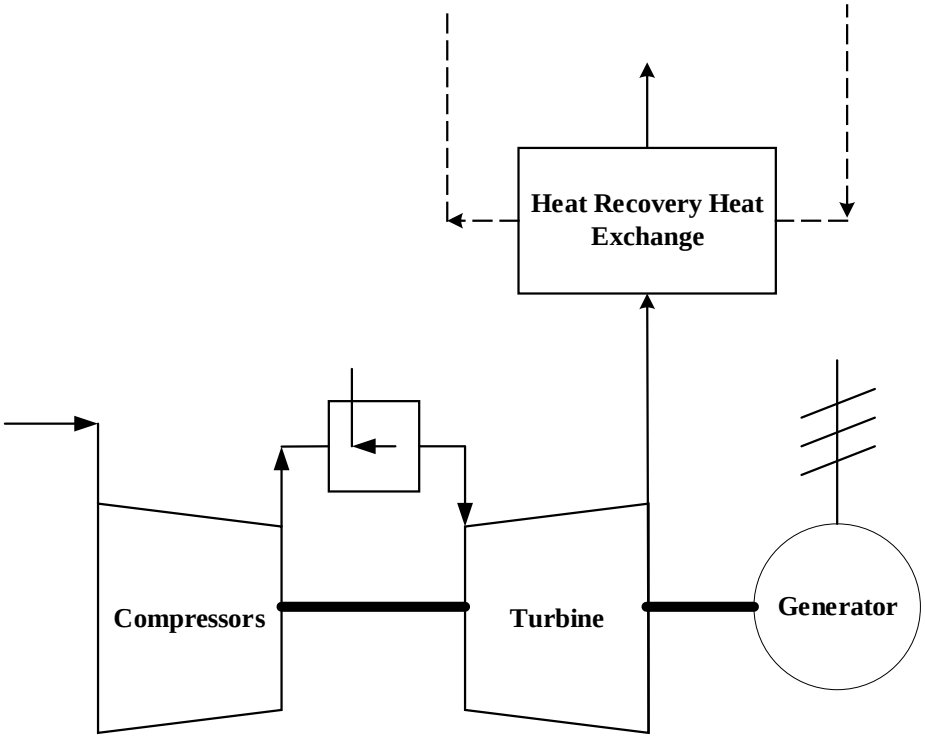

Fig. A.5 The simple gas turbine cycle

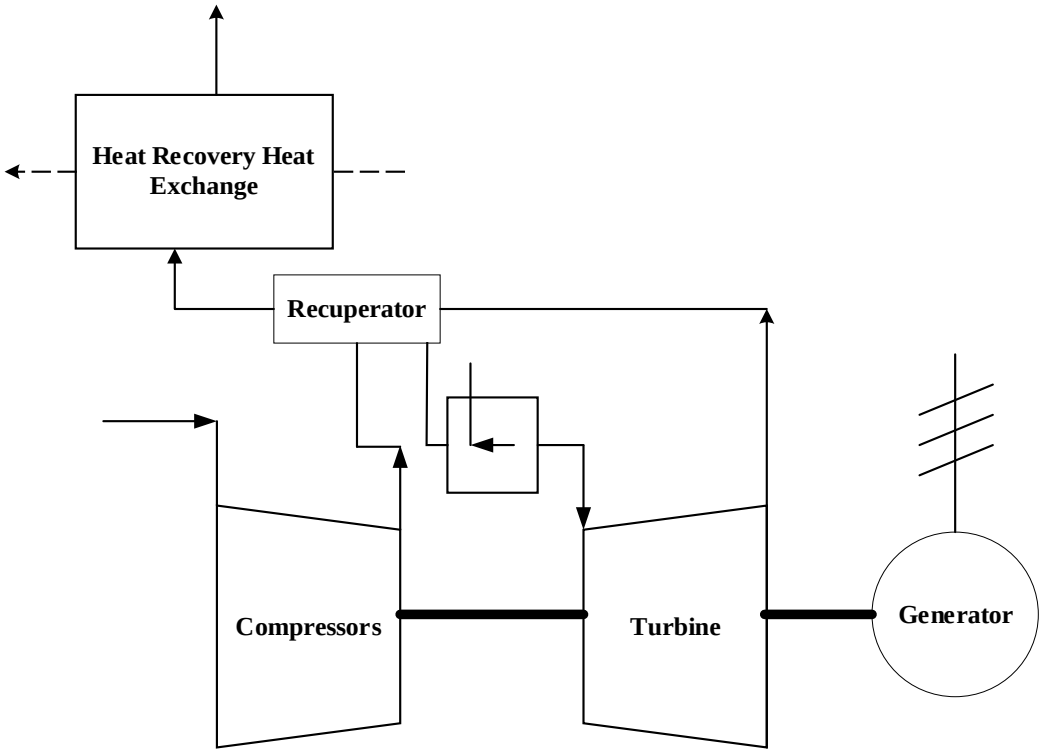

Fig. A.6 The recuperative cycle

To put the compressor, turbine and generator on a single shaft is the simplest design. When it comes to the two-shaft arrangement, the compressor on the first shaft is driven by the first turbine while the generator on the other shaft is powered by the second turbine. The capacity of 1000 kW electricity production is the highest limit of microturbine CHPs, and usually they are below 1000 kW, with some lower than 100 KW and some even less than 15 kW [208]. Therefore, the microturbine is normally used as micro or small-scale CHP systems for winter heating in hospitals, office and factory buildings.

8.1.4. Fuel cell based CHP

Fuel cell based CHP are electrochemical devices that change chemical energy of a fuel into electricity and heat in a direct manner without any involvement of the combustion process. As explained by Hawkes [209], a fuel cell can be seen as a cross

between a battery (from chemical to electrical generator) and a heat engine (from chemical to heat to generator). An anode, electrolyte and cathode are comprised in individual fuel cells, which are linked in series to build up a "stack" through electricity. Bipolar plates are utilized to allocate fuel and oxidant to the individual cells and to link them together through electricity. Common characteristic of them are high efficiency with no moving parts, quiet operation, and low or no emissions when at use.

One example is the low temperature polymer electrolyte fuel cell operated on hydrogen. Fig. A.7 illustrates the fundamental operation of fuel cell. Electrons are connected from the incoming hydrogen at the anode of the cell, which forms ions that go through a conductive electrolyte to integrate oxygen at the cathode. An electric current can be produced by the stripped electrons through the external circuit.

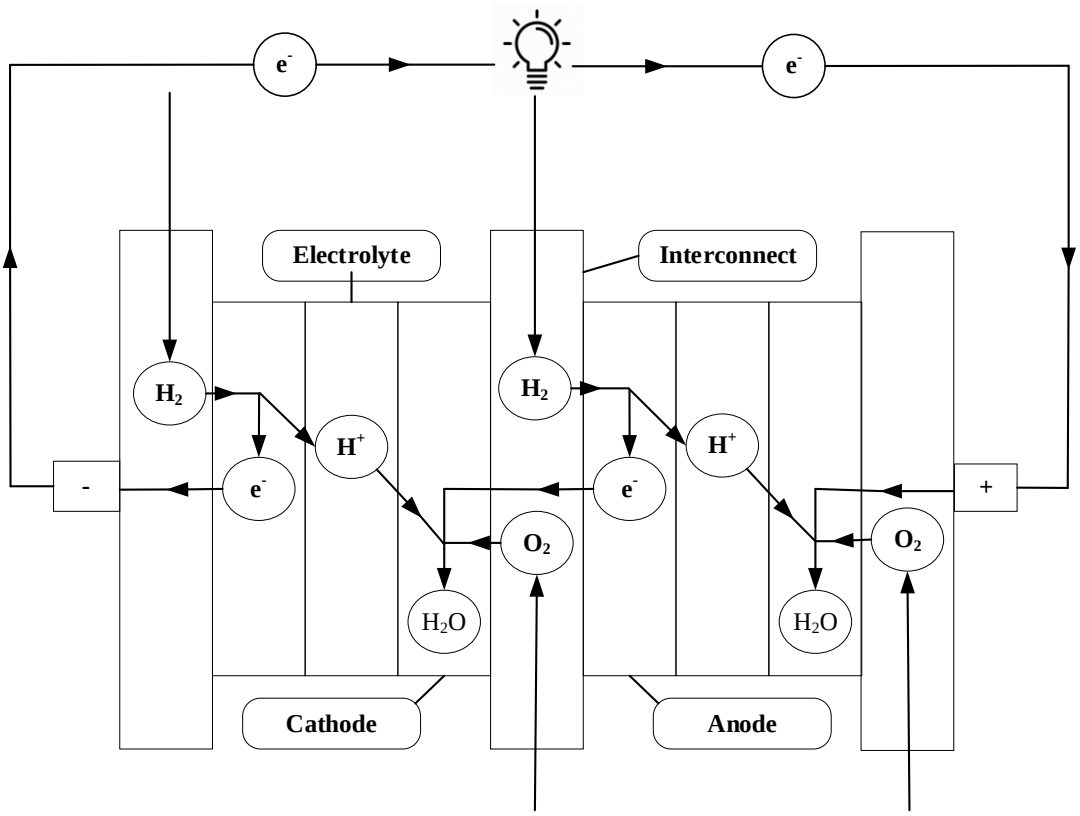

Fig. A.7 Fuel cell operation (two cells in a stack) with hydrogen fueled polymer electrolyte [210]

The ideal fuel for most of the fuel cell types is hydrogen considering performance and durability. However, direct use in homes is not practical, as there is no hydrogen generation or distribution infrastructure. Instead, hydrocarbons are regarded as the ideal fuel for micro-CHP systems, as these can be integrated into hydrogen [211]. Natural gas is inexpensive, sufficient (at least for the time being) with sufficient infrastructure in Western Europe. Natural gas, liquefied petroleum gas or kerosene is used to fuel all commercial fuel cell micro-CHP systems. However, academic research also identifies systems using gasified coal [212], diesel [213], biogas from waste [214], biomass [215], and hydrogen produced biologically from sugary waste [216].

8.1.5. Alternative CHP energy source - biomass

Alternative environment friendly energies other than fossil fuels are required for the future development of CHP. As one of these alternatives, biomass is easily found around the kitchen or agricultural waste. Biomass has been used more frequently as alternative energy resources for transportation, space heating, and power generation because of the continuously growing energy price and the urgency of carbon dioxide reduction.

Biomass consists of trees, crops and other plants, as well as residues from agriculture and forest. There are also many materials included in biomass that are regarded as waste, such as the effluents from food and drink manufacture, and the organic elements of house hold waste. Biomass can be regarded as a kind of reserved solar energy in many ways. The energy of the sun is secured and collected in the process of photosynthesis in plants that are growing [217].

Carbon dioxide is produced and emitted by burning biomass and burning fossil fuels. Nevertheless, two cases are vastly different: CO_2 released by burning fossil fuels reserved for millions of years underground could impact the natural cycle of CO_2 and

lead to the growth in the CO_2 concentration in the atmosphere. On the contrary, burning biomass simply emits CO_2 into the atmosphere, which would be absorbed as the plants grow for a relatively short period of time, e.g. a decade. The same quantity of CO_2 was absorbed from the atmosphere through the photosynthesis process when the plants were growing. However, when biomass is burned, CO_2 was released back into the air and there was no net emission of CO_2 into the atmosphere. It is neutral in terms of CO_2 when the growth cycle and harvest is remained. Therefore, biomass can be regarded as a renewable source of energy. When the production or transportation of the biomass fuel consists of the utilization of fossil fuel, some net release of CO_2 will occur. This part of CO_2 can be important for some biofuels with low ratios of energy [218].

An analysis on direct-combustion biomass CHP unit is presented in [219]. It indicates that the problem of biomass CHP unit promotion is the lower heating temperature because of less carbon.

8.1.6. Small-Scale CHP for commercial building

Small-scale CHP produces electricity and heat from the same energy source in individual buildings or homes with the purpose to substitute gas central-heating boilers in a hydronic central heating system, which proposes a huge potential sales market. The small-scale CHP is generally equipped in buildings requiring year-round demand of power and heat together with capacity of 30 kW to 2 MW [49]. The main economic and environmental advantages comparing to conventional commercial building power supply system would be the following:

i. Electricity is generated as a by-product when small-scale CHP is generating heat for existing thermal load. Such electricity can be used locally or sold to power grid.

ii. Since electricity is generated and mostly consumed on-site, power transmission losses are significantly reduced compared to the conventional generators. Moreover, we could expect that the small-scale CHP system can meet up to 50% of a home's electricity needs.

iii. CHP can save energy cost due to its high efficiency. Despite the high investment cost, the benefits of CHP still outweigh its alternatives in terms of low carbon emission and high energy efficiency.

The main types of small-scale CHP are gas turbine, microturbine and reciprocating internal combustion engine [49]. The CHP using technique of reciprocating internal combustion provides good reliability and long lifecycle. The installation is easy, and the capital cost is relatively low. The pollution emission is largely improved by the developed control techniques. However, the ability of producing steam using the recycled heat to generate electricity is insufficient, with an electric power generation efficiency of around 30% [49]. Thus, the reciprocating internal combustion CHP is suitable for the buildings with high thermal demand but low power demand.

The microturbine based CHP generally provides tens to few hundreds kW power output, but with 30% electric power efficiency and 75-85% overall energy conversion efficiency. It is suitable for residential buildings due to its lower installation cost and smaller carbon footprint compared with reciprocating internal combustion CHP and gas turbine CHP. The microturbine based CHP is generally used as a backup unit for emergency purpose.

Gas turbine generation are widely used for industrial generators as a mature technology and can also be used for small-scale CHP in commercial buildings. With the enhancement in the internal flow features of turbines and compressors and the growing turbine inlet temperatures, the efficiency of gas turbines is boosted. Gas turbines can provide 45% electric power conversion efficiency using the recycled heat

to generate electricity. Meanwhile, the CHP in this thesis is implemented in a building with higher electricity demand compared with thermal load. Therefore, the gas turbine based CHP is chosen for further study in this thesis.

8.2. ESS Technologies

8.2.1. Pumped hydroelectric storage

Pumped hydroelectric storage is a type of ESS technology featuring high maturity and large capacity. It has an installed capacity of 127-129 GW in 2012 in the world, taking up over 99% of bulk storage capacity and 3% of global electricity generated [220, 221]. There are two separate water reservoirs, exhibiting a height difference between them, for a typical pumped hydroelectric storage plant. During valley electricity price periods, the water will be pumped into the higher water reservoir. When it comes to peak periods, the water in the higher-level water reservoir will be released back to the lower water reservoir. During the water pumping process, power turbines drive electrical machines for electricity generation. Height difference between the two reservoirs and the aggregated amount of reserved water will determine the volume of energy stored. Water pressure, flow speed through turbines, and the rated power of pumps, turbines and generator/motor units, will determine the rated power of pumped hydroelectric storage plant [222].

However, since pumped hydroelectric storage plants are restricted to certain sites, they usually require a long time of construction and large capital investment. The recent technological development has enabled some pumped hydroelectric storage plants to adopt flooded mine shafts, caves underground and oceans as water reservoirs. The 300 MW ocean-based pumped hydroelectric storage plant in Hawaii, Ohio's Summit Project and New Jersey's Mount Hope project are all examples of this application [223]. Moreover, a new development is the combination of creating wind

and solar power with pumped hydroelectric storage plants, which can help the adoption of renewable energy in isolated or distributed networks [224, 225].

8.2.2. Compressed air energy storage

Compressed air energy storage is another kind of commercial ESS technology. It is able to generate power of more than 1000 MW in a single unit. During off-peak periods, extra electricity will be used to power a reversible motor or generator, which drives a set of compressors to inject air into a storage vessel. It can either be a cavern underground or a tank on the ground. High pressure air is a form of energy storage. When the demand cannot be satisfied with the power supply, the compressed air stored will be released and heated by the consumption of fossil fuels or the heat generated in the compression process. Turbines will catch the stored air energy while a recuperate unit can recycle the extra heat generated.

Compressed air energy storage systems have flexible capacities, their storage capacities can be up to hundreds of MWh and outputs can reach tens of MW [226].. The moderate speed of response and good partial-load performance can be provided by compressed air energy storage. Because of these advantages, the large-scale compressed air energy storage plants are usually used to shift loads, shave peaks and control frequency and voltage in the grid network. Intermittent renewable energy generations are also suitable to cooperate with compressed air energy storage, in particular wind power plants, which is able to smoothen the output of energy [227, 228]. The key challenge for adopting large-scale compressed air energy storage plants is to find appropriate sites, which is closely related to the investment in its construction. Another barrier for compressed air energy storage technology is the relatively low efficiency of a round trip compared with pumped hydroelectric storage and battery technologies. However, the small-scale compressed air energy storage has developed

rapidly, which can be used as an alternative to the battery in industrial applications [229].

8.2.3. Flywheel energy storage

There are five fundamental components in a modern flywheel energy storage system, i.e., a flywheel, a set of bearings, a reversible motor/generator, an electronic unit and a vacuum chamber [230]. The flywheel can be accelerated or decelerated by electricity. The energy can be stored by speeding up the flywheel, and released through an integrated motor/generator. The amount of energy stored in flywheel energy storage system depends on the rotating speed of the flywheel and its inertia [231]. Due to energy loss from air resistance and wind shear, the flywheel energy storage system is placed in a high vacuum environment.

There are two types of flywheel energy storage system. One is low-speed flywheel energy storage, where the flywheel is made of steel and its rotating speed is below $6\times10^3\ rpm$. The specific energy storing capacity of low-speed flywheels is around $5\,W\cdot h/kg$. The other is high-speed flywheel energy storage, in which the flywheel usually uses advanced composite materials, for instance carbon-fiber. The rotating speed of high-speed flywheel energy storage can rise up to $10^5\ rpm$ [232], and the high-speed composite rotor can achieve a specific energy storage capacity of around $100\,W\cdot h/kg$. In a high-speed flywheel energy storage system, the wear of bearing is reduced by using non-contact magnetic bearings, which also improves the efficiency. Low-speed flywheel energy storage are usually selected for short-term and low-power applications. High-speed flywheel energy storage systems are mainly used in high-power quality and aerospace industry [233]. However, compared with traditional metal flywheel systems, a high-speed flywheel energy storage system is much costly. But it has incomparable advantages such as high cycling efficiency (95%

of rated power), relatively high power density, zero depth-of-discharge impact and easier maintenance [234].

8.2.4. Battery energy storage

One of the most widely used ESS technologies in industrial application and daily life is the rechargeable battery. A battery energy storage system comprises different electro-chemical units. They are arranged and connected in series or paralleled structure to generate electricity from an electrochemical reaction. There are two electrodes for each cell: anode and cathode. The two electrodes have either a solid, liquid or viscous electrolyte [235]. Electricity or chemical energy can be converted by a cell. In the discharging process, electrochemical reactions will take place at both electrodes at the same time. In terms of the external circuit, anodes can provide electrons while cathodes are collecting them. In the charging process, the reverse reaction takes place and the electrodes are applied with an external voltage.

Batteries can be used widely for various applications. For instance, batteries can be used for power quality control, energy management, and transportation systems [236]. It requires a relatively short period of time to build up a system. The installation location is also very flexible, either inside a building or close to the needed infrastructure. The installation of large-scale battery storage needs to consider the degradation cost and maintenance cost. Recycling or disposal of dumped batteries should also be taken into consideration, if they contain any toxic materials. Moreover, because of the fact that batteries' life-time rely on the DOD cycle, they should not be fully discharged [237].

There is another kind of battery, flow battery storage system. It has two external liquid electrolyte tanks with two soluble redox couples, which is used to store energy. These electrolytes can be transmitted from the tanks to the cell stack. In the cell stack, there are two electrolyte flow compartments, which are isolated by ion selective

membranes. The operation of flow battery energy storage system depends on Oxidation-reduction reactions of the electrolyte solutions. In the charging process, the anode is the end where one electrolyte is oxidized and the cathode is the end where the other electrolyte is reduced.

There are two categories of flow batteries: redox flow batteries and hybrid flow batteries, which relies on the fact whether the electrolyte can dissolve all electroactive elements or not. The power of a flow battery system can be separated from its storage capacity, which constitutes a crucial advantage of the system. The scale of the electrodes and the number of stack cells will determine the power of the flow battery. The concentration and the amount of electrolytes will determine the capacity of storage [238]. Another inherent advantage of the flow battery energy storage system is its very small self-discharging loss, as electrolytes are stored in individually sealed tanks [239]. However, it also has disadvantages, such as low performance as a result of inconsistent pressure drop and the transfer limits from reactant mass, higher cost for production and more complicated structure than conventional batteries [240]. The power of flow batteries can reach a few hundred kW and even MW levels, which can be used for industrial and commercial ESS applications [241]. There are three types of flow batteries in common use: vanadium redox, zinc bromine and polysulfide bromine.

8.2.5. Capacitor and supercapacitor

There are at least two electrical conductors, which is usually made of metal foils, in one capacitor. A thin layer of insulator (usually made of ceramic, glass or plastic) is in the middle of the capacitor to separate conductors. Energy can be stored in the electrostatic field's dielectric material when a capacitor is charged. The maximum voltage of operation relies on the breakdown characteristics of separated dielectric material [242]. Small quantities of electrical energy with a varying voltage is suitable to be stored by capacitors. Comparing with traditional batteries, capacitors have a

shorter charging time and a higher power density [243]. Nevertheless, their capacity is limited because of low energy density and high dissipation of energy from self-discharging process [244]. Based on these features, capacitors are generally used for certain power quality applications, for instance, power factor correction and absorption of harmonics.

Supercapacitors, also known as electric double-layer capacitors or ultracapacitors, comprise two conductor electrodes, an electrolyte and a porous membrane separator. Because of the structures, features of both traditional capacitors and electrochemical batteries are available for supercapacitors. Energy is stored as the static form on the surfaces of two conductor electrodes. Nano-materials have increased the electrode surface area, which have improved supercapacitors' storage performance. Supercapacitors' power and energy densities are in the middle of rechargeable batteries and traditional capacitors [244]. Supercapacitors have advantages of long cycling times and high cycle efficiency, which can reach $84\%-97\%$ [245]. However, the construction cost of supercapacitors is pretty expensive and their self-discharge rate is high. Thereby, supercapacitors are suitable for short-term storage applications which requires high quality of power.

8.2.6. Superconducting magnetic energy storage (SMES)

A typical SMES system comprises a superconducting coil unit, a power conditioning subsystem, and a refrigeration and vacuum subsystem [246]. The energy of SMES system is stored in the magnetic field, which is generated by the direct current in superconducting coil. The superconducting coil is cooled down cryogenically under the critical superconducting temperature. However, when the current is passing through a coil, some electrical energy will be converted into heat because of the wire resistance. But if the coil uses the same material as the superconductor, such as mercury or vanadium, there will be no resistance under the superconducting state

(usually at an extremely low temperature) and there will be almost no losses of energy storage. Niobium-Titanium is a commonly used superconducting material at a superconducting critical temperature of 9.2 K [247]. During the discharging process, the stored electrical energy can be released back from the SMES system to the system of alternating current through a connected power converter. Coil's self-inductance and the current passing through the coil can determines the amount of stored energy [248].

Comparing with rechargeable batteries, SMES system can discharge almost all stored energy, and with little degradation even after thousands of full cycles. However, the construction cost of SMES is very expensive and may cause negative impact to the environment, because of its strong magnetic field [248]. The coil of SMES is sensitive to temperature variation, which limits its applications. Therefore, SMES is suitable for short-term storage and better to be used with intermittent renewable energy system [246].

8.2.7. ESS selection for commercial buildings

After reviewing the operating methods, advantages and disadvantages of various ESS technologies, it is recommended to choose lithium-ion battery storage system for the smart building considered in this thesis, and reasons are explained below. In view of the power demand of the building (a few hundred kW), the ESS construction cost, power and energy densities, self-discharging rate, charging/discharging time and the environmental factors, rechargeable batteries are most suitable to be selected as a buffer component participating in a smart building's operational cost minimization model. In rechargeable battery technologies, lithium-ion battery is the optimal selection for the smart building system, because of these advantages:

i. Compared to other advanced ESS technologies, such as high-speed flywheel energy storage and SMES, lithium-ion batteries have a relatively low construction cost.

ii. Compared to other rechargeable batteries, lithium-ion batteries have one of the highest energy densities.

iii. A unit lithium-ion battery (i.e. a battery cell) can drive up to 3.6 volts, which is higher than other rechargeable battery cells.

iv. Lithium-ion batteries have a relatively low maintenance cost and do not need to schedule cycling to maintain their life.

v. The self-discharging rate of lithium-ion batteries is approximately 1.5%-2% [62], which is lower than other battery technologies.

vi. Lithium-ion batteries do not contain toxic cadmium, thereby easier to be disposed.

REFERENCE

[1] S. Küfeoğlu, M. Pollitt, and K. Anaya, *Electric Power Distribution in the World: Today and Tomorrow*. 2018.

[2] !!! INVALID CITATION !!! [2, 3].

[3] S. Pazouki and M. Haghifam, "Economic and technical influences of distributed energy resources in smart energy hubs," in *2015 Smart Grid Conference (SGC)*, 22-23 Dec. 2015 2015, pp. 47-52, doi: 10.1109/SGC.2015.7857389.

[4] S. Pazouki, M. Haghifam, and J. Olamaei, "Economical scheduling of multi carrier energy systems integrating Renewable, Energy Storage and Demand Response under Energy Hub approach," in *2013 Smart Grid Conference (SGC)*, 17-18 Dec. 2013 2013, pp. 80-84, doi: 10.1109/SGC.2013.6733803.

[5] M. Mohammadi, Y. Noorollahi, B. Mohammadi-ivatloo, M. Hosseinzadeh, H. Yousefi, and S. T. Khorasani, "Optimal management of energy hubs and smart energy hubs – A review," *Renewable and Sustainable Energy Reviews,* vol. 89, pp. 33-50, 2018/06/01/ 2018, doi: https://doi.org/10.1016/j.rser.2018.02.035.

[6] M. Mohammadi, Y. Noorollahi, B. Mohammadi-ivatloo, and H. Yousefi, "Energy hub: From a model to a concept – A review," *Renewable and Sustainable Energy Reviews,* vol. 80, pp. 1512-1527, 2017/12/01/ 2017, doi: https://doi.org/10.1016/j.rser.2017.07.030.

[7] A. Sheikhi, M. Rayati, S. Bahrami, and A. M. Ranjbar, "Integrated Demand Side Management Game in Smart Energy Hubs," *IEEE Transactions on Smart Grid,* vol. 6, no. 2, pp. 675-683, 2015, doi: 10.1109/TSG.2014.2377020.

[8] M. Rayati, A. Sheikhi, and A. M. Ranjbar, "Applying reinforcement learning method to optimize an Energy Hub operation in the smart grid," in *2015 IEEE Power & Energy Society Innovative Smart Grid Technologies Conference (ISGT)*, 18-20 Feb. 2015 2015, pp. 1-5, doi: 10.1109/ISGT.2015.7131906.

[9] A. Sheikhi, S. Bahrami, and A. M. Ranjbar, "An autonomous demand response program for electricity and natural gas networks in smart energy hubs," *Energy,* vol. 89, pp. 490-499, 9// 2015, doi: http://dx.doi.org/10.1016/j.energy.2015.05.109.

[10] R. Li, W. Wei, S. Mei, Q. Hu, and Q. Wu, "Participation of an Energy Hub in Electricity and Heat Distribution Markets: An MPEC Approach," *IEEE Transactions on Smart Grid,* vol. PP, pp. 1-1, 05/04 2018, doi: 10.1109/TSG.2018.2833279.

[11] A. Akrami, M. Doostizadeh, and F. Aminifar, "Power system flexibility: an overview of emergence to evolution," *Journal of Modern Power Systems and Clean Energy,* vol. 7, no. 5, pp. 987-1007, 2019/09/01 2019, doi: 10.1007/s40565-019-0527-4.

[12] M. Mazidi, H. Monsef, and P. Siano, "Robust day-ahead scheduling of smart distribution networks considering demand response programs," *Applied Energy,* vol. 178, no. Supplement C, pp. 929-942, 2016/09/15/ 2016, doi: https://doi.org/10.1016/j.apenergy.2016.06.016.

[13] B. Nastasi and G. Lo Basso, "Power-to-Gas integration in the Transition towards Future Urban Energy Systems," *International Journal of Hydrogen Energy,* vol. 42, no. 38, pp. 23933-23951, 2017/09/21/ 2017, doi: https://doi.org/10.1016/j.ijhydene.2017.07.149.

[14] K. Zhou, C. Fu, and S. Yang, "Big data driven smart energy management: From big data to big insights," *Renewable and Sustainable Energy Reviews,* vol. 56, pp. 215-225, 2016/04/01/ 2016, doi: https://doi.org/10.1016/j.rser.2015.11.050.

[15] Y. Li, B. Feng, G. Li, J. Qi, D. Zhao, and Y. Mu, "Optimal distributed generation planning in active distribution networks considering integration of energy storage," *Applied Energy,* vol. 210, pp. 1073-1081, 2018/01/15/ 2018, doi: https://doi.org/10.1016/j.apenergy.2017.08.008.

[16] M. Geidl, G. Koeppel, P. Favre-Perrod, B. Klöckl, G. Andersson, and K. Fröhlich, "The energy hub-A powerful concept for future energy systems," *Third Annual Carnegie Mellon Conference on the Electricity Industry,* pp. 13-14, 04/01 2007.

[17] J. Wang, H. Zhong, Z. Ma, Q. Xia, and C. Kang, *Review and Prospect of Integrated Demand Response in the Multi-Energy System*. 2017.

[18] K. J. Chua, S. K. Chou, W. M. Yang, and J. Yan, "Achieving better energy-efficient air conditioning – A review of technologies and strategies," *Applied Energy,* vol. 104, pp. 87-104, 4// 2013, doi: http://dx.doi.org/10.1016/j.apenergy.2012.10.037.

[19] T. Boßmann and E. J. Eser, "Model-based assessment of demand-response measures—A comprehensive literature review," *Renewable and Sustainable Energy Reviews,* vol. 57, pp. 1637-1656, 2016/05/01/ 2016, doi: https://doi.org/10.1016/j.rser.2015.12.031.

[20] K. H. S. V. S. Nunna and S. Doolla, "Responsive End-User-Based Demand Side Management in Multimicrogrid Environment," *IEEE Transactions on Industrial Informatics,* vol. 10, no. 2, pp. 1262-1272, 2014, doi: 10.1109/TII.2014.2307761.

[21] O. Kilkki, A. Alah, x00E, iv, and I. Seilonen, "Optimized Control of Price-Based Demand Response With Electric Storage Space Heating," *IEEE Transactions on Industrial Informatics,* vol. 11, no. 1, pp. 281-288, 2015, doi: 10.1109/TII.2014.2342032.

[22] N. G. Paterakis, O. Erdinç, and J. P. S. Catalão, "An overview of Demand Response: Key-elements and international experience," *Renewable and*

Sustainable Energy Reviews, vol. 69, pp. 871-891, 2017/03/01/ 2017, doi: https://doi.org/10.1016/j.rser.2016.11.167.

[23] R. Yin *et al.*, "Quantifying flexibility of commercial and residential loads for demand response using setpoint changes," *Applied Energy,* vol. 177, pp. 149-164, 2016/09/01/ 2016, doi: https://doi.org/10.1016/j.apenergy.2016.05.090.

[24] S. Kiliccote, D. Olsen, M. D. Sohn, and M. A. Piette, "Characterization of demand response in the commercial, industrial, and residential sectors in the United States," *Wiley Interdisciplinary Reviews: Energy and Environment,* vol. 5, no. 3, pp. 288-304, 2016.

[25] S. Nolan and M. O'Malley, "Challenges and barriers to demand response deployment and evaluation," *Applied Energy,* vol. 152, pp. 1-10, 2015/08/15/ 2015, doi: https://doi.org/10.1016/j.apenergy.2015.04.083.

[26] P. Palensky and D. Dietrich, "Demand Side Management: Demand Response, Intelligent Energy Systems, and Smart Loads," *IEEE Transactions on Industrial Informatics,* vol. 7, no. 3, pp. 381-388, 2011, doi: 10.1109/TII.2011.2158841.

[27] G. Derakhshan, H. A. Shayanfar, and A. Kazemi, "The optimization of demand response programs in smart grids," *Energy Policy,* vol. 94, no. Supplement C, pp. 295-306, 2016/07/01/ 2016, doi: https://doi.org/10.1016/j.enpol.2016.04.009.

[28] P. Jahangiri, R. Sangi, A. Thamm, R. Streblow, and D. Mueller, *Dynamic Exergy Analysis - Part II: A Case Study of CHP District Heating in Bottrop, Germany*. 2014.

[29] K. Siler-Evans, M. G. Morgan, and I. L. Azevedo, "Distributed cogeneration for commercial buildings: Can we make the economics work?," *Energy Policy,* vol. 42, pp. 580-590, 2012/03/01/ 2012, doi: https://doi.org/10.1016/j.enpol.2011.12.028.

[30] M. Geidl, G. Koeppel, P. Favre-Perrod, B. Klöckl, G. Andersson, and K. Fröhlich, "Energy hubs for the future," *IEEE Power and Energy Magazine,* Review vol. 5, no. 1, pp. 24-30, 2007, doi: 10.1109/MPAE.2007.264850.

[31] G. Sundberg and D. Henning, "Investments in combined heat and power plants: influence of fuel price on cost minimised operation," *Energy Conversion and Management,* vol. 43, no. 5, pp. 639-650, 3// 2002, doi: http://dx.doi.org/10.1016/S0196-8904(01)00065-6.

[32] K. Sartor, S. Quoilin, and P. Dewallef, "Simulation and optimization of a CHP biomass plant and district heating network," *Applied Energy,* vol. 130, pp. 474-483, 10/1/ 2014, doi: http://dx.doi.org/10.1016/j.apenergy.2014.01.097.

[33] J. Liu, W. Zhang, R. Zhou, and J. Zhong, "Impacts of distributed renewable energy generations on smart grid operation and dispatch," in *2012 IEEE Power*

and Energy Society General Meeting, 22-26 July 2012 2012, pp. 1-5, doi: 10.1109/PESGM.2012.6344997.

[34] R. Boukhanouf, "15 - Small combined heat and power (CHP) systems for commercial buildings and institutions A2 - Beith, Robert," in *Small and Micro Combined Heat and Power (CHP) Systems*: Woodhead Publishing, 2011, pp. 365-394.

[35] A. D. Ondeck, T. F. Edgar, and M. Baldea, "Optimal operation of a residential district-level combined photovoltaic/natural gas power and cooling system," *Applied Energy,* vol. 156, pp. 593-606, 10/15/ 2015, doi: http://dx.doi.org/10.1016/j.apenergy.2015.06.045.

[36] D. Setlhaolo, X. Xia, and J. Zhang, "Optimal scheduling of household appliances for demand response," *Electric Power Systems Research,* vol. 116, pp. 24-28, 2014/11/01/ 2014, doi: https://doi.org/10.1016/j.epsr.2014.04.012.

[37] O. Erdinc, N. G. Paterakis, I. N. Pappi, A. G. Bakirtzis, and J. P. S. Catalão, "A new perspective for sizing of distributed generation and energy storage for smart households under demand response," *Applied Energy,* vol. 143, pp. 26-37, 2015/04/01/ 2015, doi: https://doi.org/10.1016/j.apenergy.2015.01.025.

[38] S. Behboodi, D. P. Chassin, C. Crawford, and N. Djilali, "Renewable resources portfolio optimization in the presence of demand response," *Applied Energy,* vol. 162, pp. 139-148, 1/15/ 2016, doi: https://doi.org/10.1016/j.apenergy.2015.10.074.

[39] A. S. Dagoumas and M. L. Polemis, "An integrated model for assessing electricity retailer's profitability with demand response," *Applied Energy,* vol. 198, no. Supplement C, pp. 49-64, 2017/07/15/ 2017, doi: https://doi.org/10.1016/j.apenergy.2017.04.050.

[40] M. Á. Lynch, S. Nolan, M. T. Devine, and M. O'Malley, "The impacts of demand response participation in capacity markets," *Applied Energy,* vol. 250, pp. 444-451, 2019/09/15/ 2019, doi: https://doi.org/10.1016/j.apenergy.2019.05.063.

[41] A. Ihsan, M. Jeppesen, and M. J. Brear, "Impact of demand response on the optimal, techno-economic performance of a hybrid, renewable energy power plant," *Applied Energy,* vol. 238, pp. 972-984, 2019/03/15/ 2019, doi: https://doi.org/10.1016/j.apenergy.2019.01.090.

[42] X. Wang, A. Palazoglu, and N. H. El-Farra, "Operational optimization and demand response of hybrid renewable energy systems," *Applied Energy,* vol. 143, pp. 324-335, 2015/04/01/ 2015, doi: https://doi.org/10.1016/j.apenergy.2015.01.004.

[43] X. Jin, Y. Mu, H. Jia, J. Wu, T. Jiang, and X. Yu, "Dynamic economic dispatch of a hybrid energy microgrid considering building based virtual energy storage

system," *Applied Energy,* vol. 194, pp. 386-398, 2017/05/15/ 2017, doi: https://doi.org/10.1016/j.apenergy.2016.07.080.

[44] M. Jin, W. Feng, P. Liu, C. Marnay, and C. Spanos, "MOD-DR: Microgrid optimal dispatch with demand response," *Applied Energy,* vol. 187, no. Supplement C, pp. 758-776, 2017/02/01/ 2017, doi: https://doi.org/10.1016/j.apenergy.2016.11.093.

[45] P. Firouzmakan, R.-A. Hooshmand, M. Bornapour, and A. Khodabakhshian, "A comprehensive stochastic energy management system of micro-CHP units, renewable energy sources and storage systems in microgrids considering demand response programs," *Renewable and Sustainable Energy Reviews,* vol. 108, pp. 355-368, 2019/07/01/ 2019, doi: https://doi.org/10.1016/j.rser.2019.04.001.

[46] L. Pérez-Lombard, J. Ortiz, and C. Pout, "A review on buildings energy consumption information," *Energy and Buildings,* vol. 40, no. 3, pp. 394-398, 2008/01/01/ 2008, doi: https://doi.org/10.1016/j.enbuild.2007.03.007.

[47] I. Beil, I. Hiskens, and S. Backhaus, "Frequency Regulation From Commercial Building HVAC Demand Response," *Proceedings of the IEEE,* vol. 104, no. 4, pp. 745-757, 2016, doi: 10.1109/JPROC.2016.2520640.

[48] G. Díaz and B. Moreno, "Valuation under uncertain energy prices and load demands of micro-CHP plants supplemented by optimally switched thermal energy storage," *Applied Energy,* vol. 177, pp. 553-569, 9/1/ 2016, doi: http://dx.doi.org/10.1016/j.apenergy.2016.05.075.

[49] J. Knowles, "1 - Overview of small and micro combined heat and power (CHP) systems A2 - Beith, Robert," in *Small and Micro Combined Heat and Power (CHP) Systems*: Woodhead Publishing, 2011, pp. 3-16.

[50] "Sokratherm." https://www.sokratherm.de/en/compact-chp-units/compact-chp-units-of-the-500-kw-class/ (accessed 12 April, 2020).

[51] A. D. Hawkes, "2 - Techno-economic assessment of small and micro combined heat and power (CHP) systems," in *Small and Micro Combined Heat and Power (CHP) Systems*, R. Beith Ed.: Woodhead Publishing, 2011, pp. 17-41.

[52] "UK Power." https://www.ukpower.co.uk/home_energy/tariffs-per-unit-kwh (accessed.

[53] Q. Wu, H. Ren, and W. Gao, "Economic Assessment of Micro-CHP System for Residential Application in Shanghai, China," *Energy Procedia,* vol. 88, pp. 732-737, 6// 2016, doi: http://dx.doi.org/10.1016/j.egypro.2016.06.054.

[54] D. Parra, M. Gillott, S. Norman, and G. Walker, "Optimum community energy storage system for PV energy time-shift," *Applied Energy,* vol. 137, pp. 576-587, 01/01 2015, doi: 10.1016/j.apenergy.2014.08.060.

[55] X. Luo, J. Wang, M. Dooner, and J. Clarke, "Overview of current development in electrical energy storage technologies and the application potential in power

system operation," *Applied Energy,* vol. 137, pp. 511-536, 2015/01/01/ 2015, doi: https://doi.org/10.1016/j.apenergy.2014.09.081.

[56] "Hydropower UK." https://www.hydropower.org/country-profiles/united-kingdom (accessed 20 April, 2020).

[57] "The future role for energy storage in the UK main report.," Energy Research p artnership (ERP) technology report, June 2011.

[58] H. Zhao, Q. Wu, S. Hu, H. Xu, and C. N. Rasmussen, "Review of energy storage system for wind power integration support," *Applied Energy,* vol. 137, pp. 545-553, 2015/01/01/ 2015, doi: https://doi.org/10.1016/j.apenergy.2014.04.103.

[59] A. Evans, V. Strezov, and T. J. Evans, "Assessment of utility energy storage options for increased renewable energy penetration," *Renewable and Sustainable Energy Reviews,* vol. 16, no. 6, pp. 4141-4147, 2012/08/01/ 2012, doi: https://doi.org/10.1016/j.rser.2012.03.048.

[60] B. Dunn, H. Kamath, and J.-M. Tarascon, "Electrical Energy Storage for the Grid: A Battery of Choices," *Science (New York, N.Y.),* vol. 334, pp. 928-35, 11/18 2011, doi: 10.1126/science.1212741.

[61] N. Nitta, F. Wu, J. T. Lee, and G. Yushin, "Li-ion battery materials: present and future," *Materials Today,* vol. 18, no. 5, pp. 252-264, 2015/06/01/ 2015, doi: https://doi.org/10.1016/j.mattod.2014.10.040.

[62] "Clean Energy Institute." https://www.cei.washington.edu/education/science-of-solar/battery-technology/ (accessed 18 April, 2020).

[63] D. Greenwood. "Future Lithium Ion Batteries " https://www.brighton.ac.uk/_pdf/research/cae/future-li-ion-batteries.pdf (accessed 17 October, 2018).

[64] H. Lund *et al.*, "4th Generation District Heating (4GDH): Integrating smart thermal grids into future sustainable energy systems," *Energy,* vol. 68, pp. 1-11, 2014/04/15/ 2014, doi: https://doi.org/10.1016/j.energy.2014.02.089.

[65] P. Mancarella, "MES (multi-energy systems): An overview of concepts and evaluation models," *Energy,* vol. 65, pp. 1–17, 02/01 2014, doi: 10.1016/j.energy.2013.10.041.

[66] U. Persson and S. Werner, "Heat distribution and the future competitiveness of district heating," *Applied Energy,* vol. 88, no. 3, pp. 568-576, 2011/03/01/ 2011, doi: https://doi.org/10.1016/j.apenergy.2010.09.020.

[67] Y. Li, Y. Rezgui, and H. Zhu, "District heating and cooling optimization and enhancement – Towards integration of renewables, storage and smart grid," *Renewable and Sustainable Energy Reviews,* vol. 72, pp. 281-294, 2017/05/01/ 2017, doi: https://doi.org/10.1016/j.rser.2017.01.061.

[68] H. Lund and B. V. Mathiesen, "Energy system analysis of 100% renewable energy systems—The case of Denmark in years 2030 and 2050," *Energy,* vol.

34, no. 5, pp. 524-531, 2009/05/01/ 2009, doi: https://doi.org/10.1016/j.energy.2008.04.003.

[69] J. Huang, J. Fan, and S. Furbo, "Feasibility study on solar district heating in China," *Renewable and Sustainable Energy Reviews,* vol. 108, pp. 53-64, 2019/07/01/ 2019, doi: https://doi.org/10.1016/j.rser.2019.03.014.

[70] E. Fahlén and E. O. Ahlgren, "Assessment of integration of different biomass gasification alternatives in a district-heating system," *Energy,* vol. 34, no. 12, pp. 2184-2195, 2009/12/01/ 2009, doi: https://doi.org/10.1016/j.energy.2008.10.018.

[71] L. Ozgener, A. Hepbasli, and I. Dincer, "Energy and exergy analysis of geothermal district heating systems: an application," *Building and Environment,* vol. 40, no. 10, pp. 1309-1322, 2005/10/01/ 2005, doi: https://doi.org/10.1016/j.buildenv.2004.11.001.

[72] F. Lin and L. Yan, "A New Type of District Heating System Based on Distributed Absorption Heat Pumps," *Proceedings of the ASME 3rd International Conference on Energy Sustainability 2009, ES2009,* vol. 2, pp. 163-168, 01/01 2009, doi: 10.1115/ES2009-90287.

[73] F. Sun, L. Fu, J. Sun, and S. Zhang, "A new waste heat district heating system with combined heat and power (CHP) based on ejector heat exchangers and absorption heat pumps," *Energy,* vol. 69, pp. 516-524, 2014/05/01/ 2014, doi: https://doi.org/10.1016/j.energy.2014.03.044.

[74] H. Fang, J. Xia, and Y. Jiang, "Key issues and solutions in a district heating system using low-grade industrial waste heat," *Energy,* vol. 86, pp. 589-602, 2015/06/15/ 2015, doi: https://doi.org/10.1016/j.energy.2015.04.052.

[75] A. Kapil, I. Bulatov, R. Smith, and J.-K. Kim, "Process integration of low grade heat in process industry with district heating networks," *Energy,* vol. 44, no. 1, pp. 11-19, 2012/08/01/ 2012, doi: https://doi.org/10.1016/j.energy.2011.12.015.

[76] M. Casisi, P. Pinamonti, and M. Reini, "Optimal lay-out and operation of combined heat & power (CHP) distributed generation systems," *Energy,* vol. 34, no. 12, pp. 2175-2183, 2009/12/01/ 2009, doi: https://doi.org/10.1016/j.energy.2008.10.019.

[77] L. Fu, G. Tian, J. Sui, and Y. Jiang, "Combining absorption heat pump with gas boiler for exhaust condensing heat recovery in district heating system," *Taiyangneng Xuebao/Acta Energiae Solaris Sinica,* vol. 24, pp. 620-624, 10/01 2003.

[78] L. Brange, J. Englund, and P. Lauenburg, "Prosumers in district heating networks – A Swedish case study," *Applied Energy,* vol. 164, pp. 492-500, 2016/02/15/ 2016, doi: https://doi.org/10.1016/j.apenergy.2015.12.020.

[79] G. Alva, Y. Lin, and G. Fang, "An overview of thermal energy storage systems," *Energy,* vol. 144, pp. 341-378, 2018/02/01/ 2018, doi: https://doi.org/10.1016/j.energy.2017.12.037.

[80] H. Gadd and S. Werner, "18 - Thermal energy storage systems for district heating and cooling," in *Advances in Thermal Energy Storage Systems*, L. F. Cabeza Ed.: Woodhead Publishing, 2015, pp. 467-478.

[81] D. Akinyele and R. Rayudu, "Review of energy storage technologies for sustainable power networks," *Sustainable Energy Technologies and Assessments,* vol. 8, pp. 74–91, 12/01 2014, doi: 10.1016/j.seta.2014.07.004.

[82] K. M. Powell, A. Sriprasad, W. J. Cole, and T. F. Edgar, "Heating, cooling, and electrical load forecasting for a large-scale district energy system," *Energy,* vol. 74, pp. 877-885, 2014/09/01/ 2014, doi: https://doi.org/10.1016/j.energy.2014.07.064.

[83] G. Streckienė, V. Martinaitis, A. N. Andersen, and J. Katz, "Feasibility of CHP-plants with thermal stores in the German spot market," *Applied Energy,* vol. 86, no. 11, pp. 2308-2316, 2009/11/01/ 2009, doi: https://doi.org/10.1016/j.apenergy.2009.03.023.

[84] A. Dalla Rosa and J. E. Christensen, "Low-energy district heating in energy-efficient building areas," *Energy,* vol. 36, no. 12, pp. 6890-6899, 2011/12/01/ 2011, doi: https://doi.org/10.1016/j.energy.2011.10.001.

[85] S.-I. Gustafsson and B. G. Karlsson, "Heat accumulators in CHP networks," *Energy Conversion and Management,* vol. 33, no. 12, pp. 1051-1061, 1992/12/01/ 1992, doi: https://doi.org/10.1016/0196-8904(92)90002-E.

[86] D. Schröder, "Introducing Additional Heat Storage to the Hässelby CHP Plant - A case study on economic and ecological benefits achievable with heat storage in a deregulated electricity market," 2011.

[87] A. Sciacovelli, E. Guelpa, and V. Verda, "Pumping Cost Minimization in an Existing District Heating Network," no. 56284, p. V06AT07A066, 2013, doi: 10.1115/IMECE2013-65169.

[88] E. Guelpa, C. Toro, A. Sciacovelli, R. Melli, E. Sciubba, and V. Verda, "Optimal operation of large district heating networks through fast fluid-dynamic simulation," *Energy,* vol. 102, pp. 586-595, 2016/05/01/ 2016, doi: https://doi.org/10.1016/j.energy.2016.02.058.

[89] E. Guelpa, G. Mutani, V. Todeschi, and V. Verda, "Reduction of CO2 emissions in urban areas through optimal expansion of existing district heating networks," *Journal of Cleaner Production,* vol. 204, pp. 117-129, 2018/12/10/ 2018, doi: https://doi.org/10.1016/j.jclepro.2018.08.272.

[90] M.-S. Shin, H.-S. Kim, D.-S. Jang, S.-N. Lee, Y.-S. Lee, and H.-G. Yoon, "Numerical and experimental study on the design of a stratified thermal storage

system," *Applied Thermal Engineering,* vol. 24, no. 1, pp. 17-27, 2004/01/01/ 2004, doi: https://doi.org/10.1016/S1359-4311(03)00242-4.

[91] K. Sartor and P. Dewallef, "Optimized Integration of Heat Storage Into District Heating Networks Fed By a Biomass CHP Plant," *Energy Procedia,* vol. 135, pp. 317-326, 2017/10/01/ 2017, doi: https://doi.org/10.1016/j.egypro.2017.09.523.

[92] T.-M. Tveit, T. Savola, A. Gebremedhin, and C.-J. Fogelholm, "Multi-period MINLP model for optimising operation and structural changes to CHP plants in district heating networks with long-term thermal storage," *Energy Conversion and Management,* vol. 50, no. 3, pp. 639-647, 2009/03/01/ 2009, doi: https://doi.org/10.1016/j.enconman.2008.10.010.

[93] M. Abunku and W. J. C. Melis, "Modelling of a CHP system with electrical and thermal storage," in *2015 50th International Universities Power Engineering Conference (UPEC)*, 1-4 Sept. 2015 2015, pp. 1-5, doi: 10.1109/UPEC.2015.7339926.

[94] A. Al-Qattan, A. ElSherbini, and K. Al-Ajmi, "Solid oxide fuel cell application in district cooling," *Journal of Power Sources,* vol. 257, pp. 21-26, 2014/07/01/ 2014, doi: https://doi.org/10.1016/j.jpowsour.2014.01.099.

[95] T. R. Olorunfemi and N. Nwulu, "A Review of Demand Response Techniques and Operational Limitations," in *2018 International Conference on Computational Techniques, Electronics and Mechanical Systems (CTEMS)*, 21-22 Dec. 2018 2018, pp. 442-445, doi: 10.1109/CTEMS.2018.8769181.

[96] N. O'Connell, P. Pinson, H. Madsen, and M. O'Malley, "Benefits and challenges of electrical demand response: A critical review," *Renewable and Sustainable Energy Reviews,* vol. 39, pp. 686-699, 2014/11/01/ 2014, doi: https://doi.org/10.1016/j.rser.2014.07.098.

[97] D. Setlhaolo and X. Xia, "Optimal scheduling of household appliances with a battery storage system and coordination," *Energy and Buildings,* vol. 94, pp. 61-70, 5/1/ 2015, doi: http://dx.doi.org/10.1016/j.enbuild.2015.02.051.

[98] A. Safdarian, M. Ali, M. Fotuhi-Firuzabad, and M. Lehtonen, "Domestic EWH and HVAC management in smart grids: Potential benefits and realization," *Electric Power Systems Research,* vol. 134, pp. 38-46, 5// 2016, doi: http://dx.doi.org/10.1016/j.epsr.2015.12.021.

[99] D. Caprino, M. L. Della Vedova, and T. Facchinetti, "Peak shaving through real-time scheduling of household appliances," *Energy and Buildings,* vol. 75, no. Supplement C, pp. 133-148, 2014/06/01/ 2014, doi: https://doi.org/10.1016/j.enbuild.2014.02.013.

[100] A. H. Mohsenian-Rad, V. W. S. Wong, J. Jatskevich, R. Schober, and A. Leon-Garcia, "Autonomous Demand-Side Management Based on Game-Theoretic Energy Consumption Scheduling for the Future Smart Grid," *IEEE*

Transactions on Smart Grid, vol. 1, no. 3, pp. 320-331, 2010, doi: 10.1109/TSG.2010.2089069.

[101] S. Althaher, P. Mancarella, and J. Mutale, "Automated Demand Response From Home Energy Management System Under Dynamic Pricing and Power and Comfort Constraints," *IEEE Transactions on Smart Grid,* vol. 6, no. 4, pp. 1874-1883, 2015, doi: 10.1109/TSG.2014.2388357.

[102] J. A. Gomez-Herrera and M. F. Anjos, "Optimal collaborative demand-response planner for smart residential buildings," *Energy,* vol. 161, pp. 370-380, 2018/10/15/ 2018, doi: https://doi.org/10.1016/j.energy.2018.07.132.

[103] N. Yu and J. Yu, "Optimal TOU Decision Considering Demand Response Model," in *2006 International Conference on Power System Technology*, 22-26 Oct. 2006 2006, pp. 1-5, doi: 10.1109/ICPST.2006.321461.

[104] D. S. Kirschen, G. Strbac, P. Cumperayot, and D. d. P. Mendes, "Factoring the elasticity of demand in electricity prices," *IEEE Transactions on Power Systems,* vol. 15, no. 2, pp. 612-617, 2000, doi: 10.1109/59.867149.

[105] D. Dengwei, L. Junyong, N. Huaiping, and W. Jiguang, "A risk-evasion TOU pricing method for distribution utility in deregulated market environment," in *2004 International Conference on Power System Technology, 2004. PowerCon 2004.*, 21-24 Nov. 2004 2004, vol. 1, pp. 527-531 Vol.1, doi: 10.1109/ICPST.2004.1460051.

[106] A. Etxegarai, A. Bereziartua, J. A. Dañobeitia, O. Abarrategi, and G. Saldaña, "Impact of price-based demand response programs for residential customers," in *2018 19th IEEE Mediterranean Electrotechnical Conference (MELECON)*, 2-7 May 2018 2018, pp. 204-208, doi: 10.1109/MELCON.2018.8379094.

[107] Z. Wang *et al.*, "How to effectively implement an incentive-based residential electricity demand response policy? Experience from large-scale trials and matching questionnaires," *Energy Policy,* vol. 141, p. 111450, 2020/06/01/ 2020, doi: https://doi.org/10.1016/j.enpol.2020.111450.

[108] R. Alasseri, T. J. Rao, and K. J. Sreekanth, "Institution of incentive-based demand response programs and prospective policy assessments for a subsidized electricity market," *Renewable and Sustainable Energy Reviews,* vol. 117, p. 109490, 2020/01/01/ 2020, doi: https://doi.org/10.1016/j.rser.2019.109490.

[109] H. A. Aalami, H. Pashaei-Didani, and S. Nojavan, "Deriving nonlinear models for incentive-based demand response programs," *International Journal of Electrical Power & Energy Systems,* vol. 106, pp. 223-231, 2019/03/01/ 2019, doi: https://doi.org/10.1016/j.ijepes.2018.10.003.

[110] N. I. Nwulu and X. Xia, "Multi-objective dynamic economic emission dispatch of electric power generation integrated with game theory based demand

response programs," *Energy Conversion and Management,* vol. 89, pp. 963-974, 2015/01/01/ 2015, doi: https://doi.org/10.1016/j.enconman.2014.11.001.

[111] N. I. Nwulu and X. Xia, "Optimal dispatch for a microgrid incorporating renewables and demand response," *Renewable Energy,* vol. 101, pp. 16-28, 2017/02/01/ 2017, doi: https://doi.org/10.1016/j.renene.2016.08.026.

[112] T. Chiu, Y. Shih, A. Pang, and C. Pai, "Optimized Day-Ahead Pricing With Renewable Energy Demand-Side Management for Smart Grids," *IEEE Internet of Things Journal,* vol. 4, no. 2, pp. 374-383, 2017, doi: 10.1109/JIOT.2016.2556006.

[113] C. N. Kurucz, D. Brandt, and S. Sim, "A linear programming model for reducing system peak through customer load control programs," *IEEE Transactions on Power Systems,* vol. 11, no. 4, pp. 1817-1824, 1996, doi: 10.1109/59.544648.

[114] F. N. Lee and A. M. Breipohl, "Operational Cost Savings of Direct Load Control," *IEEE Power Engineering Review,* vol. PER-4, no. 5, pp. 34-34, 1984, doi: 10.1109/MPER.1984.5526033.

[115] H. Jorge, C. H. Antunes, and A. G. Martins, "A multiple objective decision support model for the selection of remote load control strategies," *IEEE Transactions on Power Systems,* vol. 15, no. 2, pp. 865-872, 2000, doi: 10.1109/59.867186.

[116] H. Kun-Yuan and H. Yann-Chang, "Integrating direct load control with interruptible load management to provide instantaneous reserves for ancillary services," *IEEE Transactions on Power Systems,* vol. 19, no. 3, pp. 1626-1634, 2004, doi: 10.1109/TPWRS.2004.831705.

[117] A. Gomes, C. H. Antunes, and A. G. Martins, "A multiple objective evolutionary approach for the design and selection of load control strategies," *IEEE Transactions on Power Systems,* vol. 19, no. 2, pp. 1173-1180, 2004, doi: 10.1109/TPWRS.2003.821623.

[118] D. Qinwei, "A price-based demand response scheduling model in day-ahead electricity market," in *2016 IEEE Power and Energy Society General Meeting (PESGM)*, 17-21 July 2016 2016, pp. 1-5, doi: 10.1109/PESGM.2016.7741812.

[119] F. Wen and A. K. David, "Optimal bidding strategies for competitive generators and large consumers," *International Journal of Electrical Power & Energy Systems,* vol. 23, no. 1, pp. 37-43, 2001/01/01/ 2001, doi: https://doi.org/10.1016/S0142-0615(00)00032-6.

[120] H. Yang, T. Xiong, J. Qiu, D. Qiu, and Z. Y. Dong, "Optimal operation of DES/CCHP based regional multi-energy prosumer with demand response," *Applied Energy,* vol. 167, no. Supplement C, pp. 353-365, 2016/04/01/ 2016, doi: https://doi.org/10.1016/j.apenergy.2015.11.022.

[121] B. Fang *et al.*, "The contributions of cloud technologies to smart grid," *Renewable and Sustainable Energy Reviews,* vol. 59, pp. 1326-1331, 2016/06/01/ 2016, doi: https://doi.org/10.1016/j.rser.2016.01.032.

[122] A. Sheikhi, A. M. Ranjbar, and F. Safe, "Optimal dispatch of a multiple energy carrier system equipped with a CCHP," *Renewable Energy and Power Quality Journal,* pp. 1413-1418, 05/01 2011, doi: 10.24084/repqj09.675.

[123] O. Dzobo and X. Xia, "Optimal operation of smart multi-energy hub systems incorporating energy hub coordination and demand response strategy," *Journal of Renewable and Sustainable Energy,* vol. 9, p. 045501, 07/01 2017, doi: 10.1063/1.4993046.

[124] M. Alipour, K. Zare, and B. Mohammadi-Ivatloo, "Short-term scheduling of combined heat and power generation units in the presence of demand response programs," *Energy,* vol. 71, pp. 289-301, 2014/07/15/ 2014, doi: https://doi.org/10.1016/j.energy.2014.04.059.

[125] J. S. Kim and T. F. Edgar, "Optimal scheduling of combined heat and power plants using mixed-integer nonlinear programming," *Energy,* vol. 77, pp. 675-690, 2014/12/01/ 2014, doi: https://doi.org/10.1016/j.energy.2014.09.062.

[126] C. Milan, M. Stadler, G. Cardoso, and S. Mashayekh, "Modeling of non-linear CHP efficiency curves in distributed energy systems," *Applied Energy,* vol. 148, pp. 334-347, 2015/06/15/ 2015, doi: https://doi.org/10.1016/j.apenergy.2015.03.053.

[127] D. W. Wu and R. Z. Wang, "Combined cooling, heating and power: A review," *Progress in Energy and Combustion Science,* vol. 32, no. 5, pp. 459-495, 2006/09/01/ 2006, doi: https://doi.org/10.1016/j.pecs.2006.02.001.

[128] M. Newborough, "Assessing the benefits of implementing micro-CHP systems in the UK," *Proceedings of the Institution of Mechanical Engineers, Part A: Journal of Power and Energy,* vol. 218, no. 4, pp. 203-218, 2004/06/01 2004, doi: 10.1243/0957650041200650.

[129] A. D. Hawkes and M. A. Leach, "Cost-effective operating strategy for residential micro-combined heat and power," *Energy,* vol. 32, no. 5, pp. 711-723, 2007/05/01/ 2007, doi: https://doi.org/10.1016/j.energy.2006.06.001.

[130] A. Safaei, F. Freire, and C. H. Antunes, "A model for optimal energy planning of a commercial building integrating solar and cogeneration systems," *Energy,* vol. 61, pp. 211-223, 2013/11/01/ 2013, doi: https://doi.org/10.1016/j.energy.2013.08.048.

[131] D. Xie, Y. Lu, J. Sun, C. Gu, and G. Li, "Optimal Operation of a Combined Heat and Power System Considering Real-time Energy Prices," *IEEE Access,* vol. 4, pp. 3005-3015, 2016, doi: 10.1109/ACCESS.2016.2580918.

[132] A. D. Peacock and M. Newborough, "Impact of micro-CHP systems on domestic sector CO2 emissions," *Applied Thermal Engineering,* vol. 25, no.

17, pp. 2653-2676, 2005/12/01/ 2005, doi: https://doi.org/10.1016/j.applthermaleng.2005.03.015.

[133] H. Wang, H. Zhang, C. Gu, and F. Li, "Optimal design and operation of CHPs and energy hub with multi objectives for a local energy system," *Energy Procedia,* vol. 142, pp. 1615-1621, 2017/12/01/ 2017, doi: https://doi.org/10.1016/j.egypro.2017.12.539.

[134] H. R. Baghaee, M. Mirsalim, G. B. Gharehpetian, and H. A. Talebi, "A Decentralized Power Management and Sliding Mode Control Strategy for Hybrid AC/DC Microgrids including Renewable Energy Resources," *IEEE Transactions on Industrial Informatics,* pp. 1-1, 2017, doi: 10.1109/TII.2017.2677943.

[135] S. K. Tiwari, B. Singh, and P. K. Goel, "Design and Control of Microgrid Fed by Renewable Energy Generating Sources," *IEEE Transactions on Industry Applications,* vol. 54, no. 3, pp. 2041-2050, 2018, doi: 10.1109/TIA.2018.2793213.

[136] H. R. Baghaee, M. Mirsalim, G. B. Gharehpetian, and H. A. Talebi, "Reliability/cost-based multi-objective Pareto optimal design of stand-alone wind/PV/FC generation microgrid system," *Energy,* vol. 115, pp. 1022-1041, 2016/11/15/ 2016, doi: https://doi.org/10.1016/j.energy.2016.09.007.

[137] P. Bajpai and V. Dash, "Hybrid renewable energy systems for power generation in stand-alone applications: A review," *Renewable and Sustainable Energy Reviews,* vol. 16, no. 5, pp. 2926-2939, 2012/06/01/ 2012, doi: https://doi.org/10.1016/j.rser.2012.02.009.

[138] H. Karami, M. Sanjari, A. Tavakoli, and G. B. Gharehpetian, "Optimal Scheduling of Residential Energy System Including Combined Heat and Power System and Storage Device," *Electric Power Components and Systems,* vol. 41, 05/15 2013, doi: 10.1080/15325008.2013.769032.

[139] J. Ma, L. Yuan, Z. Zhao, and F. He, "Transmission Loss Optimization-Based Optimal Power Flow Strategy by Hierarchical Control for DC Microgrids," *IEEE Transactions on Power Electronics,* vol. 32, no. 3, pp. 1952-1963, 2017, doi: 10.1109/TPEL.2016.2561301.

[140] D. Pudjianto, G. Strbac, F. v. Oberbeeke, A. I. Androutsos, Z. Larrabe, and J. T. Saraiva, "Investigation of regulatory, commercial, economic and environmental issues in microgrids," in *2005 International Conference on Future Power Systems*, 18-18 Nov. 2005 2005, pp. 6 pp.-6, doi: 10.1109/FPS.2005.204223.

[141] M. T. Lawder *et al.*, "Battery Energy Storage System (BESS) and Battery Management System (BMS) for Grid-Scale Applications," *Proceedings of the IEEE,* vol. 102, no. 6, pp. 1014-1030, 2014, doi: 10.1109/JPROC.2014.2317451.

[142] M. Koller, T. Borsche, A. Ulbig, and G. Andersson, "Review of grid applications with the Zurich 1MW battery energy storage system," *Electric Power Systems Research,* vol. 120, pp. 128-135, 2015/03/01/ 2015, doi: https://doi.org/10.1016/j.epsr.2014.06.023.

[143] K. C. Divya and J. Østergaard, "Battery energy storage technology for power systems—An overview," *Electric Power Systems Research,* vol. 79, no. 4, pp. 511-520, 2009/04/01/ 2009, doi: https://doi.org/10.1016/j.epsr.2008.09.017.

[144] E. Shirazi and S. Jadid, "Cost reduction and peak shaving through domestic load shifting and DERs," *Energy,* vol. 124, pp. 146-159, 2017/04/01/ 2017, doi: https://doi.org/10.1016/j.energy.2017.01.148.

[145] K. Baker, G. Hug, and X. Li, "Energy Storage Sizing Taking Into Account Forecast Uncertainties and Receding Horizon Operation," *IEEE Transactions on Sustainable Energy,* vol. 8, no. 1, pp. 331-340, 2017, doi: 10.1109/TSTE.2016.2599074.

[146] K. Abdulla *et al.*, "Optimal Operation of Energy Storage Systems Considering Forecasts and Battery Degradation," *IEEE Transactions on Smart Grid,* vol. 9, no. 3, pp. 2086-2096, 2018, doi: 10.1109/TSG.2016.2606490.

[147] M. C. Bozchalui and R. Sharma, "Optimal operation of Energy Storage in distribution systems with Renewable Energy Resources," in *2014 Clemson University Power Systems Conference*, 11-14 March 2014 2014, pp. 1-6, doi: 10.1109/PSC.2014.6808125.

[148] S. Ikeda and R. Ooka, "Optimal Operation of Energy Systems Including Thermal Energy Storage and Battery under Different Connections," *Energy Procedia,* vol. 78, pp. 2256-2261, 2015/11/01/ 2015, doi: https://doi.org/10.1016/j.egypro.2015.11.360.

[149] D. Zhang, N. Shah, and L. G. Papageorgiou, "Efficient energy consumption and operation management in a smart building with microgrid," *Energy Conversion and Management,* vol. 74, pp. 209-222, 2013/10/01/ 2013, doi: https://doi.org/10.1016/j.enconman.2013.04.038.

[150] O. Y. Odufuwa, K. Kusakana, and B. P. Numbi, "Review of Optimal Energy Management Applied on Ice Thermal Energy Storage for an Air Conditioning System in Commercial Buildings," in *2018 Open Innovations Conference (OI)*, 3-5 Oct. 2018 2018, pp. 286-293, doi: 10.1109/OI.2018.8535839.

[151] Y. Zhao, Y. Lu, C. Yan, and S. Wang, "MPC-based optimal scheduling of grid-connected low energy buildings with thermal energy storages," *Energy and Buildings,* vol. 86, pp. 415-426, 2015/01/01/ 2015, doi: https://doi.org/10.1016/j.enbuild.2014.10.019.

[152] X. Xi, R. Sioshansi, and V. Marano, "A stochastic dynamic programming model for co-optimization of distributed energy storage," *Energy Systems,* vol. 5, no. 3, pp. 475-505, 2014/09/01 2014, doi: 10.1007/s12667-013-0100-6.

[153] J. Qin, R. Sevlian, D. Varodayan, and R. Rajagopal, "Optimal electric energy storage operation," in *2012 IEEE Power and Energy Society General Meeting*, 22-26 July 2012 2012, pp. 1-6, doi: 10.1109/PESGM.2012.6345242.

[154] D. R. Jiang, T. V. Pham, W. B. Powell, D. F. Salas, and W. R. Scott, "A comparison of approximate dynamic programming techniques on benchmark energy storage problems: Does anything work?," in *2014 IEEE Symposium on Adaptive Dynamic Programming and Reinforcement Learning (ADPRL)*, 9-12 Dec. 2014 2014, pp. 1-8, doi: 10.1109/ADPRL.2014.7010626.

[155] L. Hannah and D. Dunson, *Approximate Dynamic Programming for Storage Problems*. 2011, pp. 337-344.

[156] V. Muenzel, J. d. Hoog, M. Brazil, A. Vishwanath, and S. Kalyanaraman, "A Multi-Factor Battery Cycle Life Prediction Methodology for Optimal Battery Management," presented at the Proceedings of the 2015 ACM Sixth International Conference on Future Energy Systems, Bangalore, India, 2015. [Online]. Available: https://doi.org/10.1145/2768510.2768532.

[157] M. Koller, T. Borsche, A. Ulbig, and G. Andersson, "Defining a degradation cost function for optimal control of a battery energy storage system," in *2013 IEEE Grenoble Conference*, 16-20 June 2013 2013, pp. 1-6, doi: 10.1109/PTC.2013.6652329.

[158] D. Tran and A. M. Khambadkone, "Energy Management for Lifetime Extension of Energy Storage System in Micro-Grid Applications," *IEEE Transactions on Smart Grid,* vol. 4, no. 3, pp. 1289-1296, 2013, doi: 10.1109/TSG.2013.2272835.

[159] J. Cai, X. Jin, and H. Zhang, "Economic Model-Based Control of Sustainable Buildings with Photovoltaic (PV) and Battery Systems Considering Battery Degradation Costs," in *2018 Annual American Control Conference (ACC)*, 27-29 June 2018 2018, pp. 5406-5411, doi: 10.23919/ACC.2018.8431619.

[160] C. A. Balaras, K. Droutsa, E. Dascalaki, and S. Kontoyiannidis, "Heating energy consumption and resulting environmental impact of European apartment buildings," *Energy and Buildings,* vol. 37, no. 5, pp. 429-442, 2005/05/01/ 2005, doi: https://doi.org/10.1016/j.enbuild.2004.08.003.

[161] E. M. Malatji, J. Zhang, and X. Xia, "A multiple objective optimisation model for building energy efficiency investment decision," *Energy and Buildings,* vol. 61, pp. 81-87, 2013/06/01/ 2013, doi: https://doi.org/10.1016/j.enbuild.2013.01.042.

[162] H. Doukas, C. Nychtis, and J. Psarras, "Assessing energy-saving measures in buildings through an intelligent decision support model," *Building and Environment,* vol. 44, no. 2, pp. 290-298, 2009/02/01/ 2009, doi: https://doi.org/10.1016/j.buildenv.2008.03.006.

[163] X. Xia, J. Zhang, and W. Cass, "Energy management of commercial buildings - A case study from a POET perspective of energy efficiency," *Journal of Energy in Southern Africa,* vol. 23, pp. 23-31, 02/01 2012, doi: 10.17159/2413-3051/2012/v23i1a3153.

[164] D. Yu, Y. Meng, G. Yan, G. Mu, D. Li, and S. Le Blond, "Sizing Combined Heat and Power Units and Domestic Building Energy Cost Optimisation," *Energies,* vol. 10, p. 771, 06/01 2017, doi: 10.3390/en10060771.

[165] O. A. Shaneb, G. Coates, and P. C. Taylor, "Sizing of residential μCHP systems," *Energy and Buildings,* vol. 43, no. 8, pp. 1991-2001, 2011/08/01/ 2011, doi: https://doi.org/10.1016/j.enbuild.2011.04.005.

[166] D. Haeseldonckx, L. Peeters, L. Helsen, and W. D'haeseleer, "The impact of thermal storage on the operational behaviour of residential CHP facilities and the overall CO2 emissions," *Renewable and Sustainable Energy Reviews,* vol. 11, no. 6, pp. 1227-1243, 2007/08/01/ 2007, doi: https://doi.org/10.1016/j.rser.2005.09.004.

[167] X. Q. Kong, R. Z. Wang, and X. H. Huang, "Energy optimization model for a CCHP system with available gas turbines," *Applied Thermal Engineering,* vol. 25, no. 2, pp. 377-391, 2005/02/01/ 2005, doi: https://doi.org/10.1016/j.applthermaleng.2004.06.014.

[168] H. J. Ehmke, "Size optimization for cogeneration plants," *Energy,* vol. 15, no. 1, pp. 35-44, 1990/01/01/ 1990, doi: https://doi.org/10.1016/0360-5442(90)90062-7.

[169] R. Yokoyama, K. Ito, and Y. Matsumoto, "Optimal Sizing of a Gas Turbine Cogeneration Plant in Consideration of Its Operational Strategy," *Journal of Engineering for Gas Turbines and Power,* vol. 116, no. 1, pp. 32-38, 1994, doi: 10.1115/1.2906806.

[170] P. Hanafizadeh, J. Eshraghi, P. Ahmadi, and A. Sattari, "Evaluation and sizing of a CCHP system for a commercial and office buildings," *Journal of Building Engineering,* vol. 5, pp. 67-78, 2016/03/01/ 2016, doi: https://doi.org/10.1016/j.jobe.2015.11.003.

[171] M. A. Ehyaei and M. N. Bahadori, "Selection of micro turbines to meet electrical and thermal energy needs of residential buildings in Iran," *Energy and Buildings,* vol. 39, no. 12, pp. 1227-1234, 2007/12/01/ 2007, doi: https://doi.org/10.1016/j.enbuild.2007.01.006.

[172] J. Kim, W. Cho, and K.-S. Lee, "Optimum generation capacities of micro combined heat and power systems in apartment complexes with varying numbers of apartment units," *Energy,* vol. 35, no. 12, pp. 5121-5131, 2010/12/01/ 2010, doi: https://doi.org/10.1016/j.energy.2010.08.003.

[173] C. Diakaki, E. Grigoroudis, and D. Kolokotsa, "Towards a multi-objective optimization approach for improving energy efficiency in buildings," *Energy*

and Buildings, vol. 40, no. 9, pp. 1747-1754, 2008/01/01/ 2008, doi: https://doi.org/10.1016/j.enbuild.2008.03.002.

[174] H. Cho, P. J. Mago, R. Luck, and L. M. Chamra, "Evaluation of CCHP systems performance based on operational cost, primary energy consumption, and carbon dioxide emission by utilizing an optimal operation scheme," *Applied Energy,* vol. 86, no. 12, pp. 2540-2549, 2009/12/01/ 2009, doi: https://doi.org/10.1016/j.apenergy.2009.04.012.

[175] M. Liu, Y. Shi, and F. Fang, "Optimal power flow and PGU capacity of CCHP systems using a matrix modeling approach," *Applied Energy,* vol. 102, pp. 794-802, 2013/02/01/ 2013, doi: https://doi.org/10.1016/j.apenergy.2012.08.041.

[176] T. Fang and R. Lahdelma, "Optimization of combined heat and power production with heat storage based on sliding time window method," *Applied Energy,* vol. 162, pp. 723-732, 2016/01/15/ 2016, doi: https://doi.org/10.1016/j.apenergy.2015.10.135.

[177] R. Lahdelma and H. Hakonen, "An efficient linear programming algorithm for combined heat and power production," *European Journal of Operational Research,* vol. 148, no. 1, pp. 141-151, 2003/07/01/ 2003, doi: https://doi.org/10.1016/S0377-2217(02)00460-5.

[178] X. Xia and J. Zhang, "Operation efficiency optimisation modelling and application of model predictive control," *IEEE/CAA Journal of Automatica Sinica,* vol. 2, no. 2, pp. 166-172, 2015, doi: 10.1109/JAS.2015.7081656.

[179] A. Inc., *2008 ASHRAE handbook- HVAC systems and equipment* I-P ed. 2008.

[180] R. Sirohi, A. Singh, A. Tarafdar, and N. C. Shahi, "Application of genetic algorithm in modelling and optimization of cellulase production," *Bioresource Technology,* vol. 270, pp. 751-754, 2018/12/01/ 2018, doi: https://doi.org/10.1016/j.biortech.2018.09.105.

[181] D. E. Goldberg and J. H. Holland, "Genetic Algorithms and Machine Learning," *Machine Learning,* vol. 3, no. 2, pp. 95-99, 1988/10/01 1988, doi: 10.1023/A:1022602019183.

[182] G. Lindfield and J. Penny, "Chapter 9 - Integer, Constrained and Multi-Objective Optimization," in *Introduction to Nature-Inspired Optimization*, G. Lindfield and J. Penny Eds. Boston: Academic Press, 2017, pp. 171-184.

[183] O. E. I. U.S. "Building characteristics for residential hourly load data." https://openei.org/doe-opendata/dataset/commercial-and-residential-hourly-load-profiles-for-all-tmy3-locations-in-the-united-states (accessed 25 November, 2014).

[184] D. o. E. a. C. Change. "Further Analysis of Data from the Household Electricity Usage Study: Electricity Price Signals and Demand Response." https://assets.publishing.service.gov.uk/government/uploads/system/uploads/a

ttachment_data/file/326122/HEUS_Electricity_Price_Signals_and_Demand_Response_Final_Report_04_04_14....pdf (accessed 14 April, 2014).

[185] T. a. D. USA. "Past Weather in Miami, Florida, USA." https://www.timeanddate.com/weather/usa/miami/historic (accessed 15 November, 2016).

[186] P. N. D. Premadasa and D. P. Chandima, "An innovative approach of optimizing size and cost of hybrid energy storage system with state of charge regulation for stand-alone direct current microgrids," *Journal of Energy Storage,* vol. 32, p. 101703, 2020/12/01/ 2020, doi: https://doi.org/10.1016/j.est.2020.101703.

[187] M. S. Nazir *et al.*, "Optimization configuration of energy storage capacity based on the microgrid reliable output power," *Journal of Energy Storage,* vol. 32, p. 101866, 2020/12/01/ 2020, doi: https://doi.org/10.1016/j.est.2020.101866.

[188] A. Hoke, A. Brissette, D. Maksimović, A. Pratt, and K. Smith, "Electric vehicle charge optimization including effects of lithium-ion battery degradation," in *2011 IEEE Vehicle Power and Propulsion Conference*, 6-9 Sept. 2011 2011, pp. 1-8, doi: 10.1109/VPPC.2011.6043046.

[189] Y. Sun, H. Yue, J. Zhang, and C. Booth, "Minimization of Residential Energy Cost Considering Energy Storage System and EV With Driving Usage Probabilities," *IEEE Transactions on Sustainable Energy,* vol. 10, no. 4, pp. 1752-1763, 2019, doi: 10.1109/TSTE.2018.2870561.

[190] F. Martel, S. Kelouwani, Y. Dubé, and K. Agbossou, "Optimal economy-based battery degradation management dynamics for fuel-cell plug-in hybrid electric vehicles," *Journal of Power Sources,* vol. 274, pp. 367-381, 2015/01/15/ 2015, doi: https://doi.org/10.1016/j.jpowsour.2014.10.011.

[191] "Manufacturers and Suppliers." (accessed 1 February, 2020).

[192] K. Brown and S. Minett, "History of CHP developments and current trends," *Applied Energy,* vol. 53, no. 1, pp. 11-22, 1996/01/01/ 1996, doi: http://dx.doi.org/10.1016/0306-2619(95)00051-8.

[193] M. Ebrahimi and A. Keshavarz, "1 - CCHP Literature," in *Combined Cooling, Heating and Power*. Boston: Elsevier, 2015, pp. 1-34.

[194] J. Strömberg and P.-Å. Franck, "Gas turbines in industrial CHP applications—assessment of economics," *Heat Recovery Systems and CHP,* vol. 14, no. 2, pp. 129-141, 1994/03/01/ 1994, doi: http://dx.doi.org/10.1016/0890-4332(94)90004-3.

[195] E. Unterwurzacher, "CHP development," *Energy Policy,* vol. 20, no. 9, pp. 893-900, 1992/09/01/ 1992, doi: http://dx.doi.org/10.1016/0301-4215(92)90124-K.

[196] I. Arashnia, G. Najafi, B. Ghobadian, T. Yusaf, R. Mamat, and M. Kettner, "Development of Micro-scale Biomass-fuelled CHP System Using Stirling

Engine," *Energy Procedia,* vol. 75, pp. 1108-1113, 2015/08/01/ 2015, doi: http://dx.doi.org/10.1016/j.egypro.2015.07.505.

[197] M. E. Nazari and M. M. Ardehali, "Profit-based unit commitment of integrated CHP-thermal-heat only units in energy and spinning reserve markets with considerations for environmental CO2 emission cost and valve-point effects," *Energy,* vol. 133, pp. 621-635, 8/15/ 2017, doi: https://doi.org/10.1016/j.energy.2017.05.164.

[198] M. Farzaneh-Gord and M. Deymi-Dashtebayaz, "A new approach for enhancing performance of a gas turbine (case study: Khangiran refinery)," *Applied Energy,* vol. 86, no. 12, pp. 2750-2759, 12// 2009, doi: http://dx.doi.org/10.1016/j.apenergy.2009.04.017.

[199] J. L. Silveira, J. A. de Carvalho Jr, and I. A. de Castro Villela, "Combined cycle versus one thousand diesel power plants: pollutant emissions, ecological efficiency and economic analysis," *Renewable and Sustainable Energy Reviews,* vol. 11, no. 3, pp. 524-535, 4// 2007, doi: http://dx.doi.org/10.1016/j.rser.2004.11.007.

[200] R. E. H. Sims, H.-H. Rogner, and K. Gregory, "Carbon emission and mitigation cost comparisons between fossil fuel, nuclear and renewable energy resources for electricity generation," *Energy Policy,* vol. 31, no. 13, pp. 1315-1326, 10// 2003, doi: http://dx.doi.org/10.1016/S0301-4215(02)00192-1.

[201] W. Jan and P. Marek, "Mathematical Modeling of the Stirling Engine," *Procedia Engineering,* vol. 157, pp. 349-356, 2016/01/01/ 2016, doi: http://dx.doi.org/10.1016/j.proeng.2016.08.376.

[202] K. Wang, S. R. Sanders, S. Dubey, F. H. Choo, and F. Duan, "Stirling cycle engines for recovering low and moderate temperature heat: A review," *Renewable and Sustainable Energy Reviews,* vol. 62, pp. 89-108, 2016/09/01/ 2016, doi: http://dx.doi.org/10.1016/j.rser.2016.04.031.

[203] A. K. Almajri, S. Mahmoud, and R. Al-Dadah, "Modelling and parametric study of an efficient Alpha type Stirling engine performance based on 3D CFD analysis," *Energy Conversion and Management,* vol. 145, pp. 93-106, 8/1/ 2017, doi: https://doi.org/10.1016/j.enconman.2017.04.073.

[204] A. Abuelyamen, R. Ben-Mansour, H. Abualhamayel, and E. M. A. Mokheimer, "Parametric study on beta-type Stirling engine," *Energy Conversion and Management,* vol. 145, pp. 53-63, 8/1/ 2017, doi: https://doi.org/10.1016/j.enconman.2017.04.098.

[205] H.-S. Yang and C.-H. Cheng, "Stability analysis of thermal-lag Stirling engines," *Applied Thermal Engineering,* vol. 106, pp. 712-720, 2016/08/05/ 2016, doi: http://dx.doi.org/10.1016/j.applthermaleng.2016.06.009.

[206] B. Kongtragool and S. Wongwises, "A review of solar-powered Stirling engines and low temperature differential Stirling engines," *Renewable and*

Sustainable Energy Reviews, vol. 7, no. 2, pp. 131-154, 2003/04/01/ 2003, doi: http://dx.doi.org/10.1016/S1364-0321(02)00053-9.

[207] D. G. Thombare and S. K. Verma, "Technological development in the Stirling cycle engines," *Renewable and Sustainable Energy Reviews,* vol. 12, no. 1, pp. 1-38, 2008/01/01/ 2008, doi: http://dx.doi.org/10.1016/j.rser.2006.07.001.

[208] L. Dong, H. Liu, and S. Riffat, "Development of small-scale and micro-scale biomass-fuelled CHP systems – A literature review," *Applied Thermal Engineering,* vol. 29, no. 11, pp. 2119-2126, 2009/08/01/ 2009, doi: https://doi.org/10.1016/j.applthermaleng.2008.12.004.

[209] A. Hawkes, I. Staffell, D. Brett, and N. Brandon, "Fuel cells for micro-combined heat and power generation," *Energy & Environmental Science,* 10.1039/B902222H vol. 2, no. 7, pp. 729-744, 2009, doi: 10.1039/B902222H.

[210] J. L. H. Backman and J. Kaikko, "7 - Microturbine systems for small combined heat and power (CHP) applications A2 - Beith, Robert," in *Small and Micro Combined Heat and Power (CHP) Systems*: Woodhead Publishing, 2011, pp. 147-178.

[211] A. D. Hawkes, D. J. L. Brett, and N. P. Brandon, "Fuel cell micro-CHP techno-economics: Part 1 – model concept and formulation," *International Journal of Hydrogen Energy,* vol. 34, no. 23, pp. 9545-9557, 2009/12/01/ 2009, doi: https://doi.org/10.1016/j.ijhydene.2009.09.094.

[212] J. P. Trembly, A. I. Marquez, T. R. Ohrn, and D. J. Bayless, "Effects of coal syngas and H2S on the performance of solid oxide fuel cells: Single-cell tests," *Journal of Power Sources,* vol. 158, no. 1, pp. 263-273, 2006/07/14/ 2006, doi: https://doi.org/10.1016/j.jpowsour.2005.09.055.

[213] B. Lindström *et al.*, "Diesel fuel reformer for automotive fuel cell applications," *International Journal of Hydrogen Energy,* vol. 34, no. 8, pp. 3367-3381, 2009/05/01/ 2009, doi: https://doi.org/10.1016/j.ijhydene.2009.02.013.

[214] G. F. McLean, T. Niet, S. Prince-Richard, and N. Djilali, "An assessment of alkaline fuel cell technology," *International Journal of Hydrogen Energy,* vol. 27, no. 5, pp. 507-526, 2002/05/01/ 2002, doi: https://doi.org/10.1016/S0360-3199(01)00181-1.

[215] J. Xuan, M. K. H. Leung, D. Y. C. Leung, and M. Ni, "A review of biomass-derived fuel processors for fuel cell systems," *Renewable and Sustainable Energy Reviews,* vol. 13, no. 6, pp. 1301-1313, 2009/08/01/ 2009, doi: https://doi.org/10.1016/j.rser.2008.09.027.

[216] A. O. Olaniran, A. Balgobind, and B. Pillay, "Bioavailability of Heavy Metals in Soil: Impact on Microbial Biodegradation of Organic Compounds and Possible Improvement Strategies," *International Journal of Molecular Sciences,* vol. 14, no. 5, pp. 10197-10228, 05/15 10/08/received 04/10/revised

04/24/accepted 2013, doi: 10.3390/ijms140510197. [217] D. L. Klass, "Chapter 1 - Energy Consumption, Reserves, Depletion, and Environmental Issues," in *Biomass for Renewable Energy, Fuels, and Chemicals*. San Diego: Academic Press, 1998, pp. 1-27.

[218] R. Hoefnagels, E. Smeets, and A. Faaij, "Greenhouse gas footprints of different biofuel production systems," *Renewable and Sustainable Energy Reviews,* vol. 14, no. 7, pp. 1661-1694, 2010/09/01/ 2010, doi: https://doi.org/10.1016/j.rser.2010.02.014.

[219] M. Pirouti, J. Wu, J. Ekanayake, and N. Jenkins, "Dynamic modelling and control of a direct-combustion biomass CHP unit," in *45th International Universities Power Engineering Conference UPEC2010*, Aug. 31 2010-Sept. 3 2010 2010, pp. 1-6.

[220] "Electrical energy storage: white paper.," in "Technical report.," Prepared by electrical energy storage project team, International Electrotechnical Commission (IEC). Accessed: 15/May/ 2014. [Online]. Available: http://www.iec.ch/ whitepaper/pdf/iecWP-energystorage-LR-en.pdf

[221] M. Molina, "Dynamic Modelling and Control Design of Advanced Energy Storage for Power System Applications," 2010.

[222] F. C. Figueiredo and P. C. Flynn, "Using diurnal power price to configure pumped storage," *IEEE Transactions on Energy Conversion,* vol. 21, no. 3, pp. 804-809, 2006, doi: 10.1109/TEC.2006.877373.

[223] W. Pickard, "The History, Present State, and Future Prospects of Underground Pumped Hydro for Massive Energy Storage," *Proceedings of the IEEE,* vol. 100, pp. 473-483, 02/01 2012, doi: 10.1109/JPROC.2011.2126030.

[224] S. V. Papaefthymiou, E. G. Karamanou, S. A. Papathanassiou, and M. P. Papadopoulos, "A Wind-Hydro-Pumped Storage Station Leading to High RES Penetration in the Autonomous Island System of Ikaria," *IEEE Transactions on Sustainable Energy,* vol. 1, no. 3, pp. 163-172, 2010, doi: 10.1109/TSTE.2010.2059053.

[225] C. Bueno and J. A. Carta, "Wind powered pumped hydro storage systems, a means of increasing the penetration of renewable energy in the Canary Islands," *Renewable and Sustainable Energy Reviews,* vol. 10, no. 4, pp. 312-340, 2006/08/01/ 2006, doi: https://doi.org/10.1016/j.rser.2004.09.005.

[226] P. Breeze, "Chapter 3 - Compressed Air Energy Storage," in *Power System Energy Storage Technologies*, P. Breeze Ed.: Academic Press, 2018, pp. 23-31.

[227] R. Madlener and J. Latz, "Economics of centralized and decentralized compressed air energy storage for enhanced grid integration of wind power," *Applied Energy,* vol. 101, pp. 299-309, 2013/01/01/ 2013, doi: https://doi.org/10.1016/j.apenergy.2011.09.033.

[228] S. Succar, D. C. Denkenberger, and R. H. Williams, "Optimization of specific rating for wind turbine arrays coupled to compressed air energy storage," *Applied Energy,* vol. 96, pp. 222-234, 2012/08/01/ 2012, doi: https://doi.org/10.1016/j.apenergy.2011.12.028.

[229] E. A. Bouman, M. M. Øberg, and E. G. Hertwich, "Environmental impacts of balancing offshore wind power with compressed air energy storage (CAES)," *Energy,* vol. 95, pp. 91-98, 2016/01/15/ 2016, doi: https://doi.org/10.1016/j.energy.2015.11.041.

[230] S. M. Mousavi G, F. Faraji, A. Majazi, and K. Al-Haddad, "A comprehensive review of Flywheel Energy Storage System technology," *Renewable and Sustainable Energy Reviews,* vol. 67, pp. 477-490, 2017/01/01/ 2017, doi: https://doi.org/10.1016/j.rser.2016.09.060.

[231] A. A. K. Arani, H. Karami, G. B. Gharehpetian, and M. S. A. Hejazi, "Review of Flywheel Energy Storage Systems structures and applications in power systems and microgrids," *Renewable and Sustainable Energy Reviews,* vol. 69, pp. 9-18, 2017/03/01/ 2017, doi: https://doi.org/10.1016/j.rser.2016.11.166.

[232] R. Peña-Alzola, R. Sebastian, J. Quesada, and A. Colmenar, *Review of flywheel based energy storage systems*. 2011, pp. 1-6.

[233] F. Díaz-González, A. Sumper, O. Gomis-Bellmunt, and F. D. Bianchi, "Energy management of flywheel-based energy storage device for wind power smoothing," *Applied Energy,* vol. 110, pp. 207-219, 2013/10/01/ 2013, doi: https://doi.org/10.1016/j.apenergy.2013.04.029.

[234] I. Hadjipaschalis, A. Poullikkas, and V. Efthimiou, "Overview of current and future energy storage technologies for electric power applications," *Renewable and Sustainable Energy Reviews,* vol. 13, no. 6, pp. 1513-1522, 2009/08/01/ 2009, doi: https://doi.org/10.1016/j.rser.2008.09.028.

[235] W. Waghorne, "Viscosities of electrolyte solutions," *Philosophical Transactions of The Royal Society B: Biological Sciences,* vol. 359, 08/15 2001, doi: 10.1098/rsta.2001.0864.

[236] S. C. Smith, P. K. Sen, and B. Kroposki, "Advancement of energy storage devices and applications in electrical power system," in *2008 IEEE Power and Energy Society General Meeting - Conversion and Delivery of Electrical Energy in the 21st Century*, 20-24 July 2008 2008, pp. 1-8, doi: 10.1109/PES.2008.4596436.

[237] F. Díaz-González, A. Sumper, O. Gomis-Bellmunt, and R. Villafáfila-Robles, "A review of energy storage technologies for wind power applications," *Renewable and Sustainable Energy Reviews,* vol. 16, no. 4, pp. 2154-2171, 2012/05/01/ 2012, doi: https://doi.org/10.1016/j.rser.2012.01.029.

[238] Z. Yang *et al.*, "Electrochemical Energy Storage for Green Grid," *Chemical Reviews,* vol. 111, no. 5, pp. 3577-3613, 2011/05/11 2011, doi: 10.1021/cr100290v.

[239] C. Liu, F. Li, L.-P. Ma, and H.-M. Cheng, "Advanced Materials for Energy Storage," *Advanced materials (Deerfield Beach, Fla.),* vol. 22, pp. E28-62, 02/23 2010, doi: 10.1002/adma.200903328.

[240] K. Lin *et al.*, "Alkaline quinone flow battery," *Science,* vol. 349, no. 6255, p. 1529, 2015, doi: 10.1126/science.aab3033.

[241] A. Z. Weber, M. M. Mench, J. P. Meyers, P. N. Ross, J. T. Gostick, and Q. Liu, "Redox flow batteries: a review," *Journal of Applied Electrochemistry,* vol. 41, no. 10, p. 1137, 2011/09/02 2011, doi: 10.1007/s10800-011-0348-2.

[242] H. Chen, T. N. Cong, W. Yang, C. Tan, Y. Li, and Y. Ding, "Progress in electrical energy storage system: A critical review," *Progress in Natural Science,* vol. 19, no. 3, pp. 291-312, 2009/03/10/ 2009, doi: https://doi.org/10.1016/j.pnsc.2008.07.014.

[243] A. F. Felix and M. G. Simões, "Integration of Alternative Sources of Energy," in *Integration of Alternative Sources of Energy*: IEEE, 2006, pp. 301-332.

[244] M. Winter and R. J. Brodd, "What are batteries, fuel cells, and supercapacitors?," (in eng), *Chem Rev,* vol. 104, no. 10, pp. 4245-69, Oct 2004, doi: 10.1021/cr020730k.

[245] A. Kusko and J. Dedad, "Stored energy - Short-term and long-term energy storage methods," *IEEE Industry Applications Magazine,* vol. 13, no. 4, pp. 66-72, 2007, doi: 10.1109/MIA.2007.4283511.

[246] M. H. Ali, B. Wu, and R. A. Dougal, "An Overview of SMES Applications in Power and Energy Systems," *IEEE Transactions on Sustainable Energy,* vol. 1, no. 1, pp. 38-47, 2010, doi: 10.1109/TSTE.2010.2044901.

[247] R. B. Schainker, "Executive overview: energy storage options for a sustainable energy future," in *IEEE Power Engineering Society General Meeting, 2004.*, 6-10 June 2004 2004, pp. 2309-2314 Vol.2, doi: 10.1109/PES.2004.1373298.

[248] W. Yuan, "Second-generation high-temperature superconducting coils and their applications for energy storage (Doctoral thesis)," 2010.